Mechanism of neuronal patterning in the anthozoan cnidarian, Nematostella vectensis

Mechanism of neuronal patterning in the anthozoan cnidarian, *Nematostella vectensis*

by

Dylan Z. Faltine-Gonzalez

A Dissertation

Presented to the Graduate and Research Committee

of Lehigh University

in Candidacy for the Degree of

Doctor of Philosophy

in

Biological Sciences

Lehigh University

August 2021

Approved and recommended for acceptance as a dissertation in partial fulfillment of the requirements for the degree of Doctor of Philosophy

Dylan Z. Faltine-Gonzalez
Mechanism of Neuronal Patterning in the anthozoan cnidarian, *Nematostella vectensis*

_____

July 30th, 2021

_____

Dissertation Director
Michael J. Layden, PhD

_____

Approved Date

Committee Members:

_____

M. Kathryn Iovine, PhD

_____

Daniel Babcock, PhD

_____

Eric Rötinger, PhD

ACKNOWLEDGMENTS

First I would like to thank my advisor, Mike Layden. Ten years ago he told me I would be his graduate student. I thought this was nonsense but ten years later here I am leaving with my PhD. He saw my potential as a researcher back then, has continued to voice his support for me now, and I know he will support me as I move forward. Being his first graduate student has been an incredible experience and I wouldn't change it for the world. I sincerely hope we keep in touch and I am truly excited for to see how the lab succeeds moving forward.

I would also like to thank all the members of the Layden lab, Jamie Havrilak, Layla Al-shaer, Minghe Cheng, Justin Carlino. You all have made the lab an amazing and supportive place to work.

I would like to thank my family. They do not understand what I'm doing in graduate school but they have always been extremely supportive. My parents have always bolstered my interest in biology and instilled the stubbornness and work ethic necessary for me to finish graduate school. My grandmother has done her best to truly understand the research that I'm doing and has always seem immensely interested. I'd also like to thank my siblings who have always been supportive despite the physical distance between us.

Lastly, I would also like to thank the Faculty (including my committee), students, and friends who made up an amazing academic community. This community provided shoulders to cry on, brains to pick, and laughs to share. While they might not know it without them the stress of graduate school would have gotten to me and I am truly grateful for their help in pulling me out of those dark places.

TABLE OF CONTENTS

List of Figures

List of Tables

Abstract

Understanding nervous system patterning within the sister taxa to bilaterians provides insight into which patterning mechanisms are conserved and likely evolved prior to the evolution of bilaterians. This allows researchers to build hypotheses about which mechanisms are unique to the bilaterian nervous system development and are necessary for evolution of bilaterian nervous systems. The cnidarians (jellyfish, sea anemones, coral, etc.) are sister taxa to the bilaterians and possess an ancestral nerve net-like nervous system. A cnidarian model easily amenable to the functional assays necessary for understanding early neurogenic patterning is the anthozoan cnidarian, *Nematostella vectensis.* The nerve net of the *Nematostella vectensis* is patterned from a multipotent *NvsoxB(2)* and *Nvath-like* progenitor, these progenitor differentiate and express *NvashA,* which then patterns multiple differentiated neuronal subtypes. Despite years of research little is understand about how these individual neuronal cell types are patterned or the possible function these differentiated neurons. This dissertation focused on expanding our understanding of cnidarian neurogenesis from early progenitor dynamics to functional neuronal subtypes. I characterized the existence of a *NvsoxB(2)* only and *NvsoxB(2)* and *Nvath-like* progenitor populations which regulate unique downstream markers. I also identify a previously unknown *NvfoxD3-like* mediated mechanism of cnidocyte patterning. I then went on to characterize how axial patterning cues along the oral-aboral axis are used to pattern neuronal subtypes from broadly expressed neuronal progenitor markers. Lastly, I characterized the role of acetylcholine in the regulation of muscle contraction through an upstream still unknown cholinergic neural network. In total, this dissertation characterized multiple conserved mechanisms of neuronal patterning and

neuronal function allowing for us to build hypotheses about the evolution of these mechanisms within bilaterians.

Chapter 1: Introduction to development and neurogenesis in the starlet sea anemone, *Nematostella vectensis*

The anthozoan model, Nematostella vectensis

Understanding how the nerve net-like nervous system found within cnidarians (e.g.. jellyfish, corals, sea anemones, hydrozoans) is patterned during development can provide insight into the evolution of metazoan nervous system patterning. Cnidarian are the sister taxon to the bilaterians (e.g. humans, mice, worms, insects) who possess a centralized nervous system. It is hypothesized that the cnidarian-bilaterian ancestor likely possessed a nerve-net like nervous system, with the cnidarians maintaining this ancestral state and bilaterians eventually evolving centralized nervous systems. The possession of this ancestral nerve net coupled with the phylogenomic position of cnidarians makes this phylum an important group to study to better understand the evolution of bilaterian. If patterning mechanisms are conserved between bilaterians and cnidarians then it argues that these particular mechanisms likely arose before the cnidarians and the bilaterians diverged. If a particular conserved patterning mechanism is found to be unique to the bilaterians then it likely arose after the bilaterians diverged and could be necessary for a particular bilaterian trait. One cnidarian model which has proven easily amenable to this developmental research is the starlet sea anemone, *Nematostella vectensis*.

The annotated *Nematostella* genome has allowed for rapid development of multiple molecular tools from which functional assays could be performed within a cnidarian model. The genome was sequenced and assembled in 2007, and then repeated in 2020 (Putnam et al., 2007; Zimmermann et al., 2020). Since the annotated genome was published morpholino, shRNA-mediated, and CRISPR induced loss of expression methods have been modified to function in *Nematostella* (Layden et al., 2012, 2013; Ikmi

et al., 2014; He et al., 2018; Nakanishi and Martindale, 2018). Synthesis and injection of mRNA also allows for ubiquitous misexpression assays within *Nematostella* (Layden et al., 2013) . Lastly, utilization of restriction enzymes, TALON, and/or CRISPR/ Cas-9 systems have allowed for the synthesis of transgenic lines and the characterization of gene function within live animals (Renfer et al., 2010; Ikmi et al., 2014, 2014; Havrilak et al., 2017a; Tournière et al., 2020). The combination of these techniques has allowed for a detailed understanding of early development and neurogenesis within *Nematostella.*

Early neurogenesis in Nematostella

Early neurogenesis in *Nematostella* has been well characterized and occurs early during *Nematostella* development. Neurogenesis is induced though the MEK/MAPK pathway during early blastula stages (Layden et al., 2016). Once induced progenitors expressing low-*notch*/high *delta* then promote expression of the neuronal progenitor markers, *NvsoxB(2)/Nvath-lke* (Layden and Martindale, 2014; Richards and Rentzsch, 2015; Layden et al., 2016). Morpholino induced knockdown of *NvsoxB(2)* and *Nvath-like* has identified that this progenitor population then gives rise to both neurons and cnidocytes, the stinging cells which define the cnidarians (Richards and Rentzsch, 2015; Babonis and Martindale, 2017). This work also suggests that these two markers, *NvsoxB(2)* and *Nvath-like*, are co-expressed and likely co-regulate all downstream cell types from this progenitor lineage (Richards and Rentzsch, 2014, 2015; Busengdal and Rentzsch, 2017). Once these broad neural progenitors are induced to differentiate, a mechanism currently unknown to the field, they express either the post-mitotic markers *NvashA,* or the unipotent progenitor marker, *Nvfoxq2d* (Layden et al., 2012; Richards and Rentzsch,

2015; Busengdal and Rentzsch, 2017). *Nvfoxq2d* is currently the only downstream progenitor identified and later differentiates into *Nvfoxq2d+* sensory neurons within the ectodermal nerve net (Busengdal and Rentzsch, 2017). Those cells which express *NvashA* then give rise to multiple neuronal subtypes, including *NvLWamide-like* and *Nvserum amyloidA-like*. A subset of *NvsoxB(2)/Nvath-like* daughter cells will differentiate and express *NvpaxA* which then goes on to specify cnidocytes (Babonis and Martindale, 2017). Most recently *NvsoxB(2)* has also been found to regulate the neuronal and secretory marker *Nvism1* as well as other secretory maker markers in *Nematostella* (Tournière et al., 2021). These data suggest that *NvsoxB(2)* and *Nvath-like* positive progenitors can differentiate into neurons, cnidocytes, and sensory cells (Richards and Rentzsch, 2015; Babonis and Martindale, 2017; Tournière et al., 2021). Despite improved understanding of the pathways downstream *NvsoxB(2)* and *Nvath-like* our understanding for how these pathways interact with each other to pattern neurons, cnidocytes, or secretory cells is completely unknown.

Oral-aboral patterning and restricted neuronal subtypes

The spatial restriction of targets downstream *NvashA* suggest that neuronal subtypes are regulated by spatial genes. The expression patterns of multiple downstream targets of *NvashA* (e.g. *NvLWamide, Nvserum amyloidA-like,* and *Nvpaladin*) display varying levels of spatial restriction when compared to the broad expression of *NvashA* itself (Layden et al., 2012). Most interestingly, ubiquitous expression of *NvashA* does not result in ubiquitous expansion of *NvLWamide* or *Nvpaladin* but instead increased expression within their wildtype domains (Layden et al., 2012). These spatial restrictions are

reminiscent of spatial markers, like *Nvsix3/6*, expressed along the oral-aboral axis in *Nematostella*.

Spatial genes along the oral-aboral axis are patterned through a gradient of Wnt along the oral-aboral. Early expression of multiple Wnt ligands (*Nvwn1, Nvwnt2,* and *Nvwnt3*) defines the site of gastrulation at the oral pole of the animal (Kraus et al., 2016) . This Wnt activity can be read out as a gradient of stabilized nuclear ß-catenin, with high nuclear ß-catenin at the oral pole and low nuclear ß-catenin at the aboral pole (Leclère et al., 2016). This gradient of nuclear ß-catenin then activates expression of distinct spatial markers along the oral-aboral axis (Leclère et al., 2016). For instance, the aboral marker *Nvsix3/6* requires low nuclear ß-catenin at the aboral pole, is activated, then functions to further inhibit Wnt activity within this aboral domain (Sinigaglia et al., 2013; Leclère et al., 2016). Pharmacological overactivation of Wnt activity then oralizes the embryo with an expansion of oral and trunk markers at the loss of aboral expression (Marlow et al., 2013; Sinigaglia et al., 2013; Leclère et al., 2016). Once established these spatial domain genes then go on to pattern their specific domain. However, this has only been characterized for the aboral marker *Nvsix3/6*. Loss of *Nvsix3/6* results in loss of aboral cell types with a subsequent expansion of trunk markers into the aboral domain while overactivation of *Nvsix3/6* expands aboral identity at a loss of oral tissue (Sinigaglia et al., 2013; Leclère et al., 2016). This Wnt mediated mechanism of oral-aboral patterning in cnidarians follows the same regulatory logic as the anterior-posterior axis of bilaterians. However, the neurogenic role found within bilaterians spatial domain genes has not been observed within cnidarians.

Anterior-posterior patterning genes within the bilaterian brain pattern neuronal subtypes but this neurogenic function has not been identified in *Nematostella.* Along the anterior-posterior axis of the bilaterian brain, spatial genes pattern regionally specific neuronal subtypes. Six3 expression is found within the most anterior-most region of the brain and patterns neuronal cell types which originate in that anterior tissue, this mechanism is highly conserved among multiple bilaterians models (mice, sea urchins, sea stars, and zebrafish) (Oliver et al., 1995; Lagutin, 2003; Cheatle Jarvela et al., 2016; Range and Wei, 2017). Within *Nematostella* some neuronal subtypes seem to be restricted to this *Nvsix3/6* domain (Leclère et al., 2016; Busengdal and Rentzsch, 2017). When *Nvsix3/6* expression was knocked down the predicted neuronal marker *Nvdmrtb* expression was reduced, however it wasn't lost and *Nvsix3/6* was argued to not have a critical role in neurogenesis (Sinigaglia et al., 2013). Pharmacological overactivation of Wnt activity resulted in aboral domain shifts in the expression of the predicted neural marker *Nv-op85309* and the broad neural subtype marker *Nvantho-rfamide* (Marlow et al., 2013). These data suggest that some aspect of spatial patterning along the oral-aboral axis likely patterns individual neuronal subtypes however, the mechanism for this is still uncharacterized.

The adult nervous system and neuronal subtype function

The nervous system of *Nematostella* is characterized as a nerve net composed of multiple neuronal subtypes and has been hypothesized to be an organized nervous system. The classic description of the cnidarian nerve net is that it consists of soma with disorganized

neurite projections occurring across the body, which results in a nervous system that resembles a net. Early work determined that *Nvelav1* labeled a large portion of the adult nervous system and characterized three common neuronal cell types; sensory, glial, and bipolar (Nakanishi et al., 2012). Research within the last five years though has expanded on this early nervous system research and utilization of subtype markers has allowed for more detailed understanding of the adult nervous system.

Synthesis of the NvLWamide::mCherry transgenic line showed distinct neuronal subtypes within *Nematostella.* Characterization of this transgenic line identified five distinct neuronal cell types based of neuronal morphologies and the tissue they were identified in; the tripolar, quadripolar, mesentery, longitudinal, tentacular, and pharyngeal neurons (Havrilak et al., 2017). Further characterization of this transgenic line identified that the nervous system, when identified at the subtype level, scaled the number of neuronal subtypes as the adult polyp grew in size suggesting organization to the "disorganized' nerve net (Havrilak et al., 2017). Several more neuronal subtypes have been identified since then including a terminal differentiation marker Nvpou4, NvGLwamide, and a sensory neuron marker Nvfoxq2d (Busengdal and Rentzsch, 2017; Nakanishi and Martindale, 2018; Tournière et al., 2020). Despite identification of new neuronal subtypes, the functions of these neurons remains largely unstudied within *Nematostella*.

Early research suggested that many of the neurotransmitters found within bilaterians are utilized in *Nematostella* but, little work has been done to characterize the roles of these

neuronal subtypes. To date the only neuronal subtype which has been found to have a function in *Nematostella* is the neural peptide marker, NvGLWamide. Treatment with endogenous GLwamide during development was found to inhibit larval metamorphosis and maintain the free swimming planula larvae a few days longer than controls (Nakanishi and Martindale, 2018). This is the extent for what we know about neuronal subtype function in *Nematostella*. Interestingly though many of the mechanism necessary for neuronal transmission within bilaterians has been identified within *Nematostella* (Putnam et al., 2007; Anctil, 2009; Sebé-Pedrós et al., 2018). These consists of acetylcholine, dopamine, serotonin, GABAnergic, and several cnidarian-specific neuropeptides (Anctil, 2009). In fact recent single cell sequencing data has found that many of these genes are expressed within neuronal cells types and could be used as neurotransmitters, in a similar fashion to the bilaterian neurotransmitters (Sebé-Pedrós et al., 2018). The characterization of these neurotransmitters within *Nematostella* could provide insight into the evolution of neurotransmitter function within metazoans.

Summary

Research within *Nematostella* has identified many of the transcription factors necessary for early neurogenesis within the ectodermal nervous system however how individual neuronal cells type are patterned and the functional role of these neurons is unknown. The first chapter within this dissertation aims to identify gene regulatory pathways that determine how cell types are patterned from *NvsoxB(2)* and *Nath-like* progenitor population. My work within chapter 2 identifies a *NvsoxB(2)* only progenitor pool as well as a previously uncharacterized role for *NvfoxD3-like* in patterning cnidocytes. Chapter 3

focuses on characterizing the role of spatial domain genes in patterning known neuronal subtype markers. I found that *Nvsix3/6* is necessary and sufficient to pattern aborally restricted neuronal subtypes while trunk domain markers are likely patterned through Wnt signaling. This work is the first to characterize a conserved role for axial patterning genes in patterning neuronal subtypes outside the bilaterians. Lastly, within chapter 4, I identified a neurotransmitter role for acetylcholine in muscle contraction within *Nematostella*. The culmination of this work identified that cnidarians utilize use a combination of multiple progenitor populations and spatial information to pattern cell types along the oral-aboral axis as well as a conserved role of acetylcholine as a neurotransmitter.

Chapter 2: Establishment of a preliminary gene regulatory network for early neurogenesis in *Nematostella* gastrula

Abstract

The nerve net of *Nemtostella vectensis* is thought to arise from a pool of *NvsoxB(2)* and *Nvath-like* positive progenitors however, this progenitor population also gives rise to cnidocytes, neurons, and secretory cell types. Despite interest in understanding cell type specification within *Nematostella,* how individual cell types are patterned remains poorly understood. Knockdown of *NvsoxB(2), Nvath-like,* and dual knockdown of *NvsoxB(2)* and *Nvath-like* reveals eleven novel targets of *NvsoxB(2)/Nvath-like.* These knockdowns also suggest the existence of a *NvsoxB(2)* progenitor population which regulates a subset of downstream markers consisting of all three cell types. Loss of *Nvath-like* resulted in loss of *NvsoxB(2)* expression suggesting that *Nvath-like* promotes *NvsoxB(2)* expression and is largely redundant in its regulation of early cell type patterning. Interestingly *NvfoxD3-like ,*which is not downstream *NvsoxB(2)* or *Nvath-like,* regulates expression of the cnidocyte marker, *NvpaxA,* suggesting it may have a role in cnidocyte differentiation. These findings expand previously published gene regulatory pathways and provides some insight on cnidocyte specification during early neurogenesis.

Introduction

The nervous system of the anthozoan cnidarian, *Nematostella vectensis,* is most commonly described as a diffuse nerve net with neural soma projecting neurites across the animal in seemingly haphazard directions (Nakanishi et al., 2012). This is in stark contrast to the highly organized and structured central nervous system found within the cnidarian sister taxa, the bilaterians (e.g. mouse, chick, c. elegans, etc.). Despite differences in the structure of the final nervous system many of the early regulatory

components necessary for bilaterian nervous system development have been found to be functionally similar within *Nematostella.* Generally within bilaterians neural precursors are selected through notch signaling, with high notch maintaining a stem cell population and low notch activating the expression of proneural and sox genes (Bylund et al., 2003; Simpson). Sox gene expression is maintained and necessary for maintenance of actively dividing neural precursor cells (Graham et al., 2003; McClay et al., 2018) . Utilizing a combination of spatial-temporal information these multipotent neural precursor cells will either differentiate into specific developmentally restricted progenitor populations before differentiating or will differentiate into the fully differentiated neural subtypes (Guillemot, 2007; Berndt et al., 2015) . Despite years of research we only have a preliminary understanding of early neurogenesis within *Nematostella.* In order to make more informed hypotheses about the evolution of nervous systems, evolution of nervous system patterning, or subtype specification mechanisms in cnidarians we need to expand on what is currently known about early neurogenesis in *Nematostella.*

The onset of *Nematostella* neurogenesis occurs via MEK/MAPK signaling at the late blastula stage with the expression of the neural progenitor markers, *NvsoxB(2)* and *Nvath-like* (Layden et al., 2016). Notch signaling is then used to maintain *Nvath-like* positive neuronal progenitors and it has been hypothesized that low *Nvnotch/* high *Nvdelta* induces differentiation of these *NvsoxB(2)/Nvath-like* positive progenitors (Layden and Martindale, 2014; Richards and Rentzsch, 2015). Progenitors that are *NvsoxB(2)* positive then give rise to three separate cell types within *Nematostella*: cnidocytes, a stinging cell type unique to the cnidarians; neurons; or secretory cells

(Layden et al., 2012; Richards and Rentzsch, 2015; Babonis and Martindale, 2017; Tournière et al., 2021). Differentiating cnidocytes will then express *NvpaxA* while differentiating neurons will express either the postmitotic marker, *NvashA,* or the unipotent progenitor marker, *Nvfoxq2d* (Layden et al., 2012; Busengdal and Rentzsch, 2017). After differentiation occurs both fully differentiated cnidocytes and neuronal subtypes will express the terminal marker *NvPou4* (Tournière et al., 2020). This pathway then gives rise to the several neuronal, cnidocyte, and secretory markers identified within adult polyps (pathway summarized in Figure 3.1)(Layden et al., 2012, 2016; Babonis and Martindale, 2017; Busengdal and Rentzsch, 2017; Sebé-Pedrós et al., 2018; Sunagar et al., 2018; Tournière et al., 2020, 2021). While this preliminary gene regulatory network is informative, how individual subtypes (cnidocytes vs neuron vs secretory cells) are patterned is currently unknown. Utilizing a pool of previously identified genes thought to be neuronal we can begin to expand on this gene regulatory network and understand how cell types are patterned.

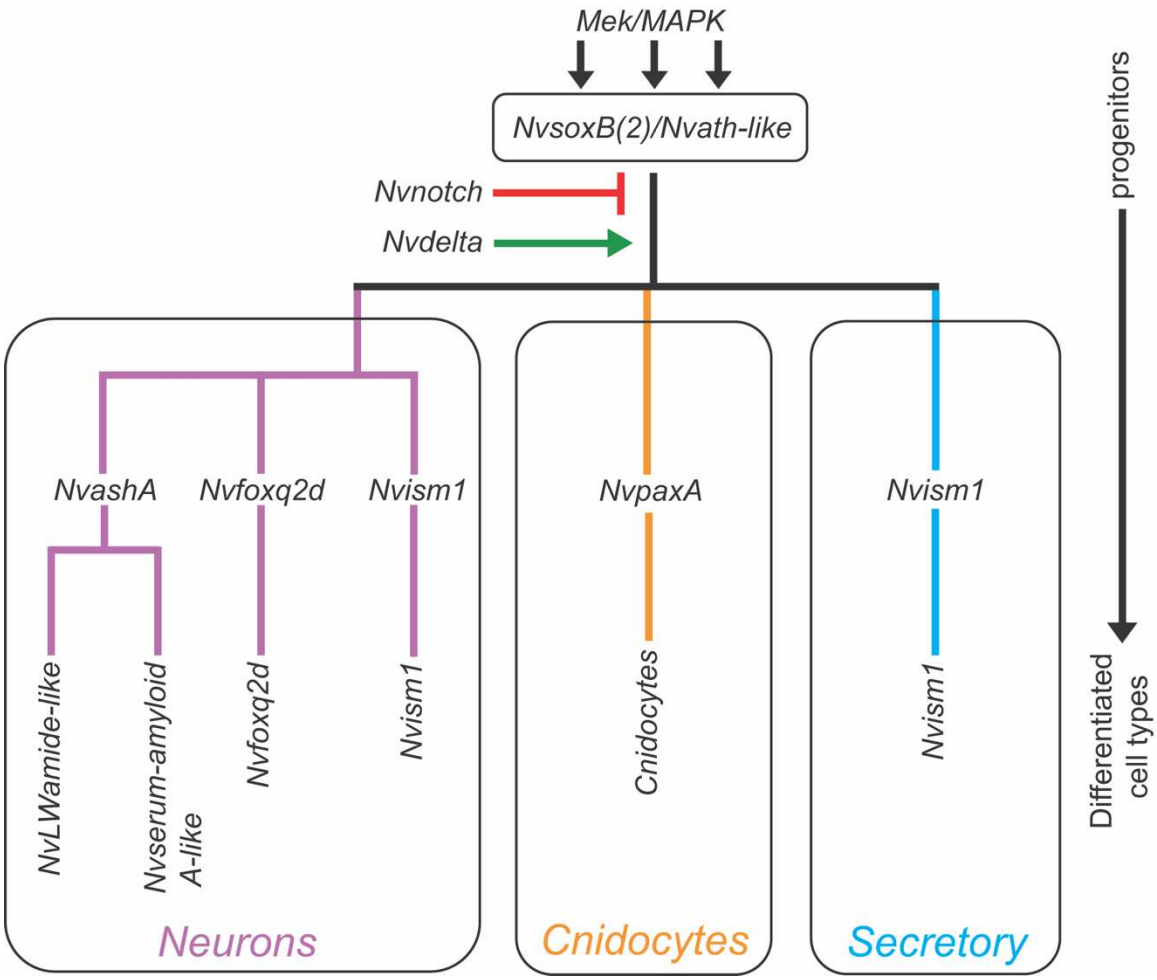

Figure 3.1 *Gene regulatory pathways for the three cell types downstream NvsoxB(2) and Nvath-like progenitors during development*: Expression of *NvsoxB(2)* and *Nvath-like* is initiated through Mek/MAPK signaling. *Nvnotch* signaling will maintain progenitor identity while low *Nvnotch/* high *Nvdelta* expression induces differentiation. Progenitors can then give rise to neurons (purple), cnidocytes (orange), or secretory cells (blue). As neuronal progenitors begin to differentiate they will the postmitotic marker *NvashA,*which will they give rise to multiple neuronal subtypes, or the unipotent progenitor marker *Nvfoxq2d,* which gives rise to *Nvfoxq2d* positive sensory neurons. Recent work also identified *Nvism1* positive neurons downstream *NvsoxB(2)/Nvath-like* + cells. As cnidocyte progenitors differentiate expression of *NvpaxA* will be initiated, which goes on to activate expression of the cnidocyte marker *Nvminicollagen3*. Lastly, recent work has found that *NvsoxB(2)/Nvath-like* positive cells also give rise to the secretory/gland cell marker *Nvism1*.

Previous work which aimed to identify the neurogenic role of the MAPK pathway used a microarray to identify genes that were affected by U0126, a MAPK inhibitor (Layden et al., 2016). This microarray revealed 19 potentially neural transcription factors whose gene expression becomes upregulated after the expression of *NvsoxB(2)* and *Nvath-like*

(Layden et al., 2016). Of these 19, one was found to be the broad cnidocyte regulator *NvpaxA* and the other was later characterized as the unipotent progenitor marker *Nvfoxq2d* (Layden et al., 2016; Babonis and Martindale, 2017; Busengdal and Rentzsch, 2017). It was also found that *NvashA* positively regulated two of the 17 potential neural markers, *NvemxLX* and *Nvvsx-like,* likely supporting neuronal function of these two genes (Layden et al., 2016). Here we aim to characterize whether the other 15 potential transcription factors are downstream the neural progenitor markers *Nvath-like* and *NvsoxB(2).* We identified that all genes except for *NvfoxD3-like, Nvvegf-like, Nvhox2, and Nvsox10* are downstream *NvsoxB(2)/Nvath-like*. We then individually knocked down *Nvath-like* or *NvsoxB(2)* and observed evidence of a population of *NvsoxB(2)* only progenitors. We then individually knocked down *NvfoxD3-like* to identify neurogenic regulation independent of the *NvsoxB(2)/Nvath-like* positive progenitors cells. We found that *NvfoxD3-like* seems to regulate cnidocyte patterning independent of *NvsoxB(2)/Nvath-like*. Taken together these data expand our current understanding of gene regulation and cell type patterning within *Nematostella*.

Materials and Methods

Animal Care and microinjection: Sexually mature *Nematostella* polyps were maintained in 11-12ppt artificial sea water (Instant Ocean), maintained at 17ºC, and fed as previously described (Havrilak et al., 2017b, 2021). One week before spawning polyps were fed oyster. To induce spawning polyps were placed at 25ºC and a light was turned on 12 hours before spawning occurred. Egg clutches were fertilized for 10 minutes, de-jellied in 4% L-cysteine, pH=7-8, and then rinsed with 11-12ppt artificial sea water three times

before microinjection as previously described (Havrilak et al., 2021). Microinjections were performed using a Nikon SMZ1270 scope and Narishige MO-2020U rig and embryos were then raised at 22C until the late gastrula stages, cleaned, and then placed into Tripure as previously described (SIGMA 93289) (Layden et al., 2016).

shRNA synthesis: shRNAs were synthesized as mentioned in He et al. 2018 (He et al., 2018). shRNAs were then stored at -80ºC in single injection aliquots. For all shRNAs where a single gene was targeted the shRNAs were injected at 1µg/µL concentrations. shRNA targeting *NvsoxB(2)* were used at a concentration of 2µg/µL and the control was then injected at the same concentration. For double knockdowns of *Nvath-like* and *NvsoxB(2)* sampled were injected with a mix that included 1µg/µL of *Nvath-like shRNA* and 2µg/µL of *NvsoxB(2)* totally 3µg/µL shRNA. The control shRNA for these double injections were then injected at 3µg/µL. The controls used were a previously published scramble shRNA (He et al., 2018). Gene knockdown was confirmed through qPCR analysis.

RNA isolation and qPCR analysis:

RNA isolation were performed as previously reported with some modifications to the protocols (Layden et al., 2012). cDNA was synthesized from 1µg of isolated RNA and was performed using the qScript CDNA SuperMix (QuantaBio 84034) according to manufactured protocols. qPCR analysis was performed using the Qiagen Rotorgene 3000 and PerfeCTa SYBR Green FastMix (Quanta bio 84071). ATP-Synthase was to normalize fold change between the experiment and the control samples. Control fold

change was calculated using one control replicate to normalize the data and then three other control replicates were used to calculate relative fold change ratios. Statistical significance between experimental and control sampled were performed by comparing fold change ratio values between experimental and control genes using a student t-test. Each qPCR consisted of four biological replicates.

Results

NvfoxD3-like, Nvvegf-like, Nvsox10-like, and *Nvhox2* are not regulated by *NvsoxB(2)* and *Nvath-like while Nvhd052* is inhibited

The neurogenic markers used for this study were previously identified as downstream the MEK/MAPK pathway, which regulates early neurogenesis in *Nematostella* (Layden et al., 2016). Due to the multiple roles MAPK plays during development in *Nematostella*, the characterization of these markers as downstream targets of *NvsoxB(2)/Nvath-like* needed to be confirmed (Layden et al., 2016; Amiel et al., 2017). To confirm downstream targets of *Nvath-like/NvsoxB(2)* we coinjected shRNAs targeting both *Nvath-like* and *NvsoxB(2)* (Figure 2.2) . Expression of *Nvsox2*, *Nvvsx-like, Nvgfi-like, Nvpea3-like, Nvtailless-like*, *Nvgcm*, *Nvhes-like3, Nvelav-like, Nvdkk-like3, Nvcoup-like1, Nvcoup-like2,* and *Nvhd145* all showed reduced expression when both neuronal progenitor markers were knocked down (Figure 2.2). *Nvhd052* was upregulated, and no significant change in expression was observed for *NvfoxD3-like, Nvhox2, Nvsox10,* and *Nvvegf-like* (Figure 2.2). This confirmed downstream targets for at least 14 of the 19 MAPK markers. Interestingly, previously reported single cell sequencing analysis identified *Nvvegf-*

within neurons while *NvfoxD3-like* was expressed within cnidocytes and neurons (Table 2.1).

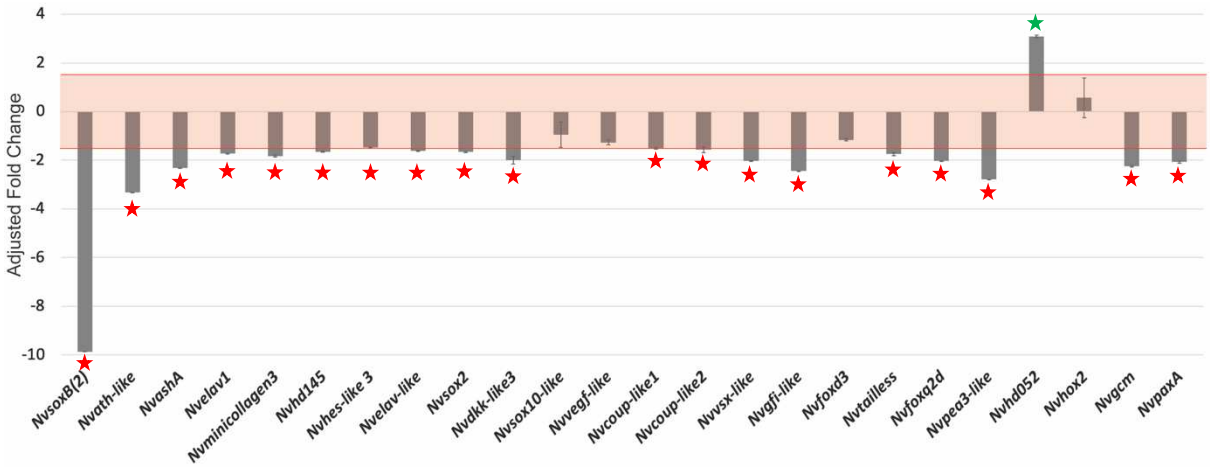

Figure 2.1: Knockdown of *NvsoxB(2)* and *Nvath-like* reveals 11 new downstream targets of *NvsoxB(2)* and *Nvath-like*. Adjusted fold change values of MAPK target genes were calculated using qPCR. Knockdown of both *NvsoxB(2)* and *Nvath-like* resulted in loss of expression for all genes except *Nvhd052,* which was upregulated, and *Nvsox10-like, Nvvegf-like, NvfoxD3-likeNvfoxD3-like, Nvhox2* which were downregulates. Known neuronal markers *NvashA, Nvelav, Nvminicollagen3, Nvfoxq2d,* and *NvpaxA* were used as known positive control targets of both *NvsoxB(2)* and *Nvath-like* and showed loss of expression in the knockdowns. Red stars indicate significant ($p<0.05$) downregulation of target genes while green stars indicate significant upregulation of targets markers. The highlighted box demarcates values between 1.5 and -1.5 adjusted fold change which marks no change in expression. Error bars were calculated using standard error and significance was calculated using a student t-test.

	JGI Number	Cnidocytes (Adult)	Neurons (Adult)	Gland/Secretory (Adult)	Muscle Gastroderm (Adult)	Larval cells (planula)
Nvhd145	8907			C1,C2,C3		C35
Nvhes-like 3	242118					
Nvelav-like	214798	C2	C32-C34		C2,C26	C25,C28,C26
Nvsox2	239130	C8				C20
Nvdkk-like3	247589					
Nvsox10-like	120772					
Nvvegf-like	247798		C35			C25-C26
nvcoup-like1	165424	C5, C8		C20		C20
Nvcoup-like2	203423					
Nvvsx-like	43460		C8,C37	C17		C25, C37
Nvgfi-like	182742		C13			
Nvfoxd3	39632	C8	C6,C7			C20,C22
Nvtailless	132075		C1,C4-C7			C22
Nvfoxq2d	96685			C22		C38
Nvpea3-like	211452/16815		C37	C17,C20	C26	C28,C37
Nvhd052	92785					
Nvhox2	91593					
Nvgcm	157036					
NvpaxA	243681	C5				C20, C34

Table 2.1. Identification of MAPK targets within the Sebé-Pédros et al. single cell sequencing data set. Single cell transcriptomics identified some of these MAPK markers, classified here by their name and the genome identification number (jgi number), within different adult cell types and within planula larvae. Each cell indicates the cluster number these genes were identified within for each cell type class (cnidocytes, neurons, gland/secretory, muscle gastroderm, and larval cells).

NvsoxB(2) and *Nvath-like* regulate unique populations of downstream MAPK targets

We then wanted to confirm that *Nath-like* and *NvsoxB(2)* actually coregulate all downstream cell types. *Nematostella* possess *NvsoxB(2)* and *Nvath-like* positive multipotent neural progenitor population that regulates all neuronal differentiation markers known to date (Richards and Rentzsch, 2014, 2015). Recent work identified a unipotent progenitor population downstream *NvsoxB(2)*/*Nvath-like* progenitors*, Nvfoxq2d,* which differentiates into ectodermal sensory neurons (Busengdal and Rentzsch, 2017). This recently identified progenitor population could imply that *Nematostella*, like bilaterians, segregate progenitors during development to pattern unique neuronal subtypes. Co-expression assays of *NvsoxB(2)* and *Nvath-like* suggest the existence of three distinct progenitor populations early during neurogenesis: *NvsoxB(2)* only cells, *Nvath-like* only cells, and cells which express both *NvsoxB(2) and Nvath-like* (Richards and Rentzsch, 2015). This could indicate that multipotent neural progenitors diverge early during development to regulate unique subsets of differentiated cell types. We hypothesized that if progenitors segregate early during specific cell type differentiation then a unique subset of these makers should be lost when *Nvath-like* or *NvsoxB(2)* expression is reduced. To test this hypothesis knockdowns were performed using shRNAs which targeted either *Nvath-like* or *NvsoxB(2)* and gene expression was quantified at the late gastrula stage.

shRNA mediated knockdown of *NvsoxB(2)* alone resulted in a loss of *Nvsox2, Nvcoup-like1, Nvvsx-like, Nvgfi-like, Nvtailless-like, Nvpea3-like, and Nvgcm* expression ($p<0.05$,

Figure 2.3). Loss of *Nvath-like* resulted in significant loss of *Nvgfi-like, Nvfoxq2d,* and *Nvhox2* ($p<0.05$, Figure 2.4). While not significant, previous work has traditionally defined an adjusted fold change value above 1.5 or lower than -1.5 as markers for a significant change in gene expression (Layden et al., 2012; Richards and Rentzsch, 2015). Utilizing this method to identify "significance", *Nvath-like* knockdown also resulted in loss of expression of *NvsoxB(2), Nvsox2, Nvvegf-like, Nvvsx-like,* and upregulation of *Nvhd052* (Figure 2.4). The knockdown of *NvsoxB(2)* associated with loss of *Nvath-like* expression indicates a role for *Nvath-like* in maintaining *NvsoxB(2)* expression. This would suggest that we cannot separate *Nvath-like* progenitors from *NvsoxB(2)/Nvath-like* progenitors within this study. However, these data still allow for the characterization of *NvsoxB(2)* and *NvsoxB(2)/Nvath-like* progenitor populations.

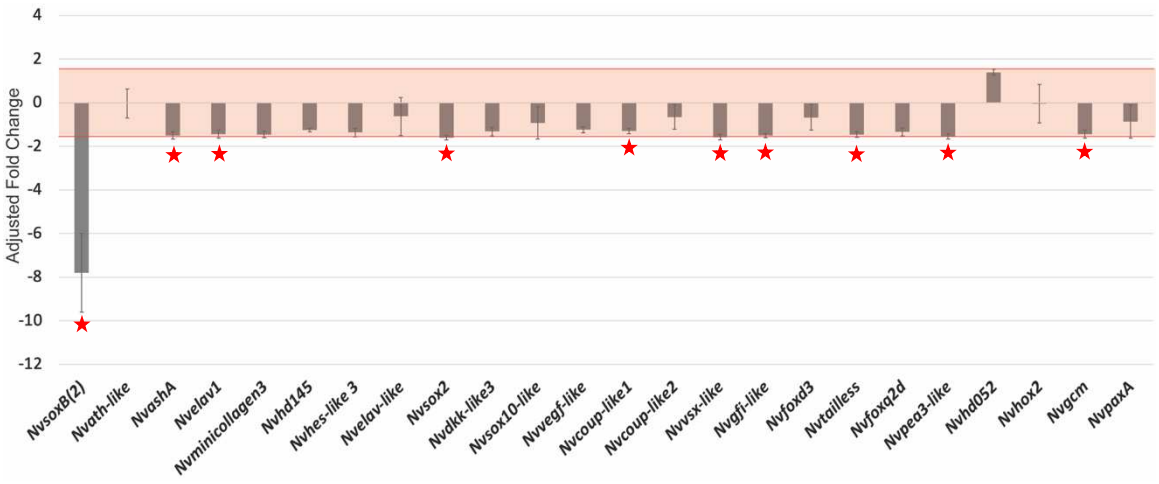

Figure 2.3: Knockdown of *NvsoxB(2)* alone results in loss of a unique subset of MAPK markers. Adjusted fold change values of MAPK target genes were calculated using qPCR. Knockdown of *NvsoxB(2)* resulted in loss of expression *Nvsox2, Nvcoup-like1, Nvvsx-like, Nvgfi-like, Nvtailless, Nvpea3-like,* and *Nvgcm.* Known neuronal markers *NvashA* and *Nvelav* showed loss of expression however *Nvminicollagen3, Nvfoxq2d,* and *NvpaxA* remained unchanged despite all being positive control targets for *NvsoxB(2).* Red stars indicate significant ($p<0.05$) downregulation of target genes while green stars indicate significant upregulation of targets markers. The highlighted box demarcates values between 1.5 and -1.5 adjusted fold change which marks no change in expression. Error bars were calculated using standard error and significance was calculated using a student t-test.

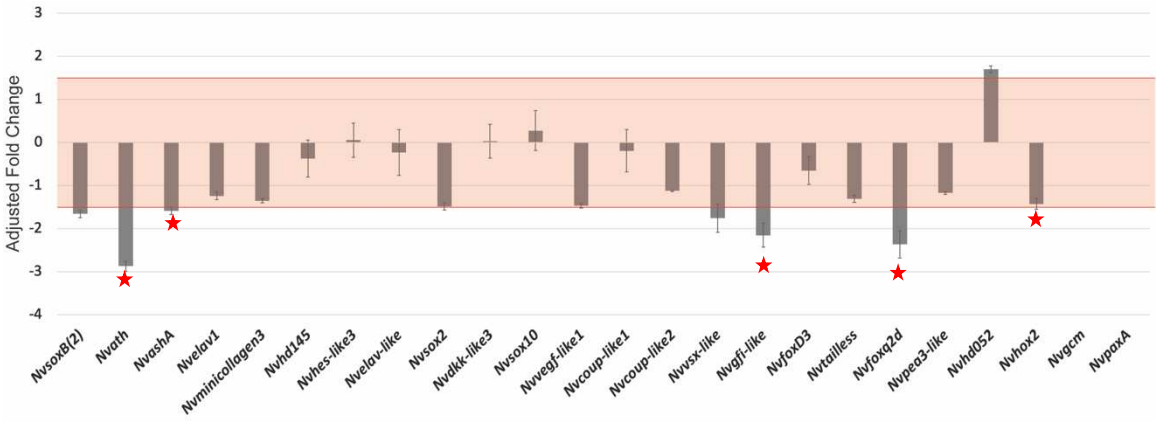

Figure 2.4: Loss of *Nvath-like* results in loss of some but not all target genes. Adjusted fold change values of MAPK target genes were calculated using qPCR. Knockdown of *Nvath-like* resulted in loss of expression *Nvgfi and Nvhox2.* Knockdown also resulted in statistically nonsignificant loss of expression of *Nvsox2, Nvvegf-like, Nvvsx-like* and statistically nonsignificant upregulation of *Nvhd052.* Known neuronal markers *NvashA* and *Nvfoxq2d* showed loss of expression however *Nvelav1, Nvminicollagen3,* and *NvpaxA* remained unchanged despite all being known positive control targets for *Nvath-like.* Red stars indicate significant ($p<0.05$) downregulation of target genes while green stars indicate significant upregulation of targets markers. The highlighted box demarcates values between 1.5 and -1.5 adjusted fold change which marks no change in expression. Error bars were calculated using standard error and significance was calculated using a student t-test.

NvfoxD3-like regulates cnidocyte patterning independently of *NvsoxB(2)/Nvath-like* progenitors

Knockdown of *NvsoxB(2)* and *Nvath-like* does not alter *NvfoxD3-like* expression however previous data supports a possible neuronal or cnidocyte regulatory role for *NvfoxD3-like.* Previous work found expression of *NvfoxD3-like* occurred early during development, is broadly expressed, and has been characterized within both cnidocytes and neurons (Table 1.1) (Layden et al., 2016; Sebé-Pedrós et al., 2018). This led us to hypothesize that *NvfoxD3-like* cells consists of a *NvsoxB(2)/Nvath-like* independent lineage of neuronal or cnidocyte cell type. To test this, we created shRNAs for *NvfoxD3-like* and tested the effect of their knockdown on previously published neurogenic markers, cnidocyte markers, and those markers characterized in this study. Knockdown of *NvfoxD3-like* resulted in no statistically significant change in gene expression (Figure 2.5). Utilizing an

adjusted fold change of +/-1.5 as a biologically significant change in expression, we found that loss of *NvfoxD3-like* expression resulted in knockdown of the cnidocyte markers *NvpaxA* and *Nvminicollagen3* (Figure 2.6). Knockdown of *Nvfoxd* also resulted in increased expression of *Nvsox10-like, Nvhd052,* and *Nvhox2* (Figure 2.5). The loss of *NvpaxA* expression when *NvfoxD3-like* expression was lost supports the hypothesis that *NvfoxD3-like* regulates cnidocytes independent of both *NvsoxB(2)* and *Nvath-like* expression.

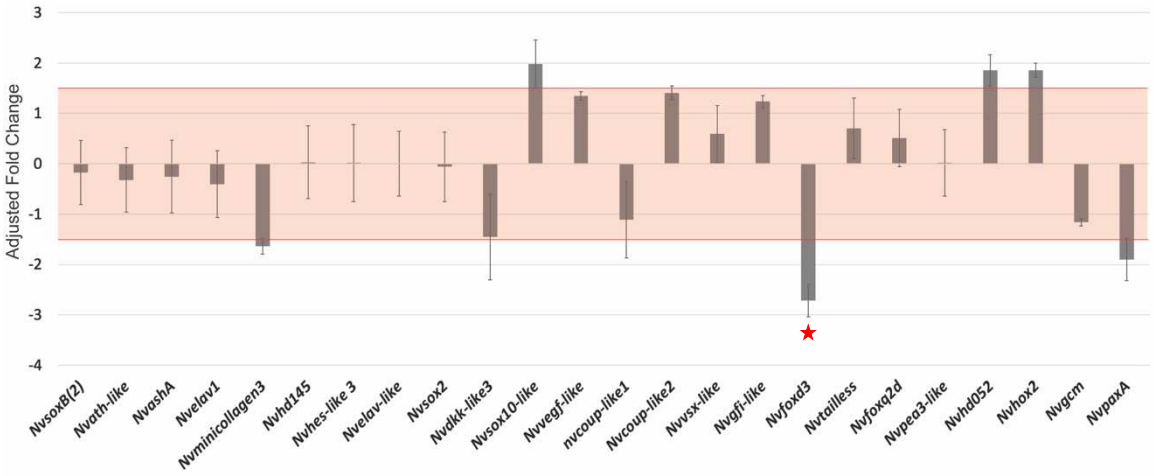

Figure 2.5: Knockdown of *NvfoxD3-like* reveals a positive regulatory role on cnidocytes with possible inhibition of several other targets. Adjusted fold change values of MAPK target genes were calculated using qPCR. Knockdown of *NvfoxD3-like* resulted statistically significant in loss in expression for just *NvfoxD3-like*. Statistically nonsignificant knockdown of *Nvminicollagen3,NvpaxA,* and *Nvdkk-like3* were observed. Statistically nonsignificant upregulation was also observed of *Nvsox10-like, Nvhd052,* and *Nvhox2* when *NvfoxD3-like* expression was lost. Red stars indicate significant ($p<0.05$) downregulation of target genes while green stars indicate significant upregulation of targets markers. The highlighted box demarcates values between 1.5 and -1.5 adjusted fold change which marks no change in expression. Error bars were calculated using standard error and significance was calculated using a student t-test.

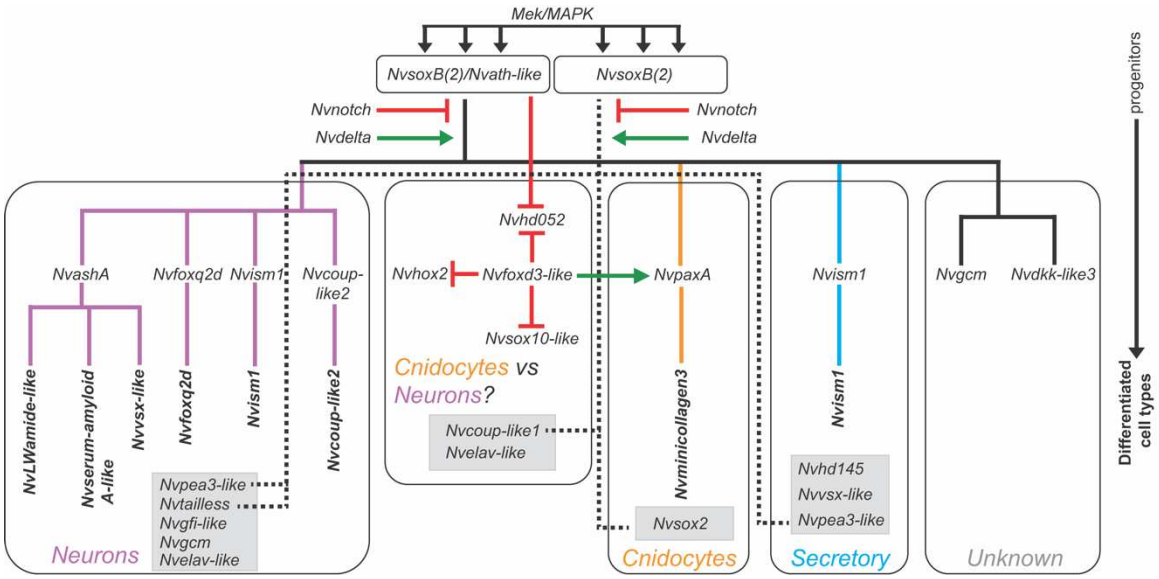

Figure 2.6: Model of gastrula neuronal, cnidocyte, and secretory differentiation within *Nematostella*. Boxes indicate different patterning mechanisms for neuronal, cnidocyte, and secretory cell types.

Discussion

Identification of a *NvsoxB(2)* only progenitor population and the redundant role of *Nvath-like* expression during early development

Here we expand on the gene regulatory network necessary for cnidocyte and neuronal development within late gastrula *Nematostella* (Figure 2.6). We confirm at least 15 downstream targets of *NvsoxB(2)* and *Nvath-like* progenitors. We show that *NvsoxB(2)* and *NvsoxB(2)/Nvath-like* progenitor populations regulate different downstream markers despite traditionally thought to coregulate all downstream targets (Richards and Rentzsch, 2015). We find that *NvsoxB(2)* is specifically necessary for expression of *Nvsox2, Nvcoup-like1, Nvtailless-like,* and *Nvpea3-like*. This does not consist of one specific cell type and all these genes have been identified in cnidocytes, neurons, or secretory cells (Table 1.1) (Richards and Rentzsch, 2015; Sebé-Pedrós et al., 2018; Tournière et al., 2021). This then supports a scenario where expression of *Nvath-like* is capable of regulating all other targets downstream *NvsoxB(2)/Nvath-like* except *Nvvsx-*

like, Nvgfi-like, and *NvashA* during late gastrulation. Previous work has shown that morpholino induced loss of *NvashA* reduced expression of *Nvvsx-like* which could suggest that loss of *Nvvsx-like* expression is due to loss of *NvashA* (Layden et al., 2016). The redundant function of *Nvath-like* then ensures development of multiple cells types if *NvsoxB(2)* expression is temporarily reduced. This redundancy is not a novelty within *Nematostella* and has been characterized within bilaterian nervous system development (Vallstedt et al., 2001; Cau and Wilson, 2003; Madelaine et al., 2011). It should be noted while *Nvsoxb(2)* knockdown was observed at gastrula stages, morpholino induced knockdown of *NvsoxB(2)* was found to be a more effective knockdown target genes when tested during later larval stages (Richards and Rentzsch, 2015). It has also been observed that loss of *NvsoxB(2)* at the planula stage results in loss of *Nvath-like* expression (Richards and Rentzsch, 2015). This could suggest initial *Nvath-like* expression, and potential to rescue loss of *NvsoxB(2),* is restricted to early stages of development.

The identification of these progenitor population and the hypothesis of this redundancy relies heavily on the qPCR analyses performed here. To date no detailed characterization of *Nvath-like* has been performed, at least to the same extent as the other progenitor marker *NvsoxB(2)* (Richards and Rentzsch, 2015, 2015). The creation of a transgenic line for *Nvath-like,* which could then be crossed into the NvsoxB(2):mOrange transgenic line, would allow for *in situ* characterization within developing embryos. This Nvath-like transgenic would then allow for characterization of their early differentiated cell types, within cells that maintain the fluorescence before it's degradation. Lastly, utilization of single cell sequencing to compare cells types which express and then develop from *NvsoxB(2)* and/or *Nvath-like* expressing cells would be instrumental in

understanding, at least at the transcriptional level, any differences between these two genes. However, the data collected here still suggests a redundant role for *Nvath-like* and the existence of two progenitor populations; *NvsoxB(2)* only progenitors and *NvsoxB(2)/Nath-like* progenitors.

NvfoxD3-like **expression is necessary for cnidocyte differentiation independent of** ***NvsoxB(2)*** **and** ***Nvath-like*** **expression**

Knockdown of *NvfoxD3-like* results in loss of cnidocyte expression and increased expression of *Nvsox10-like*, *Nvhd052*, and *Nvhox2* (Figure 2.5). Interestingly, none of these upregulated genes were found within the single cell sequencing analysis within adults or larval planula (Table2.1) (Sebé-Pedrós et al., 2018). However, expression of *NvfoxD3-like* was found within both cnidocytes and neurons, is expressed fairly early during development, and shares a similar expression pattern to *NvsoxB(2)* and *Nvath-like* (Table 2.1) (Layden et al., 2016; Sebé-Pedrós et al., 2018). Work within bilaterians has shown that vertebrate FoxD3 suppresses neuronal differentiation while promoting neural crest-like cell differentiation (Dottori et al.). Bilaterian Foxd3 has also been shown to regulate broader progenitors during early neural crest development and then function later to differentiate specific neural crest markers (Lister et al., 2006). It should be emphasized, that neural crest cells have not been identified outside of vertebrate lineages and is thought to have evolved within vertebrates. However, the function of Foxd3 in the inhibition of one cell type and the positive regulation of another could be and ancestral role and might be maintained within cnidarians. With these data taken into account we hypothesize that early during development *NvfoxD3-like* expression is involved in

promoting early cnidocyte differentiation by inducing expression of *NvpaxA*. *NvfoxD3-like* expression within cnidocytes could support the idea that *NvfoxD3-like* represses early neurogenesis, however the markers which are inhibited have not been implicated in neurogenesis at all within *Nematostella*. Further characterization of the roles of *Nvhox2* and *Nvsox10-like* could be instrumental in understanding what cell types are being inhibited during early development. Another possibility is that *NvfoxD3-like* also regulates or demarcates a subset of neurons within adult polyps, this is likely the case do to its expression within adult neurons (Table 2.1) (Sebé-Pedrós et al., 2018). It is obvious that further characterization of *NvfoxD3-like* is necessary to confirm the decision-making mechanism hypothesized here. However, these data suggest a role in cnidocyte development which was previously unknown.

Downstream targets of *NvsoxB(2)/Nvath-like* and a preliminary gene regulatory network

Here we identified 13 novel downstream targets of *NvsoxB(2)* and *Nvath-like* utilizing a pool of potential markers previously identified to be expressed within *Nematostella* gastrula stages (Layden et al., 2016). It was hypothesized that based on the expression patterns of these markers that these markers likely consist of broad neuronal regulators or individual neuronal subtypes. We were not able to determine what cell types these 13 markers regulate within this study but single cell analysis suggest that these markers likely make up multiple secretory, neuronal, and cnidocyte cell types (Table 2.1) (Sebé-Pedrós et al., 2018). However, this single cell analysis was performed in adult polyps and the study performed here only consists of late gastrula embryos so discrepancies within

the two datasets are likely to occur. The research performed here did not include a marker for secretory cells, recent work has identified that *Nvism1* is a neuronal marker and a secretory marker (Tournière et al., 2021). However, it would not be possible to separate differences in neuronal and the secretory *Nvism1* expression utilizing qPCR at the gastrula stage tested here. Future studies should include the secretory marker *Nvmucin* within qPCR analyses. *Nvmucin* has been found to be downstream *NvsoxB(2)* and is expressed broadly within late gastrula stages, when this analysis was performed (Steinmetz et al., 2017; Tournière et al., 2021). Despite the flaws within this study we built a preliminary gene regulatory network for cell types downstream *NvsoxB(2)* and *Nvath-like* (Figure 2.9). We expanded the number of known downstream targets and identified a cnidocyte regulatory pathway for *NvfoxD3-like* expression (Figure 2.6). Further characterization of these 13 markers and the effects each gene has on the others is important to build a more informed gene regulatory network for late gastrula embryos. As this gene regulatory expands we should be able to identify the mechanisms necessary for cell type specification (cnidocyte vs neuron vs secretory cell) and for downstream subtype specification.

.

Chapter 3: *Nematostella vectensis* nerve net patterning indicates an ancestral neurogenic role for axial patterning genes during early neurogenesis

Abstract

Spatial patterning along the anterior-posterior axis of the bilaterian brain patterns neuronal subtypes and is thought to be highly conserved. The conserved expression profile of these spatial genes is then used to homologize the brains of extremely divergent animal models. However, this work presumes that the neurogenic regulatory function of axial patterning genes is unique to the bilaterian brain. Here we characterize the role of axial patterning mechanisms, including the aboral marker *Nvsix3/6*, in patterning neuronal subtype expression along the oral-aboral axis. We find that knockdown or misexpression of *Nvsix3/6* results in loss and expansion, respectively, of aborally restricted neuronal subtypes. While graded Wnt activity along the oral-aboral axis patterns the trunk neuronal marker *Nvpea3-like* and inhibits aboral neuronal subtype patterning. We hypothesize a model where *Nvsix3/6* and graded Wnt function together to pattern domain restricted neuronal subtypes. We propose the idea that axial patterning genes were used within the cnidarian-bilaterian ancestor to pattern the ancestral nerve net and that this mechanism is not necessary for the evolution of bilaterian brains.

Introduction

Centralization of the nervous system is a conserved trait among the bilaterians (e.g. mice, frogs, insects) and the evolution of this trait has been hypothesized to have occurred once during bilaterian evolution. Early work within traditional bilaterian models (e.g. mice, xenopus, chicks, and drosophila) identified a conserved function for bone morphogenic protein (BMP) in establishing the dorsal-ventral axis and in the inhibition of neurogenic tissue. Neurogenic ectoderm is initiated within the opposite end

of BMP expression, which occurs ventrally within protostomes (ex. insects and worms) and within the dorsal tissue in deuterostomes (ex. vertebrates). Along the D-V nerve cord BMP then establishes a morphogen gradient from which spatial domain genes arise which go on to pattern specific neuronal subtypes. A similar patterning mechanism has been identified within the developing brain of bilaterians as well. With a gradient of Wnt activity along the posterior (high Wnt) to anterior (low Wnt) axis patterning known spatial domain markers, which go on to pattern specific neuronal subtypes along this AP axis of the brain (Holland et al., 2013). These A-P patterning genes have been identified within multiple bilaterians and their expression within the brain appears to be highly conserved across multiple bilaterians (Steinmetz et al., 2010; Holland et al., 2013; Cheatle Jarvela et al., 2016; Darras et al., 2018; McClay et al., 2018). Do to these two highly conserved patterning mechanisms along the A-P and D-V axis, it is often used to support the single origin hypothesis for the central nervous systems (Holland et al., 2013). Recent work however, has started to challenge just how conserved these mechanisms are within bilaterian and ultimately challenges support for a single origin of the central nervous system.

Recent research within non-traditional models questions previous assumptions about the conservation of DV and AP neurogenic patterning mechanisms. Work within the spiralian,*Capitella teleta* observed that endogenous BMP did not inhibit formation of the brain or the ventral nerve cord (Webster et al., 2021). A lack of response to BMP was also identified within the hemichordate, *Saccoglossus kowalevskii*, which does not possess a centralized nervous system (Lowe et al., 2006). Characterization of the conserved spatial markers of the DV nerve cord within rotifers, did not observe the

staggered expression typical of these genes within the rotifer trunk nerve cord (Martín-Durán et al., 2018). Lastly, manipulation of BMP within the xenocoelomorphs, sister taxa to the rest of the bilaterians, did not affect nervous system development (Martín-Durán et al., 2018). These data argue that nerve cords and the utilization of BMP to pattern the nervous system along the DV axis likely convergently evolved (Martín-Durán et al., 2018; Martín-Durán and Hejnol, 2021). However, less work has gone into confirming the neurogenic role of conserved spatial genes along the A-P axis and these genes expression profiles are still used as support for the single evolution of centralized nervous systems within bilaterians and used to homologize bilaterian brains. Identification of a neurogenic function for AP patterning genes within an outgroup to bilaterians would suggest that a neurogenic function occurred before the bilaterians diverged and that it is not a trait unique to the bilaterian brain.

Cnidarians are the sister taxa to bilaterians and utilize similar AP patterning mechanisms to pattern their oral-aboral axis. Research within the cnidarian, *Nematostella vectenesis,* suggests that axial programs once thought to be unique to bilaterians were present in the cnidarian-bilaterian ancestor (Marlow et al., 2013; Sinigaglia et al., 2013; Leclère et al., 2016). Along the oral-aboral axis, graded Wnt activity establishes distinct molecular domains, many of which express homologs in the same relative order in which they are observed in bilaterian centralized nervous systems (Marlow et al., 2013). Lastly, expression of neuronal subtype markers along the oral-aboral axis suggests that neuronal subtypes arise within these distinct molecular domains (Layden et al., 2012; Busengdal and Rentzsch, 2017). Despite what appears to be similarities in neuronal patterning

mechanisms with bilaterians, cnidarians do not possess a centralized nervous system. The cnidarian nervous system consists of nerve nets comprised of neurons with soma distributed in a scattered pattern intermixed with other differentiated cell types (Marlow et al., 2009; Nakanishi et al., 2012). These observations suggest that some or all of the bilaterian central nervous system AP patterning programs existed in the cnidarian-bilaterian ancestor, and that further investigation into neuronal patterning programs in *Nematostella* and other cnidarians could shed light on the origin and evolution of CNS patterning programs and provide further insight about the homology or lack thereof of bilaterian central nervous systems.

To gain insights about whether conserved A-P neuronal patterning programs were present in the cnidarian-bilaterian common ancestor we investigated these molecular mechanisms in *Nematostella.* In this article we determine that neuronal subtypes are not restricted to distinct molecular domains but appear to be restricted to the domains of specific axial markers. Pharmacological manipulation of Wnt activity results in subsequent shifts in axial domain genes and neuronal subtypes, supporting the hypothesis that axial patterning patterns neuronal subtypes. We then found that shRNA mediated knockdown of the four axial markers researched (*Nvsp6/9, Nvwnt2, Nvdlx* and *Nvsix3/6*) only the aboral marker *Nvsix3/6* displayed a neurogenic role. We then attempted to differentiate the Wnt inhibitory role of *Nvsix3/6* from the neurogenic role identified here. We combined the molecular manipulation of *Nvsix3/6* and pharmacological manipulation of Wnt activity to further characterize the axial mechanisms patterning neurogenesis. This data suggests that *Nvsix3/6* positively regulates neuronal subtypes within this *Nvsix3/6* domain while Wnt activity inhibits expression of these aboral neuronal markers

in favor of trunk neuronal markers. Lastly, we show evidence suggesting that Wnt patterns the aborally restricted endodermal marker *NvotxC,* which could suggest that *NvotxC* might follow the same regulatory logic as *Nvsix3/6*. Together these data support a neurogenic function for the spatial marker *Nvsix3/6* and that axial markers had neurogenic role before bilaterians diverged from the cnidarians. The evolutionary implications of this data brings into question the ability to use spatial genes along the AP axis of bilaterians to argue the single origin of the central nervous system.

Methods

Animal Care, microinjection, and fixation

Sexually mature *Nematostella* polyps were raised in 11-12ppt artificial sea water (Instant Ocean), maintained at 17˚C, and fed as previously described (Havrilak et al., 2017) One week before spawning polyps were fed oyster. To induce spawning polyps were placed at 25˚C and a light was turned on 12 hours before spawning occurred. Egg clutches were fertilized for 10 minutes, dejellied in 4% L-cysteine pH=7-8, and then rinsed with 11-12ppt artificial sea water three times before treatments, as previously described (Havrilak et al., 2017). Microinjections were performed using Nikon SMZ1270 scope and Narishige MO-2020U rig. Embryos that were not treated with a pharmacological drug were then raised at 22˚C for 24hpf (late gastrula), cleaned, and then prepped for fixation (Havrilak et al., 2017). Embryos treated with a pharmacological agent were raised at 17C for 48hpf (late gastrula), unless explicitly stated to be different, until fixation, and then prepped for fixation (Havrilak et al., 2017). Embryos were fixed as described in Havrilak et al. 2017 and then stored at -20C in methanol.

shRNA, mRNA and Pharmacological treatments

shRNAs were synthesized as mentioned in He et al. 2019 (He et al., 2018). They were then stored at -80 in single injection aliquots. A previously published scramble shRNA was used as the control for all shRNA injections (He et al., 2018). Gene knockdown was confirmed through *in situ* hybridization and/or qPCR. *Nvsix3/6:venus* mRNA using previously published methods (Layden et al., 2013). Embryos were maintained at 17˚C until early gastrulation (~24hpf), once observed gastrulation was observed, embryos were then treated with azakenepaullone (sigma A3734) or iCRT14 in 1/3X (Sigma SML0203) until the last gastrula/early planula stage (~48hpf). Control embryos were treated with DMSO. Embryos were then washed with fresh *Nematostella* media prior to fixation.

In situ hybridization, imaging, and domain quantifications

In situ hybridization was performed using previously published methods (Havrilak et al., 2017b). DIC images of *Nematostella* embryos were taken on a Nikon NTi with a Nikon DS-Ri2 color camera using the Nikon Elements software. To quantify domain size animals were imaged so that the pharyngeal ectoderm was visible and centered within lateral images. Images were then uploaded to Fiji where domain size was measured using the segmented line tool (Schindelin et al., 2012). The first point of the segmented line tool was positioned at the most endodermal location of the pharyngeal ectoderm. The first measurement was then taken from the pharyngeal ectoderm to the most oral location of gene expression, following the curve oft he embryo, and the length of this line was recorded. The second measurement was then taken from the pharyngeal ectoderm to the

location where the apical tuft will develop. This second measurement determined the total size of the embryo. The last measurement was taken from this apical tuft region to the most aboral expression domain for our gene of interest. We then used these three measurements to determine the start of and aboral end of the expression domains. We divided the first domain measurement , pharyngeal ectoderm to oral most region of gene expression, and divided that by the total size of embryo multiplied by 100. This results in a value that demarcates the start of domain expression on a 0-100 scale. We then repeated this method for the third measurement, apical organ to aboral end of expression, and subtracted this number by 100 to get value which demarcates the end of the expression domain.

Results

Neuronal subtypes appear to be restricted to axial domains

The expression boundaries of axial domain markers and neuronal subtypes were quantified to determine the correlation between axial domains and neuronal subtype position in gastrula stage embryos. Positional information was normalized to percent embryo length with the tip of pharyngeal ectoderm assigned zero and the aboral pole assigned one hundred (Figure 3.2A). Axial domains were grouped into three main categories oral (*Nvslouch-like*), trunk (*Nvwnt2, Nvsp6/9,* and *Nvdlx)*, and aboral (*Nvsix3/6),* (Figure 3.1, Figure 3.2). The expression domains of the neuronal subtype markers fell into three distinct categories aboral (*Nvfoxq2d* and *Nv239910*), aboral and trunk *(NvLWamide*), and trunk (*Nvpea3-like)* (Figure 3.1, Figure 3.2). We then quantified the expression domains and mapped them onto a molecular domain map (Figure 3.2).

Nvfoxq2d and *Nv239910* were both restricted to the *Nvsix3/6* aboral domain but only *Nv239910's* expression boundary coincided with the oral most boundary of *Nvsix3/6* (Figure 3.2C). The expression boundaries for *Nvfoxq2d* ended within the aboral domain and did not correspond to any identified molecular domain boundary. *NvLWamide-like* expression spanned multiple aboral and trunk domains terminating before the expression domain of *Nvslouch-like* (Figure 3.2C). Lastly, *Nvpea3-like* was primarily restricted to the *Nvwnt2* positive domains trunk but was also expression within the *Nvdlx Nvsix3/6*+ aboral domain (Figure 3.2C). *Nvpea3-like* expression also terminated in the middle of the *Nvwnt2/Nvsp6/9/Nvslouch-like* domain (Figure 3.2). These data suggest that axial domain genes, like *Nvsix3/6* and *Nvwnt2*, may contribute to regulating neuronal subtype patterning. However, the fact that some neuronal subtype expression ended within a domain rather than at domain boundaries suggests that either our catalog of molecular domains is incomplete, or that additional factors contribute to neuronal subtype patterning.

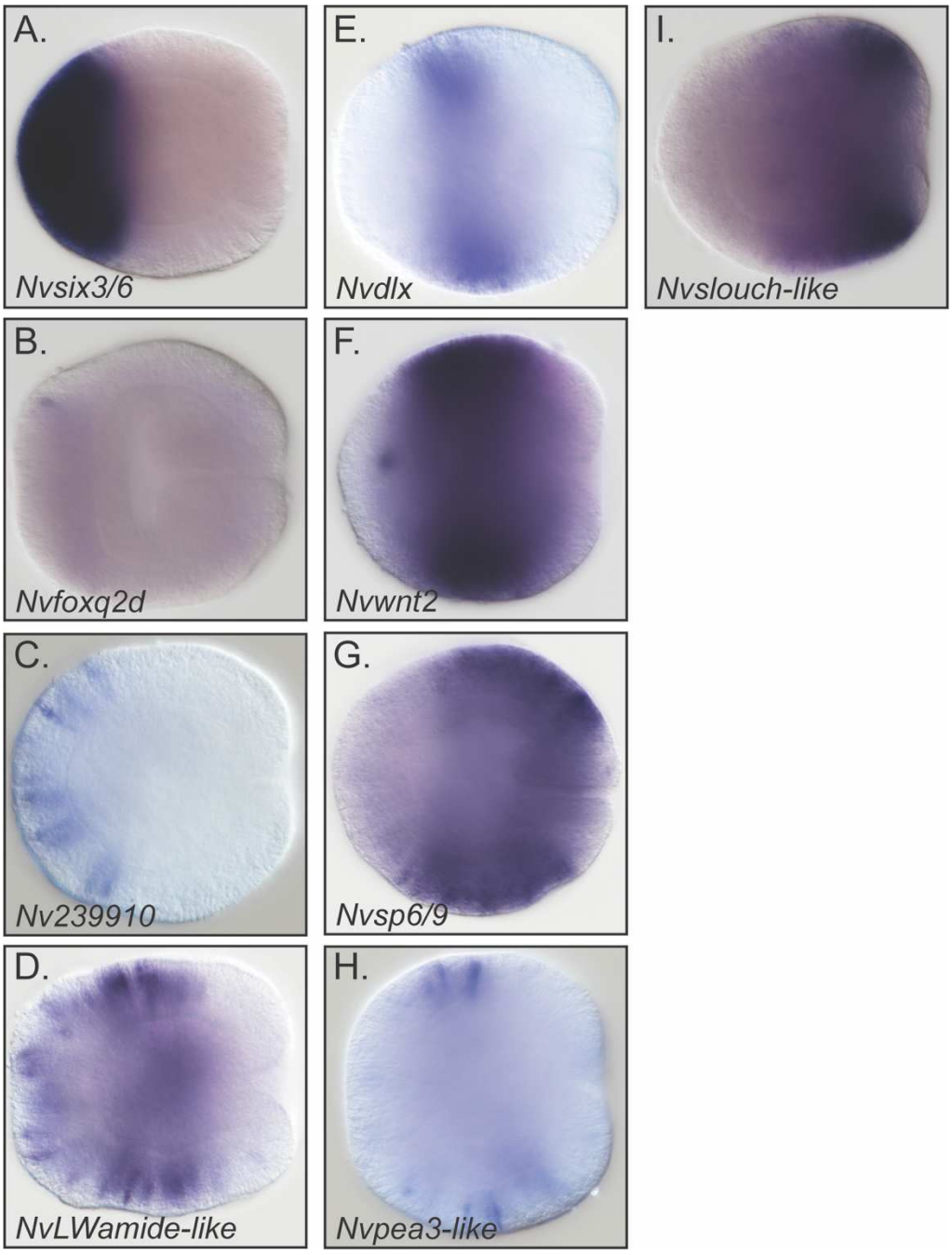

Figure 3.1: Expression of markers used to create the molecular domain map along the oral-aboral axis, and the neuronal markers used to determine molecular restriction. The aboral marker *Nvsix3/*6 (A), the trunk markers *Nvdlx* (E)/*Nvwnt2* (F)/*Nvsp6/*9 (G), and the oral marker *Nvslouch-like* (I) were used to determine molecular domains along the oral-aboral axis. Previously published neuronal marker *Nvfoxq2d* (B), *Nvserum amyloidA-like* (C), *NvLWamide-like* (D), and *Nvpea3-like* (H) were used to identify the domains neuronal subtypes are restricted to. Lateral with oral pole to the left.

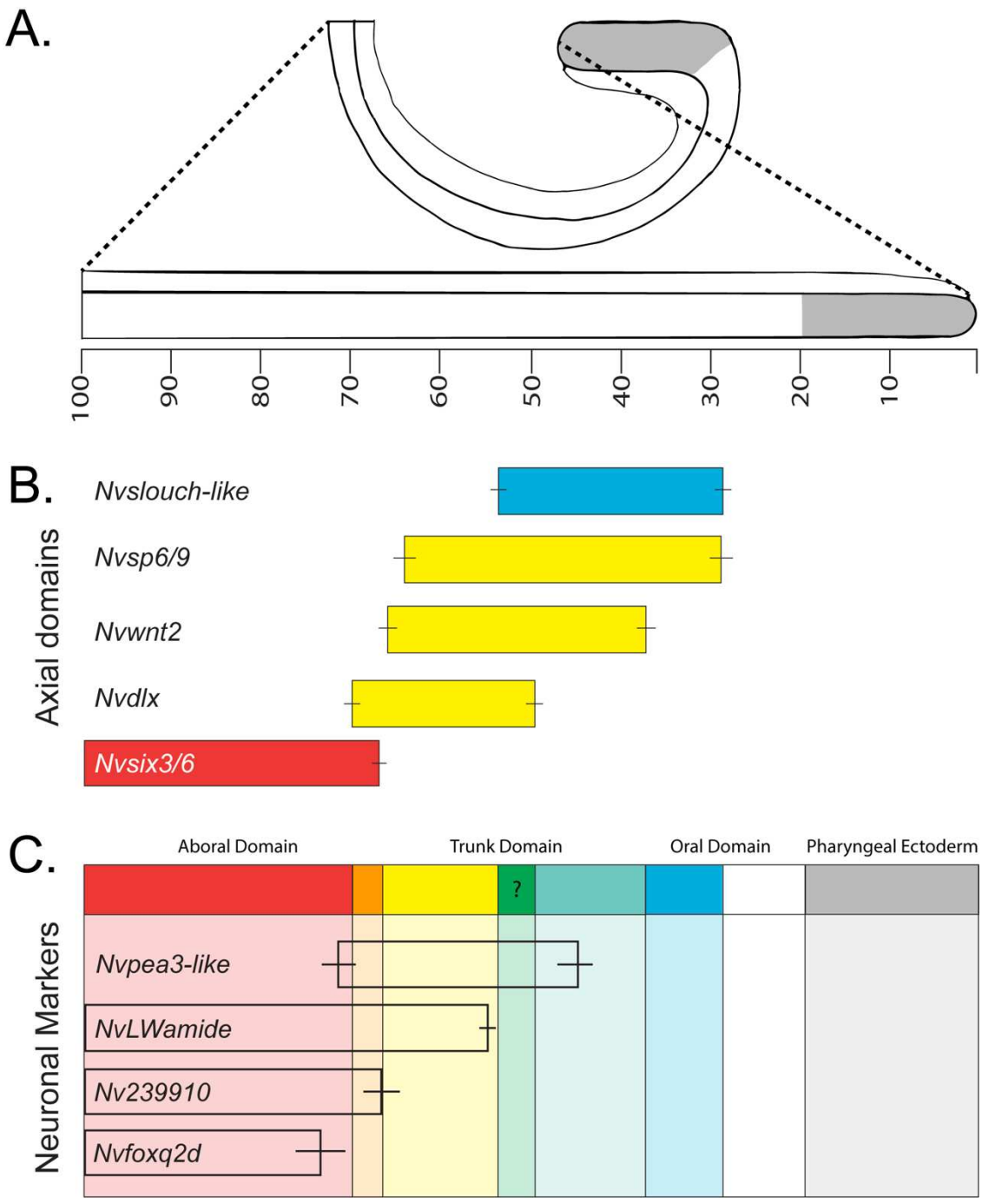

Figure 3.2: Unique molecular domains established along the oral-aboral axis do not coincide with expression of known neuronal subtype markers. Positional information was normalized along the oral-aboral axis with 0 at the pharyngeal ectoderm (grey) and 100 at the aboral end (A). The domain measurements for the spatial markers used within this study (B). The combinatorial molecular domains established by overlapping regions of expression and the expression domains for published neuronal subtypes (C). Bars at the end of the domain measurements are calculated from standard error of the mean (SEM).

Pharmacological manipulation of Wnt activity alters domains of these neuronal subtypes

After identifying that some neuronal markers were restricted to the expression domains of axial markers we wanted to identify whether manipulation of these domains would also shift neuronal subtype expression. Previous work has shown that treatment with the Wnt agonist, azakenpaullone, reduced the domain size of aboral markers while expanding the expression of trunk markers (Marlow et al., 2013; Leclère et al., 2016; Lebedeva et al., 2021). While treatment with iCRT14, a Wnt antagonist, was capable of expanding the aboral domains (Marlow et al., 2013). We then repeated these experiments treating embryos from fertilization to gastrulation (Figure 3.3). Interestingly we observed that early treatment with 10µM or 20µM iCRT14 resulted in reduced expression of the neuronal progenitor marker, *Nvath-like,* and loss in *Nv239910* expression (Figure 3.3 D-I). Treatment with azakenpaullone or iCRT14 after the start of gastrulation to the late gastrula stage reduced this knockdown of *Nvath-like* expression though treatment with 10µM azakenpaullone still significantly reduced expression of *NvashA* (Figure 3.3 J). We then utilized this delayed treatment to characterize whether shifts in axial domain size also shifts neuronal expression domains.

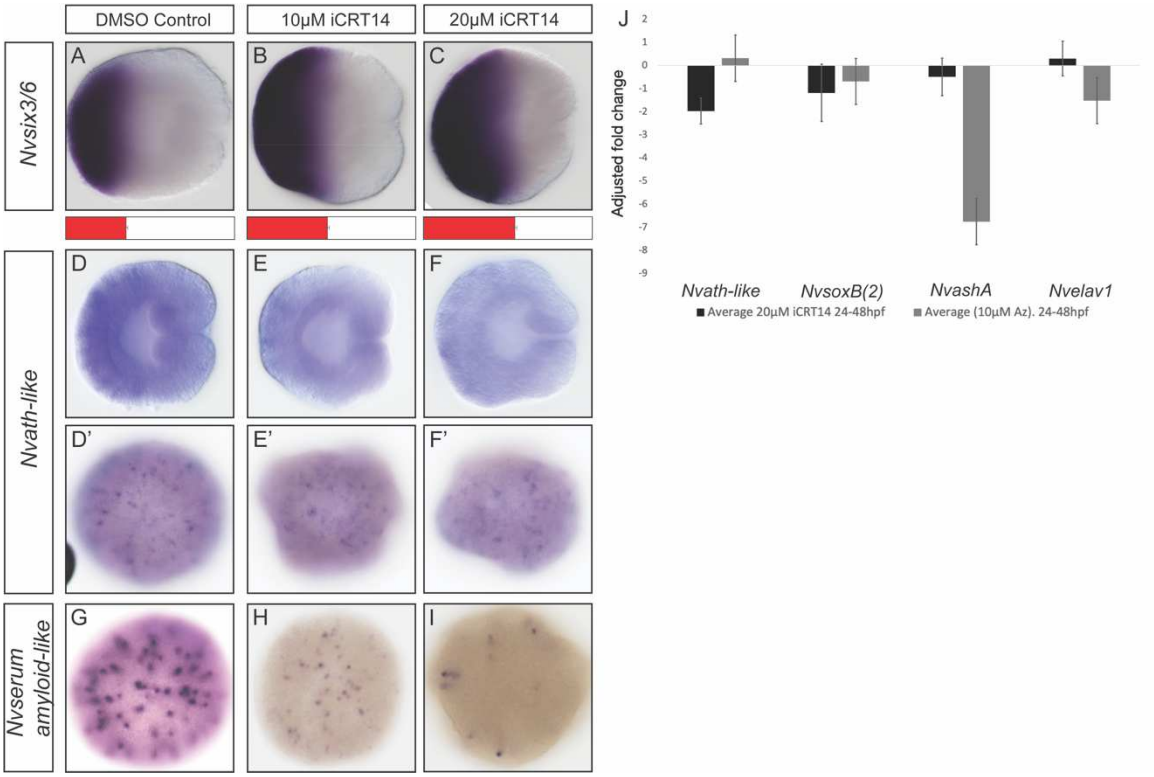

Figure 3.3: Pharmacological wnt manipulation from fertilization to late gastrulation inhibits neurogenesis in *Nematostella* which is not observed when treatment occurs after the start of gastrulation. Treatment with iCRT14 from fertilization to late gastrulation at published concentrations expands expression of *Nvsix3/6* (A-C). This treatment regimen also reduces expression of the progenitor marker *Nvath-like* (D-F, D'-F') and the differentiation marker *Nvserum amyloidA-like* (G-H). Treatment with azkenpaullone does not affect neural progenitor markers but does knockdown expression of *NvashA* (J, grey bars). Delayed treatment with iCRT14 after gastrulation occurs slightly reduces *Nvath-like* expression but does not significantly reduce expression of other neuronal markers (J, black bars). Error bars are standard error of the mean. (A-E) Lateral view with oral pole to the left. (D'-F' and G-I) aboral views.

Manipulation of the Wnt gradient, altered axial domain genes and shifted expression of neuronal markers. Previous work has already shown that treatment with 20µM iCRT14 is capable of expanding aboral markers at the expense of oral markers (Marlow et al., 2013). We observed an expansion of the aboral marker *Nvsix3/6* however treatment with 20µM iCRT14 did not significantly shift expression of trunk domain markers (Figure 3.4 D-E, G-H, J-K, P-Q). Interestingly we did observe a significant reduction in the domain size of the trunk neural marker *Nvpea3-like* (Figure 3.4M-N, $p<0.05$). Expression of

Nvfoxq2d expanded when treated with iCRT14, however the expression domain of *Nv239910* and *NvLWamide-like* remain unchanged (Figure 3.4 S-T, V-W, Y-Z, $p<0.05$). Treatment with 2μM azakenpaullone significantly expanded the expression domains for all trunk domain and the trunk specific neuronal marker, *Nvpea3-like*, at a significant loss of all aboral marker expression (Figure 3.4 C, F, I, L, O, R, U, X, A'). Interestingly the oral marker *Nvslouch-like,* did not expand but its expression shifted aborally and was significantly reduced (Figure 3.4 A, C). These data augments previous work characterizing the role of Wnt activity on axial domain shifts by identifying that these domain shifts also alter the domain sizes of known neuronal markers as well. This would support the hypothesis that axial information along the oral-aboral axis functions to pattern neuronal subtypes.

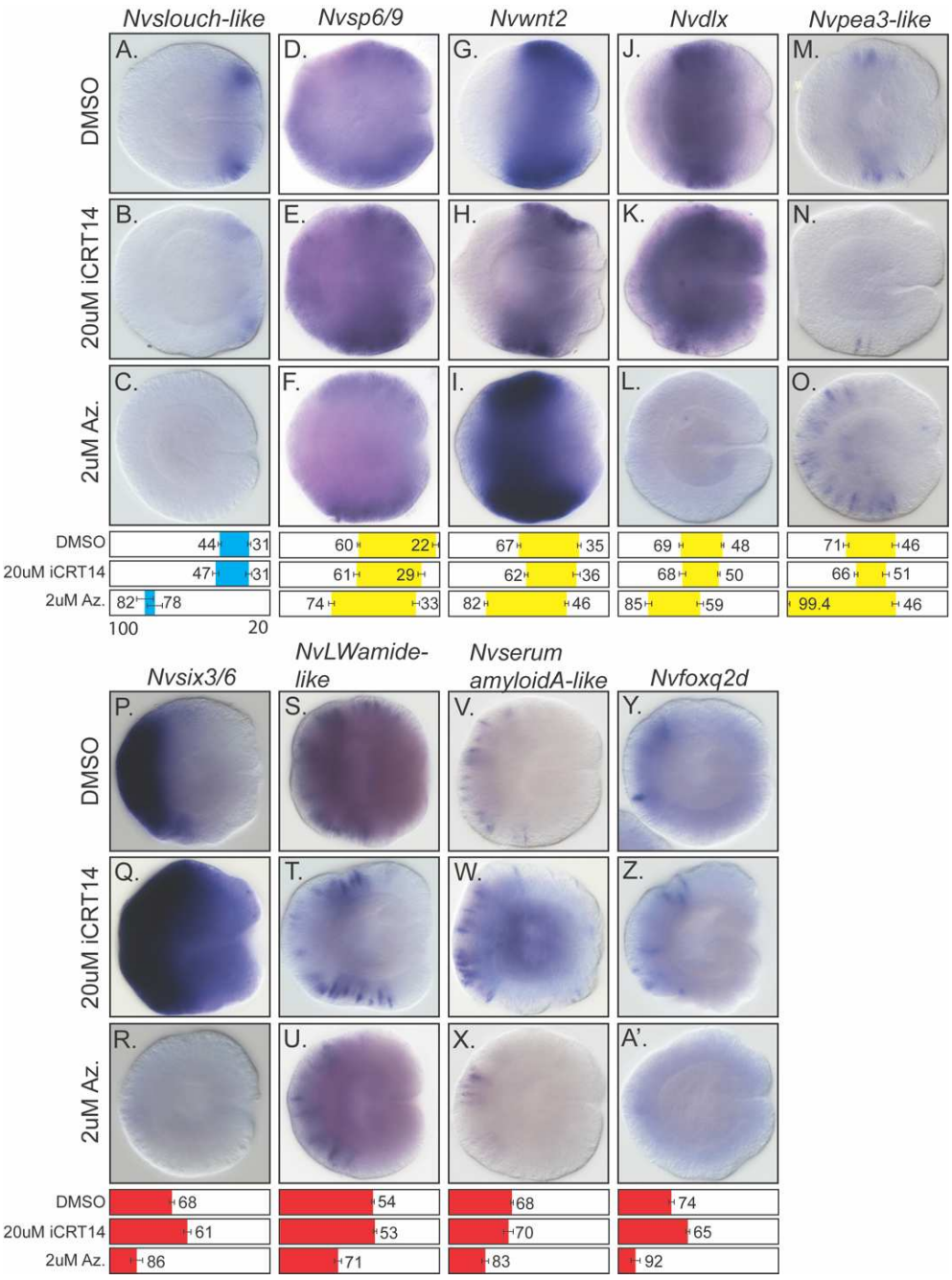

Figure 3.4: Pharmacological overactivation of wnt results in aborilized shifts in neuronal subtype expression. (A-O) Treatment with 20µM iCRT14 does not significantly reduce expression of the oral or trunk domain markers but does reduce expression of *Nvpea3-like*. Treatment with 2µM azakenpaullone significantly shifts the oral marker *Nvslouch-like* and expands trunk identity, both domain and neuronal markers, into the aboral domain. (P-A') Treatment with 20µM iCRT14 significantly ($p<0.05$) expands expression of *Nvsix3/6* and *Nvfoxq2d* expression while treatment with 2µM azakenpaullone significantly reduces domain sizes for the aboral domain and neuronal markers. Lateral view with oral to the left. Bars at the bottom of the page show domain measurements, from 20 to 100%, across all three treatment groups. Error bars were calculated using standard error of the mean. Significance was determined using student t.test.

Nvsix3/6 is necessary and sufficient to pattern aboral neuronal subtypes

To determine if axial domains contribute to neuronal patterning, axial domains genes were disrupted and changes to neuronal patterning assessed. The initial focus was on the *Nvsix3/6*+ aboral domains, in part, due to the presence of multiple neuronal subtypes found within its expression domain. shRNA mediated knockdown of *Nvsix3/6* produced the previously identified expansion of trunk markers into the aboral domain confirming the functionality of the shRNA (Figure 3.5C-D) (Sinigaglia et al., 2013). Loss of *Nvsix3/6* reduced the expression of and domain boundaries for the neuronal markers restricted to the *Nvsix3/6* domain (Figure 3.5 H-I', $p<0.05$). However, *NvLWamide* expression, which spans both the aboral and trunk domains, remained unchanged in *Nvsix3/6* shRNA injected animals (Figure 3.5 G-G', $p>0.05$). Additionally, the aboral boundary of the trunk neuronal subtype *Nvpea3-like* expanded into the apical domain in *Nvsix3/6* knockdowns (Figure 3.5 E-E', $p<0.005$), which is consistent with the expansion of the trunk axial domain aborally in the absence of *Nvsix3/6*. We found no significant change in the domain size for the oral marker *Nvslouch-like* when *Nvsix3/6* was knocked down (Figure 3.5 A-A'; $p>0.05$). Conversely, global misexpression of *Nvsix3/6* resulted in an expansion of the oral expression limit for all neuronal subtypes (Figure 3.6 G-I/GI'-'$p<0.005$). The ubiquitous misexpression of *Nvsix3/6* also resulted in loss of the oral and trunk domain markers while *Nvpea3-like* expression was significantly reduced and shifted orally (Figure 3.6 A-E'A-E/). These data suggest that *Nvsix3/6* is necessary and sufficient to promote patterning of aboral neuronal subtypes. This would support the overall hypothesis that axial markers within the cnidarian-bilaterian ancestor also used axial markers to pattern neuronal subtypes.

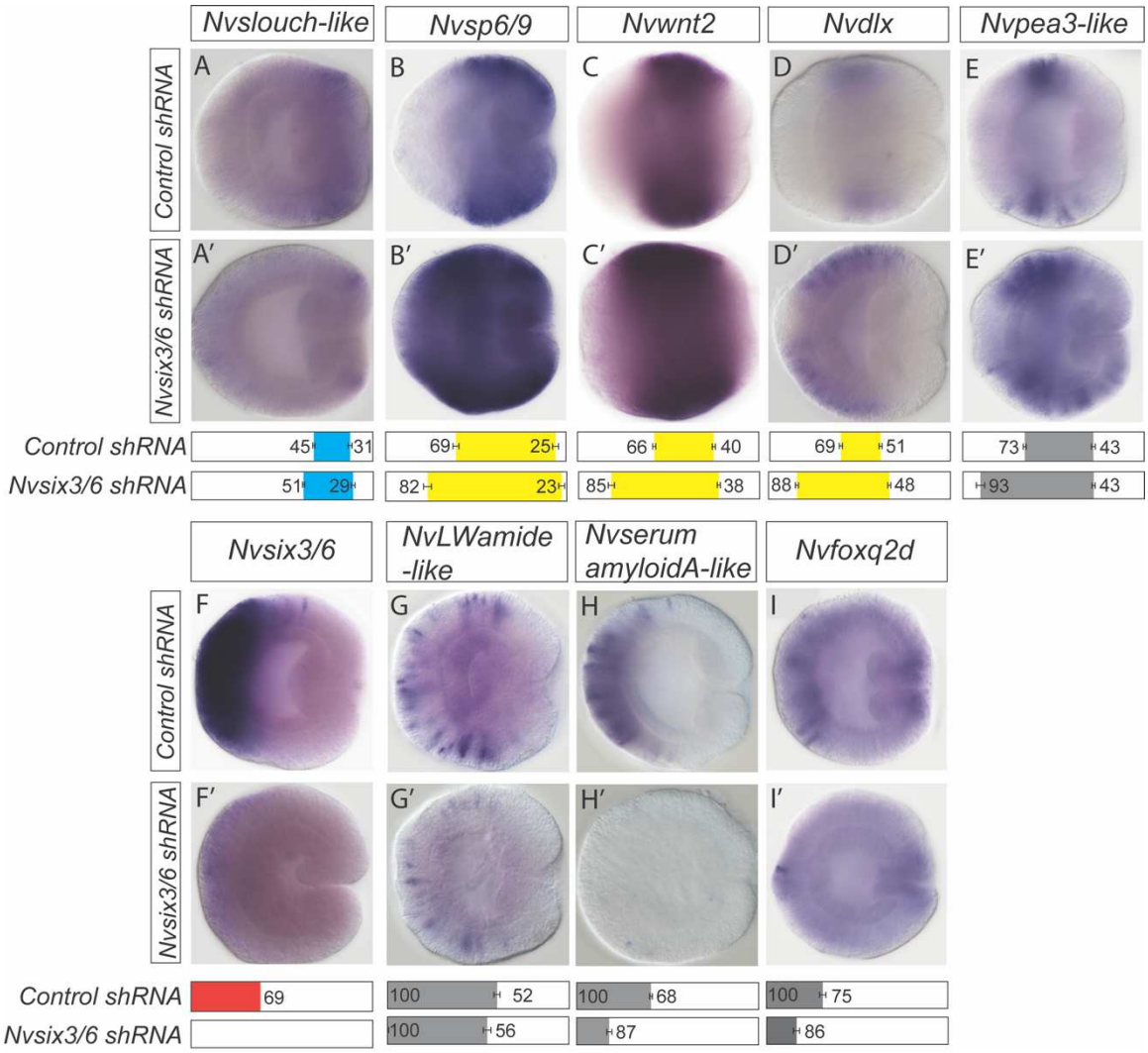

Figure 3.5: shRNA mediated loss of *Nvsix3/6* expression results in aboral shifts in trunk and aboral markers. Loss of *Nvsix3/6* did not alter the domain size of the oral marker *Nvslouch-like* (A/A'). Loss of expression expanded expression of the trunk domain and neuronal markers (B-E/B-E'). Loss of *Nvsix3/6* also resulted in reduction in the domain size of *Nvserum amyloidA-like* and *Nvfoxq2d* while having no effect on *NvLwamide* expression (G-I/G'-I'). Lateral view with oral to the left. Bars at the bottom of the page show domain measurements, from 20 to 100%, across all three treatment groups. Error bars were calculated using standard error of the mean. Significance was determined using student t.test.

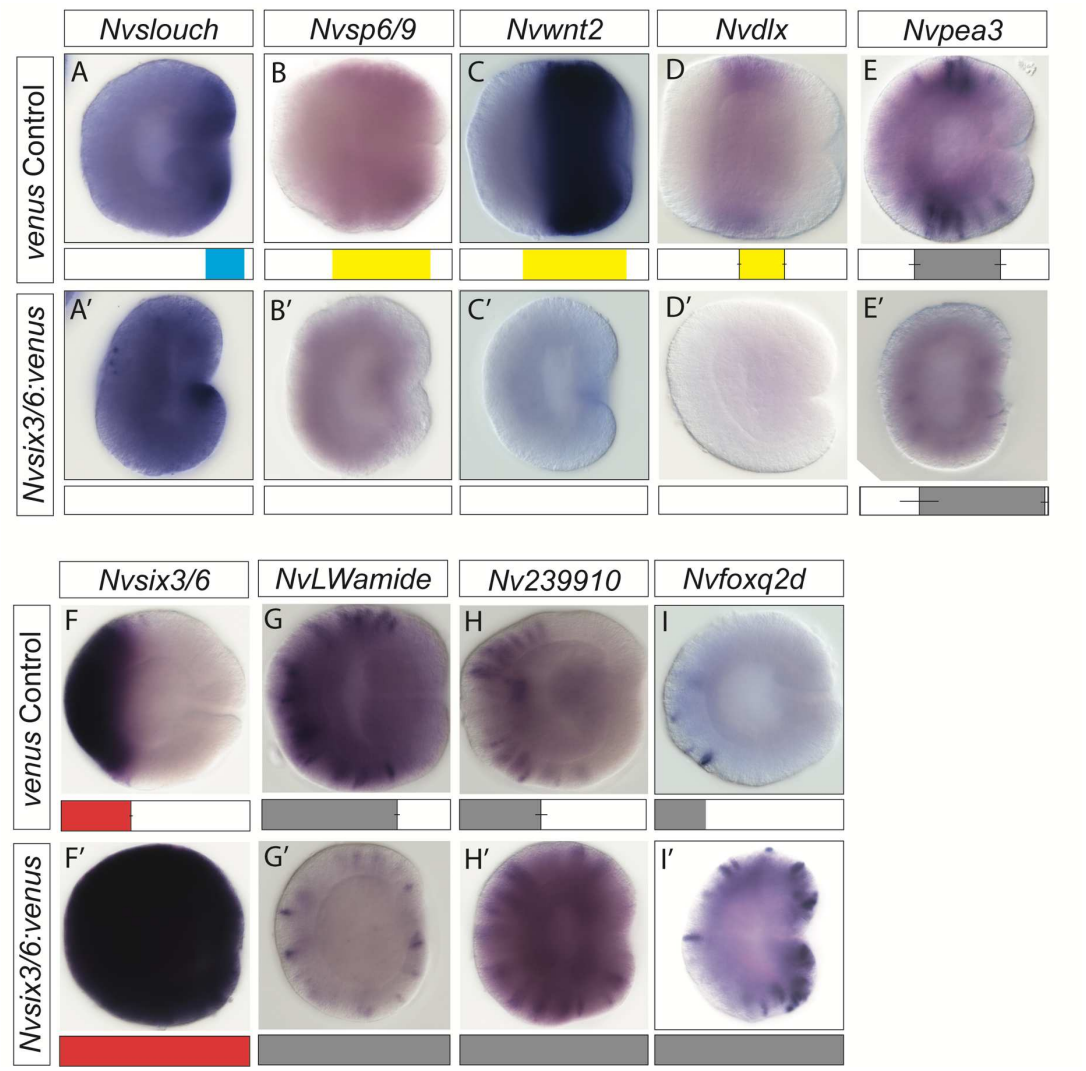

Figure 3.6: Ubiquitous expression of *Nvsix3/6* result in oral shifts in expression of trunk and aboral markers. Misexpression of *Nvsix3/6* resulted in loss of expression for the oral marker, *Nvslouch-like*, and all trunk domain markers (A-D/A'-D'). The trunk neuronal domain marker, *Nvpea3-like,* however still maintained expression at the oral-most region of the embryo (E/E'). Ubiquitous expression of *Nvsix3/6* was capable of expanding expression of all aborally expressed neuronal markers into the trunk and oral domains (H-I/H'-I'). Lateral view with oral to the left. Bars at the bottom of the page show domain measurements, from 20 to 100%, across all three treatment groups. Error bars were calculated using standard error of the mean. Significance was determined using student t.test.

The trunk marker *Nvwnt2* regulates trunk expressed neuronal subtypes

Next we tested the role of trunk domain markers on the regulation of the neuronal subtype marker *Nvpea3-like.* While our molecular domain data would suggest that *Nvwnt2* regulates *Nvpea3*-like, *Nvpea3-like* also overlaps with *Nvdlx* and *Nvsp6/9* (Figure

1). If *Nvdlx, Nvwnt2,* and/or *Nvsp6/9* regulates neuronal subtypes then knockdown of one of these genes should result in loss of *Nvpea3-like* expression. We created shRNAs for *Nvdlx, Nvwnt2,* and used a previously published shRNA for *Nvsp6/*9 to identify which trunk marker regulates *Nvpea3-like* expression (Lebedeva et al., 2021). We also tested whether loss of these genes would result in expansion of the flanking axial genes, suggesting a role in axial patterning

Loss of *Nvdlx* expression resulted in no change in the expression domain of the oral markers, trunk neural and domain markers, or aboral domain and neuronal markers (Figure 3.7 A--E'); $p>0.05$). This suggest that *Nvdlx* is not a regulator of trunk identity or trunk neuronal subtypes during these late gastrula stages. Knockdown of *Nvsp6/9* reduced the expression domain of *Nvslouch-like* and *Nvwnt2* however, the expression domain of *Nvdlx* and *Nvpea3-like* were largely unaffected (Figure 3.7 A/A''-E/E''$p<0.05$). Loss of *Nvsp6/9* did result in the slight expansion of *Nvsix3/6, NvLWamide-like,* and *Nvserum amyloidA-like* expression into the trunk domain (Figure 3.7 F/F''-H/H'', $p<0.005$). However, expression of *Nvfoxq2d* remained unchanged when *Nvsp6/9* expression was reduced (Figure 3.7G/G''; $p>0.05$). We then knocked down the trunk marker, *Nvwnt2,* and observed shifts in domain sizes for all markers tested (Figure 3.7A-I'''). The aboral-end of domain expression for *Nvslouch-like*, *Nvsp6/9, Nvdlx,* and *Nvpea3-like* were all slightly shifted orally reducing the overall domain size (Figure 3.7 A/A'''-E/E'''). We also observed expanded expression of the aboral marker *Nvsix3/6*, the aboral-trunk neuronal marker *NvLWamide-like,* and the aboral neuronal marker *Nvfoxq2d* into the trunk domain (Figure 3.7 F/F'''-G/G'''). Interestingly, expression of *Nvserum amyloidA-like* appeared to be slightly reduced, though this was not significant, when *Nvwnt2*

expression is reduced. Despite knockdown of the three trunk neuronal markers none of them dramatically reduced expression of *Nvpea3-like* and suggests that the published trunk markers do not regulate neuronal subtype patterning. Overall the data could suggest that another axial patterning mechanism could be regulating trunk neuronal subtypes.

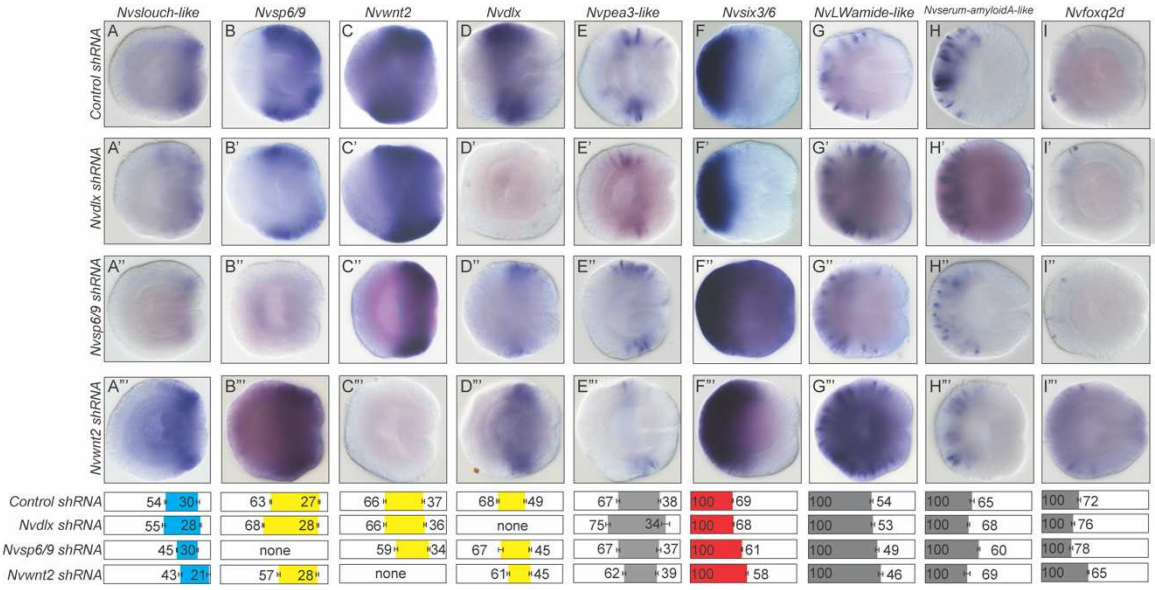

Figure 3.7: Known trunk markers (*Nvdlx, Nvsp6/9, and Nvwnt2*) do not pattern trunk neuronal identity. Knockdown of *Nvdlx* does not alter spatial domain or neuronal markers (A'-I'). Loss of *Nvsp6/9* results in domain shifts orally of *Nvslouch-like, Nvwnt2, Nvsix3/6, NVLwamide-like,* and *Nvserum amyloidA-like* (A''-G''). Knockdown of *Nvwnt2* expands expression of *Nvsix3/6* and *Nvfoxq2d* at the expense of the trunk marker *Nvsp6/9, Nvdlx, Nvpea3-like* and the oral marker *Nvslouch-like* (A'''-I'''). Lateral view with oral to the left. Bars at the bottom of the page show domain measurements, from 20 to 100%, across all three treatment groups. Error bars were calculated using standard error of the mean. Significance was determined using student t.test.

NvSix3/6 regulates aboral neuronal subtype expression and wnt signaling patterns trunk neuronal subtypes

Our inability to identify a trunk domain marker with a neuronal function led us to question whether the neurogenic role of *Nvsix3/6* was true. Previous work within *Nematostella* characterized a role for *Nvsix3/6* in the stabilization of the oral-aboral axis by inhibiting Wnt activity at the aboral pole (Sinigaglia et al., 2013; Leclère et al., 2016).

This led us to hypothesize that early embryonic manipulation of *Nvsix3/6* likely altered Wnt activity along the oral-aboral axis. To separate the Wnt inhibitory role of *Nvsix3/6* with the neurogenic function we treated embryos injected with *Nvsix3/6 shRNA* or *Nvsix3/6:venus* with iCRT14 or azakenpaullone, respectively. If *Nvsix3/6* has a neurogenic function, then pharmacological manipulation of Wnt activity should not rescue *Nvsix3/6* mediated loss or misexpression of the aboral neuronal subtypes identified above (Figure 3.5 and 3.6).

Embryos injected with *Nvsix3/6 shRNA* and treated with a DMSO control resulted in expansion of *Nvpea3-like* and domain reduction of *Nvserum amyloidA-like,* replicating the above phenotypes (Figure 3.8 A/A' and C/C'). Treatment with 20µM iCRT14 did not rescue this expansion of *Nvpea3-like* and loss of *Nvserum amyloid-like* (Figure 3.8A-D'). Embryos injected with *Nvsix3/6:venus* resulted in expansion of *Nvfoxq2d* expression while orally restricting expression of *Nvpea3-like*, as was previously observed (Figure 3.6). Treatment with 2µM azakenpaullone resulted in expansion of *Nvpea3-like* expression and a significant reduction in the domain size of *Nvfoxq2d* (Figure 3.8 E-H'). This is reminiscent of the domain measurements observed when embryos were treated with 2µM azakenpaullone (Figure 3.4M/O and Y/A'). The culmination of the data from these rescue experiments suggests that *Nvsix3/6* is necessary for aboral neuronal subtypes while graded Wnt activity patterns trunk neuronal subtypes and inhibits aboral neuronal subtypes. Lastly, previous work identified the predicted enhancer domain for *Nvsix3/6* within *Nematostella* (Sebé-Pedrós et al., 2018). Previous work also identified the upstream regulatory necessary to synthesize a *Nvserum amyloidA-like* transgenic line

(Layden et al., 2016). We found that the upstream regulatory domain for *Nvserum amyloidA-like* possessed three potential enhancer binding domains for *Nvsix3/6* and contained binding domains for *Nvtcf*, the transcription factor activated by wnt signaling. We also identified potential binding domains in the upstream regulatory components used to synthesize transgenic lines for *NvLWamide-like* and *Nvfoxq2d* (Layden et al., 2016; Busengdal and Rentzsch, 2017; Havrilak et al., 2017). This could lend support to the hypothesis that *Nvsix3/6* directly patterns regulation of those neuronal subtypes expressed within the aboral domain.

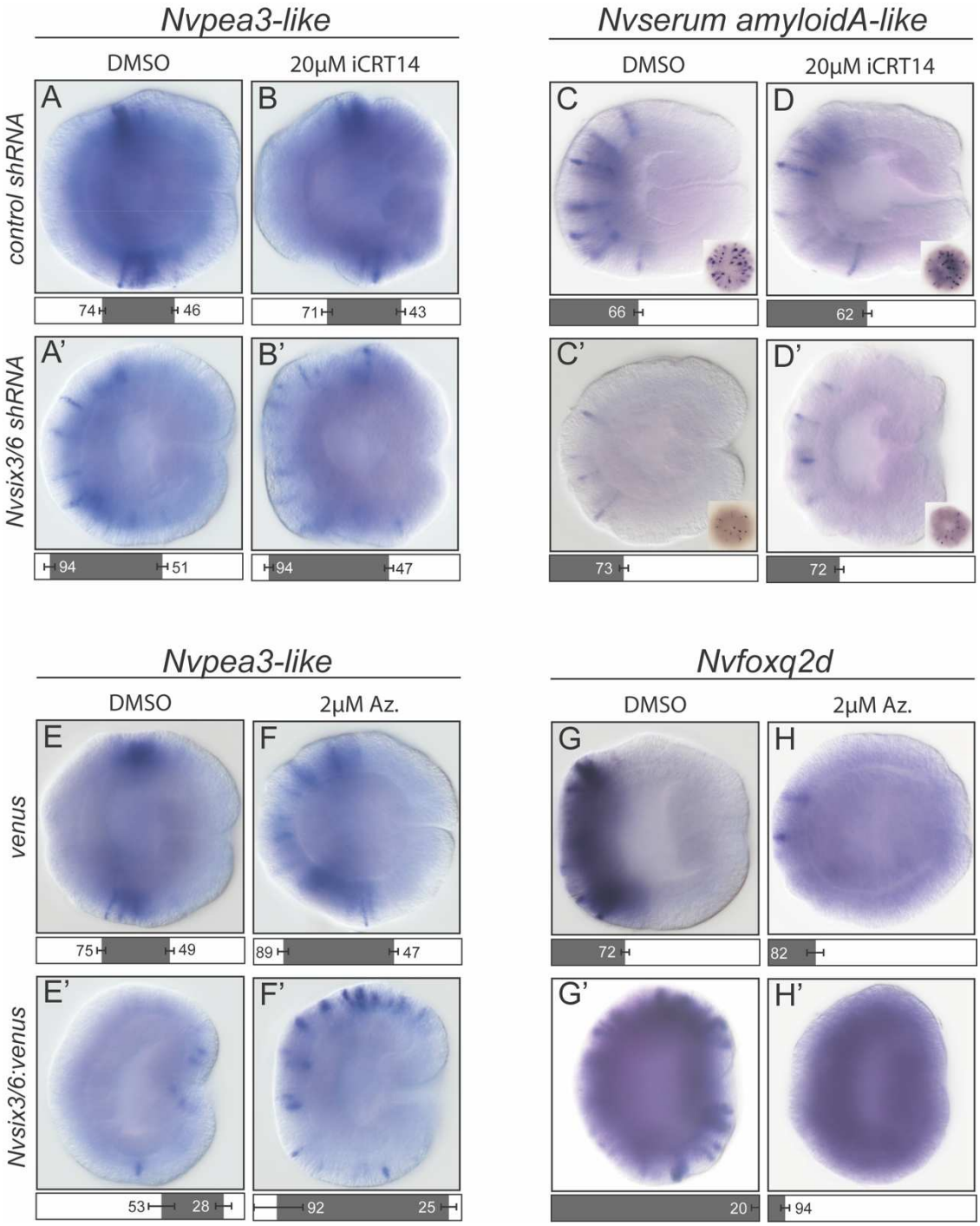

Figure 3.8: Pharmacological wnt manipulation rescues ubiquitous misexpression of *Nvsix3/6* but not shRNA mediated loss of *Nvsix3/6* expression. Injection of *Nvsxi3./6* shRNA and treatment with iCRT14 is not capable of rescuing expansion of *Nvpea3-like* or loss of *Nvserum amyloidA-like* (A-D'). Treatment with 2µM azakenpaullone in embryos ubiquitously misexpressing *Nvsix3/6* rescues loss of *Nvpea3-like* expression and reduces expression of *Nvfoxq2d* (E-H'). Lateral view with oral to the left. Insets within C-D are images with aboral ends in focus. Bars at the bottom of the page show domain measurements, from 20 to 100%, across all three treatment groups. Error bars were calculated using standard error of the mean. Significance was determined using student t.test.

Wnt signaling also affects endodermal expression of *NvotxC*

Here we focused on characterizing a neurogenic role for *Nvsix3/6* however, other bilaterian AP patterning domain markers have been identified within *Nematostella* and could also perform neural regulatory roles. Within bilaterians expression of six3 defines the forebrain, the genes otx and irx define the midbrain, and gbx defines the hindbriain within bilaterians (Holland et al., 2013). *Nvirx* is expressed adjacently to expression domain of *Nvsix3/6* and Wnt activity regulates its expression along the oral-aboral axis (Marlow et al., 2013). However, expression of *Nvirx* seems to be restricted to individual cells instead of the broad expression typical of domain markers in *Nematostella* (Marlow et al., 2013). While *NvotxC* expression is restricted to the aboral end of the endoderm of *Nematostella* within gastrula and this expression is maintained as development occurs (Mazza et al., 2007). Interestingly, within *Nematostella* the endodermal nerve net is patterned independently of the ectodermal nervous system (Nakanishi et al., 2012). It is possible that *NvotxC* patterns expression of endodermal neurons in a similar manner to *Nvsix3/6.* However, no work has been done to determine whether Wnt patterns this endodermal spatial marker in *Nematostella.* Treatment with 2µM azakenpaullone resulted in complete loss of expression of *NvotxC* while treatment with 20µM iCRT14 increased expression of *NvotxC*. This would suggest that *NvotxC* is responsive to alterations in Wnt activity and could be functioning to pattern neuronal subtypes within the endoderm.

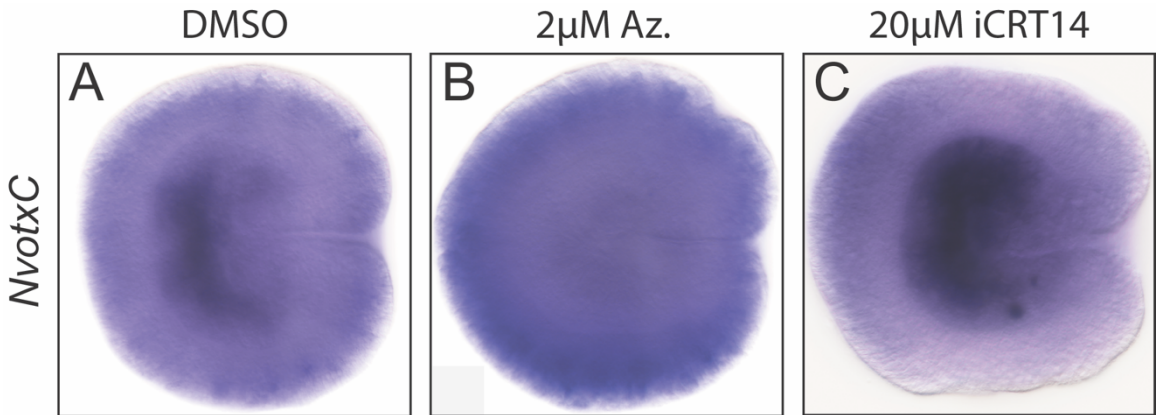

Figure 3.9: Pharmacological manipulation of wnt affects expression of the endodermal marker *NvotxC*. *NvotxC* expression is restricted to the aboral end of the endoderm within late gastrula (A). Treatment with 2µM azakenpaullone results in a loss of *NvotxC* expression (B). Treatment with 20µM iCRT14 then increased expression of *NvotxC* (C). Lateral view with oral to the left

Discussion

Axial patterning mechanisms pattern neuronal subtypes within Nematostella

Here we show that *Nvsix3/6* is both necessary and sufficient for the expression of neuronal subtypes expressed within its own domain (Figure 3.8). We then hypothesize that graded Wnt activity along the oral-aboral axis inhibits expression of these aboral neuronal markers while promoting expression of trunk neuronal identity. It is this dual role of spatial markers and graded Wnt activity which go on to pattern different neuronal subtypes along the oral-aboral axis. However, it is entirely possible that the spatial domain genes necessary for neuronal patterning within the trunk domains have just not been identified.

The trunk domain is patterned through Wnt mediated mechanism but the upstream regulatory gene necessary for trunk development is still unknown. Our model of Wnt mediated trunk neuronal patterning was hypothesized due to our inability to identify a domain marker which patterns the trunk domain of *Nematostella*. To date the best characterized trunk marker is *Nvsp6/9* whose domain is repressed by oral markers

and whose expression represses the domain of *Nvsix3/6* (Lebedeva et al., 2021). However, loss of *Nvsp6/9* expression does not result in loss of trunk domain identity (Figure 3.7). Instead, loss of *Nvsp6/9* reduced the domain size of known trunk genes, including expression of *Nvwnt2*, and similar to the iCRT14 treatments (Figure 3.7). This reduced domain phenotype is also observed within *Nvwnt2* knockdown embryos and it is possible that these two genes function together to pattern the trunk domain and trunk neuronal subtypes, in a similar mechanism to how the oral domain is patterned in *Nematostella* (Lebedeva et al., 2021). It is also possible that we have not yet identified the spatial domain gene necessary for trunk identity. Several markers were recently identified as trunk markers within *Nematostella,* including the homeodomain marker *NvmsxA,* but their function within *Nematostella* remains largely uncharacterized (Lebedeva et al., 2021). Characterization of how the trunk domain is patterned and the roles individual trunk markers play in patterning this tissue could provide further insight into our understanding of how trunk neurons are patterned.

The role of anterior-posterior patterning and the evolution of central nervous systems

The ability for *Nvsix3/6* to pattern aborally restricted neuronal subtypes within *Nematostella* brings into question the utilization of these spatial markers to homologize bilaterian brains. Loss of six3 within multiple bilaterian models results in loss of forebrain development (Oliver et al., 1995). It is this highly conserved function of six3 which is used to support homologizing brain tissue across distinctly different bilaterian brain (Steinmetz et al., 2010; Holland et al., 2013; Darras et al., 2018). Functional studies characterizing a patterning or neurogenic role for these axial markers, like six3,

have not been extensively performed outside of traditional models (Steinmetz et al., 2010; Martín-Durán et al., 2018). The data collected here confirmed a neurogenic role for *Nvsix3/6* within cnidarians and suggest that this neurogenic function evolved prior to when cnidarians and bilaterians diverged. This would suggest that the utilization of axial genes to pattern bilaterian brains and neuronal subtypes is not necessary for central nervous system patterning and likely should not be used to homologize different brain regions. The other hypothesis that could be postulated is that the bilaterian forebrain and the aboral domain of *Nematostella* are homologous. This is not a novel hypothesis and has been previously hypothesized due to the conserved regulatory role of *Nvsix3/6* in patterning the aboral domain (Sinigaglia et al., 2013). However, expression of other spatial markers typically identified within the midbrain and hindbrain are not expressed within the same tissue in *Nematostella*.

It is possible that the condensation of these spatial domain markers into the same neuroectoderm is necessary for the evolution of the centralized nervous system. The bilaterian markers six3, irx, otx, and gbx are expressed within staggered domains in the neuroectoderm and give rise to the three generally homologized regions of the bilaterian brain. In *Nematostella* these markers are expressed within the ectoderm (*Nvsix3/6* and *Nvirx*) and the endoderm (*Nvgbx* and *NvotxC*) (Mazza et al., 2007; Marlow et al., 2013; He et al., 2018). Interestingly, *Nematostella* also develop nervous systems independently from the ectoderm and the endoderm with no data supporting that either nervous system is more homologous to bilaterian nervous system (Nakanishi et al., 2012). These data culminates in the hypothesis that within the bilaterian ancestor these anterior posterior markers coalesced into the same tissue, became staggered, and then patterned distinct

regions within the brain. An alternative hypothesis previously postulated however, is that central nervous system convergently evolved in a stepwise manner utilizing genes which already play a spatial patterning role (Pani et al., 2012; Martín-Durán and Hejnol, 2021). It then becomes important to study the expression profiles of these AP axial markers within non-traditional bilaterian system to functional determine whether they have a neurogenic function. For instance in the hemichordate, *Saccoglossus kowalevskii*, Six3 is expressed anteriorly yet, it does not possess a central nervous system (Lowe et al., 2006). This would suggest that it is involved in axial patterning but not utilized for neurogenic patterning. The xenocoelomorphs have been postulated to be the earliest branching bilaterian and it has been hypothesized that the ancestral nervous system for this model is likely a nerve net (Cannon et al., 2016; Gavilán et al., 2016). Characterization of the expression patterns for these AP spatial domain markers within xenocoelomorphs found anterior restriction of *six3/6* but expression of *otx* occurs across the entire body column. If these spatial markers play both a spatial and neuroregulatory role then it would lend support to the idea that this neurogenic role is highly conserved and is not involved in the evolution of complex brains. If these spatial markers regulate spatial patterning but are not involved in neurogenesis then it would support the hypothesis that these spatial patterning markers are being convergently co-opted within bilaterians to pattern different brain regions.

Chapter 4: Identification and characterization of the role of acetylcholine in *Nematostella vectensis*

Abstract

Recent worked has characterizing the nerve net of *Nematostella vectensis* found that it consists of multiple neuronal subtypes. However, the function of these neurons has remained largely uncharacterized. Nicotinic and muscarinic acetylcholine receptors are best known for their role at chemical synapses in bilaterian animals. It is not clear when neuronal function for nicotinic or muscarinic receptors evolved. Previous studies in cnidarians suggest that acetylcholine's neuronal role existed prior to the cnidarian–bilaterian divergence, but has not been well characterized. To determine the origins of neuronal functions of nicotinic acetylcholine receptors, we investigated the phylogenetic position of cnidarian acetylcholine receptors, characterized the spatiotemporal expression patterns of nicotinic receptors in *Nematostella*, and compared pharmacological studies in *N. vectensis* to the previous work in other cnidarians. Treatment with acetylcholine-and nicotine induced tentacular contractions while the nAChR antagonist mecamylamine suppressed tentacular contractions induced by both acetylcholine and nicotine. This indicated that tentacle contractions are in fact mediated by nAChRs. Nicotine also induced the contraction of radial muscles, which contract as part of the peristaltic waves that propagate along the oral–aboral axis of the trunk. Radial contractions and peristaltic waves were suppressed by mecamylamine. The ability of nicotine to mimic acetylcholine responses, and of mecamylamine to suppress acetylcholine and nicotine-induced contractions, supports a neuronal function for acetylcholine in cnidarians. Phylogenetic analysis suggests that the *Nematostella* genome encodes 26 nicotinic (nAChRs), no muscarinic (mAChRs) acetylcholine receptors were observed, and that nAChRs independently radiated in cnidarian and bilaterian linages. Examination of the

spatiotemporal expression of *N. vectensis nAChRs* during development and in juvenile polyps identified that *NvnAChRs* are expressed in neurons, muscles, gonads, and large domains known to be consistent with a role in developmental patterning. These patterns are consistent with nAChRs functioning in a neuronal and suggested non-neuronal functions as well. Our data suggest that nAChR receptors functioned at chemical synapses in *N. vectensis* to regulate tentacle contraction. Similar responses to acetylcholine are well documented in cnidarians, suggesting that the neuronal function represents an ancestral role for nAChRs. Together, these observations suggest that both neuronal and non-neuronal functions for the ancestral nAChRs were present in the cnidarian–bilaterian common ancestor. Thus, both roles described in bilaterian species likely arose at or near the base of nAChR evolution.

Introduction

Neuronal subtypes in *Nematostella vectensis* have largely been identified through large scale experiments, such as RNA sequencing, microarray, or identification of neuropeptide expression (Marlow et al., 2009; Layden et al., 2012; Havrilak et al., 2017b). More recent work has started to link these neuronal subtypes to their functional role, such GLWamide's role in metamorphosis (Nakanishi and Martindale, 2018). Yet there has been less focus on the characterization of the developmental origins of these functional neuronal subtypes in Nematostella. One functional neuronal subtype that has been developmentally characterized within multiple bilaterian are cholinergic neurons [5](Dani and Bertrand, 2007). Cholinergic neurons release acetylcholine at the synaptic junction where it will bind to either nicotinic or muscarinic acetylcholine receptors.

Interestingly the components necessary for cholinergic signaling have been identified within the multiple cnidarian genomes but cholinergic neurons have not been characterized any cnidarian, including *Nematostella vectensis* (Anctil, 2009; Chapman et al., 2010; Shinzato et al., 2011; Leclère et al., 2019). The focus of this aim was to (1) characterize the role of acetylcholine in *Nematostella* and (2) to identify the cholinergic neurons producing acetylcholine.

The role of acetylcholine within cnidarians has largely been investigated through pharmacological experiments(Kass-Simon and Pierobon, 2007). Within anthozoans treatment with acetylcholine or nicotine has shown to induce contractions within the oral and body tissues of *Bunodosoma caissarum (Mendes and De Freitas, 1984)*. In the hydrozoan, *Liriope tetraphylla*, nicotine induced an initial bell contraction, which constitute their swimming behavior, while acetylcholine itself showed no effect (Scemes and Mendes, 1986). Interestingly atropine, an agonist of muscarinic acetylcholine receptors, inhibited these swimming bell contractions (Scemes and Mendes, 1986). Pharmacological treatment of *Hydra attenuate* with nicotinic receptor agonists resulted in reduced contraction burst pulses while treatment with atropine increased the number of contraction burst pulses (Kass-Simon and Passano, 1978). Within another Hydra species, *Hydra piradi*, treatment with acetylcholine resulted in increased contraction response (Singer, 1964). Despite differences in data collection and behavioral response to acetylcholine, nicotine, or muscarinic agonist, these data support the likelihood that cnidarians use acetylcholine to regulate muscle contraction.

Advances in genomics within recent years has increased the number of cnidarians with whole annotated genomes. Access to the annotated genomes of *Nematostella vectensis, Acropora digitifera, Clytia hemisphaerica*, and *Hydra* have allowed researchers to identify and characterize different components of the cnidarian cholinergic nervous system with the goal of better understanding some of the conflicting pharmacological data (Putnam et al., 2007; Chapman et al., 2010; Shinzato et al., 2011; Leclère et al., 2019). Previous work within *Nematostella* identified 14 potential nicotinic acetylcholine receptors (nAchRs), no muscarinic acetylcholine receptors (mAchRs), three potential choline acetyltransferases, necessary for acetylcholine synthesis, and five potential acetylcholinesterases, necessary for the degradation of acetylcholine once bound to the receptor (Anctil, 2009). Single-cell RNA sequencing within *Nematostella* has shown expression of nAchRs within neuronal cells, muscle cells, gonads, and the apical tuft, though this is lacking temporal resolution (Sebé-Pedrós et al., 2018). Single-cell RNA sequencing within *Hydra* has shown similar results with expression of nAchRs within the tentacles, nematocytes, neural cells, ectodermal cells, and gland cells while mAchRs were expressed within neural and gland cells (Siebert et al., 2019). The shared expression of nicotinic acetylcholine receptors within muscle and neuronal cells along with the pharmacological experiments further supports the role of acetylcholine as a neurotransmitter within cnidarians.

Here, we identify the role of acetylcholine in muscle contraction and characterize the expression of acetylcholine receptors in the anthozoan cnidarian *Nematostella vectensis*. In *Nematostella*, acetylcholine treatment induced tentacle contraction. Treatment with the

nicotine, an agonist of nAChR, reproduced the acetylcholine response, and the nAChR antagonist mecamylamine suppressed both acetylcholine and nicotine mediated tentacular contractions. Nicotine also induced contractions of the radial muscles present in endodermal tissue, and mecamylamine suppressed nicotine mediated radial contractions. Treatment with lidocaine, a voltage-gated ion channel inhibitor, blocked all acetylcholine and nicotine induced contractions. We found that Nematostella has 26 nicotinic acetylcholine receptors encoded in its genome. Phylogenetic analysis suggests that the cnidarian receptors radiated independently from bilaterian receptors. To gain a broader insight into the potential role(s) of acetylcholine in Nematostella, we used mRNA in situ hybridization to identify potential nAChR positive neuronal. Several previously published neuronal nAChRs appeared to be expressed within neurons and muscles. Non-neuronal-like expression in large regions such as ubiquitous expression, endodermal expression, and large domains that encompassed the pharynx and the apical tuft were observed for seven of the 15 genes assessed. While we were not able to identify nAChRs positive neuronal subtypes the data presented here suggest that acetylcholine plays a neuronal role in muscle contraction and likely plays multiple non-neuronal roles within Nematostella. These data also support the hypothesis that both neuronal and non-neuronal functions were present in the ancestral nAChR(s) that gave rise to both the cnidarian and bilaterian receptors.

Results:

Acetylcholine mediates tentacle and radial muscle contractions

Before identifying cholinergic neurons we wanted to determine whether acetylcholine played any role within *Nematostella*. To characterize the role of acetylcholine in *Nematostella,* polyps were treated with increasing concentrations of acetylcholine dissolved in 1/3X artificial sea water (ASW) (0-25mM acetylcholine). As other cnidarians treated with acetylcholine, or nicotine, have a contractile response we expected to observe some contraction within *Nematostella* (Singer, 1964; Mendes and De Freitas, 1984; Scemes and De-Freitas, 1989). *Nematostella* have been shown to display multiple types of contractions: tentacle contractions, which occurs along the proximal-distal axis, tentacle retractions, when tentacles are pulled into their pharynx, radial contractions, and lateral contractions, which occur along the oral-aboral axis of the polyps. When animals were treated with 1/3XASW 15% of animals display tentacular contractions (Figure 4.1A-D, 3H, 4A-C,P). Lower dosages of acetylcholine (1μM-5mM) resulted in no statistically significant changes in tentacle contractions, while higher concentrations of acetylcholine, 10mM and 25mM, ≥86% of animals contracted their tentacles. (p<0.05) (Figure 4.1A,F). After the initial tentacle contractions no additional contractions were observed, instead tentacles relaxed, likely due to acetylcholinesterase which have been shown to be broadly expressed in *Nematostella*(Anctil, 2009; Sebé-Pedrós et al., 2018). No tentacle retractions were observed when polyps were treated with acetylcholine and there was no change in the number of peristaltic contraction waves (Figure 4.2). Juvenile, 1-month, 2-month, and 3-month old polyps were then treated with 10mM acetylcholine to determine whether this tentacle contraction role was established once the polyp nervous system develops. There was no significant difference in the number of polyps with tentacle contractions, tentacle contractions occurred, on

average, in ≥84% of animals regardless of age (p>0.05; Figure 4.1H). This supports a previous publication which found that the juvenile polyp nervous system resembled the adult nervous system, just exhibiting fewer neurons (Havrilak et al., 2017).

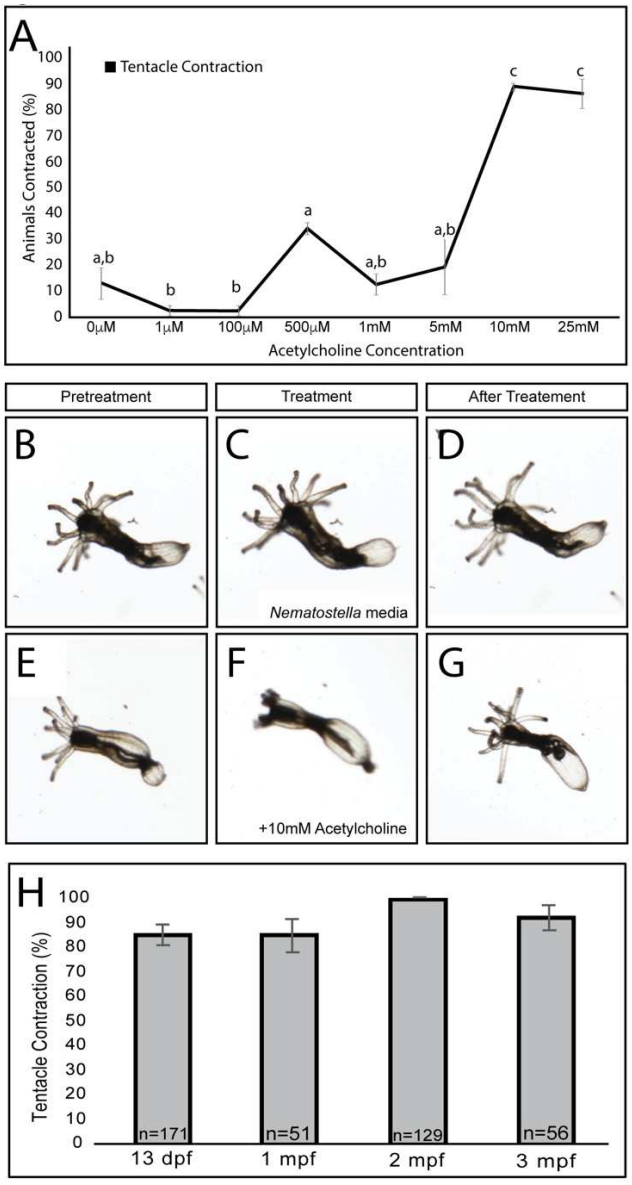

Figure 4.1: Acetylcholine induces tentacular contractions. (A) Contractile response to 0μM-25mM acetylcholine in three-month old polyps. The first response to acetylcholine occurred at 500μM acetylcholine with 33.6 ± 2.4% of animals contracting their tentacles but was not significantly different than the controls (p=0.339). At 1 mM tentacular contractions occurred in 12 ± 3.97% of polyps tested. At 5 mM tentacular contractions occurred in 18 ±10.82% of polyps. Tentacular contractions occurred in 88 ± 1.42% of polyps treated with 10mM and 85.9 ± 5.63% of polyps treated with 25mM acetylcholine. Tentacular contractions observed at 10mM and 25mM were statistically significant from contractions

observed polyps treated with control and lower concentrations of acetylcholine ($p \leq 0.05$). (B-D) Single frame images from movies showing tentacular response to the addition of Nematostella growth medium. (E-G) Single frame images from movies showing tentacular response to the addition of 10mM acetylcholine (F), and the subsequent relaxation that occurs after treatment (G). Response to acetylcholine is not significantly different ($p=0.196$)) between 13 days post fertilization (13dpf), two-months post fertilization (2mpf), or three-month post fertilization (3mpf) old polyps (H). In all images oral is to the left. These data were calculated using a one-way ANOVA. (A) Contractile response to 0μM-25mM acetylcholine in three-month old polyps $F_{7,18}=53.7$, $p<0.001$; (H) Response to acetylcholine at different time points $F_{3,8} = 1.98$, $p=0.196$. Each experiment was performed $N > 3$ times with an $n \geq 8$/replicate. Points that do not share letters in (A) are statistically different from each other. (mpf) months post fertilization. (dpf) days post fertilization.

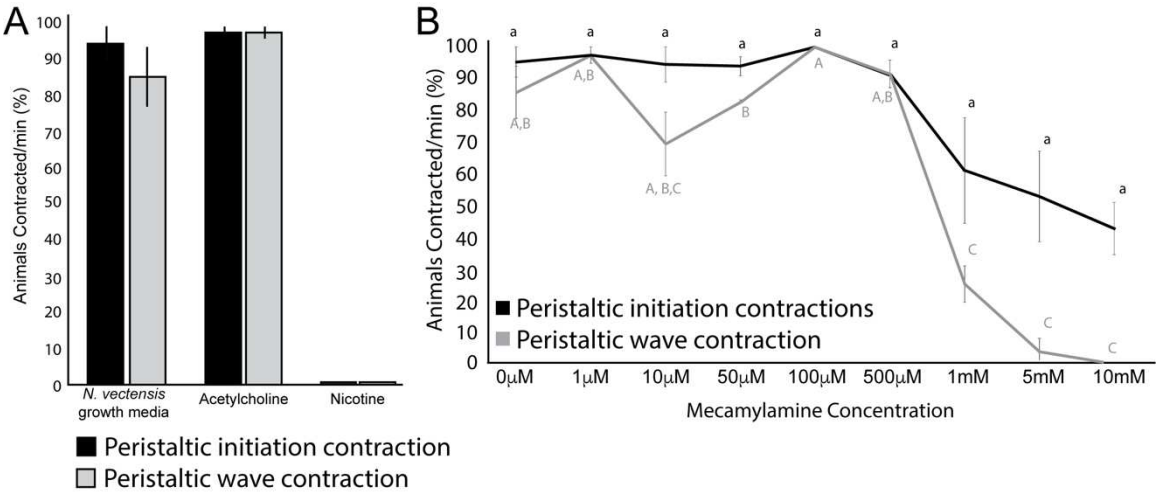

Figure 4.2: Quantifications of radial contractions and peristaltic waves in the presence of N. vectensis medium, acetylcholine, nicotine, and mecamylamine**.** (A) Treatment with acetylcholine did not induce a statistically significant difference in the number of animals with peristaltic initiation contractions (black) or peristaltic wave contractions (grey) ($p \geq 0.05$). Treatment with nicotine alone resulted in complete radial contractions, thus no peristaltic wave contractions or peristaltic initiation contractions occurred. (B) Treatment with mecamylamine at 1mM reduced the percentage of animals with peristaltic initiation contractions from ~91.53 ± 4.33% to 61.1 ± 16.6%. The peristaltic initiation contractions continued to drop to 42.6 ± 8.24% with 10mM mecamylamine. A similar drop was observed in the percentage of animals who performed peristaltic wave contractions from 91.53 ± 4.33% at 500μM to 25.39 ± 5.7%at 1mM mecamylamine. The radial contractions were reduced to 0 ± 0% when treated with 10mM mecamylamine. Each experiment was performed $N > 3$ times with an $n \geq 7$/replicate. P-values were calculated using a student t-test for (A) and a one-way ANOVA for (B). (B, black) Peristaltic initiation contractions in three-month old polyps pretreated with 0μM-10mM mecamylamine $F_{7,16}=7.06$, $p<0.005$ (B, gray) Peristaltic 843 wave contractions in three-month old polyps pretreated with 0μM-10mM mecamylamine $F_{8,18}=60.56$, $p<0.001$. Points that do not share letters, either uppercase or lowercase (B), are statistically different from each other

All of the acetylcholine receptors found within the genome of *Nematostella* have been nicotinic acetylcholine receptors, named for their ability to be activated by nicotine (Dani

and Bertrand, 2007). To further support that these tentacle contractions are due to binding to a nAChR polyps were treated with a dose response curve of nicotine (Figure 4.3H). Treatment with 1μM-1mM of nicotine resulted in no significant change in the number of animals that displayed tentacle contractions (Figure 4.3H). By 5mM 100% of polyps displayed contraction of their tentacles. These polyps did not relax after the initial contraction, likely due to the inability acetylcholinesterase to degrade nicotine (Figure 4.3-H, 4J-L, P). Nicotine treatment also induced contraction of the endodermal radial muscles, with these contractions occurring in 71-81% of polyps tested ~4mins after 5 or 10mM nicotine was added, respectively (Figure 4.3G). The nicotine induced contractions of the endodermal radial muscles were unexpected as they were not observed when polyps were treated with acetylcholine.

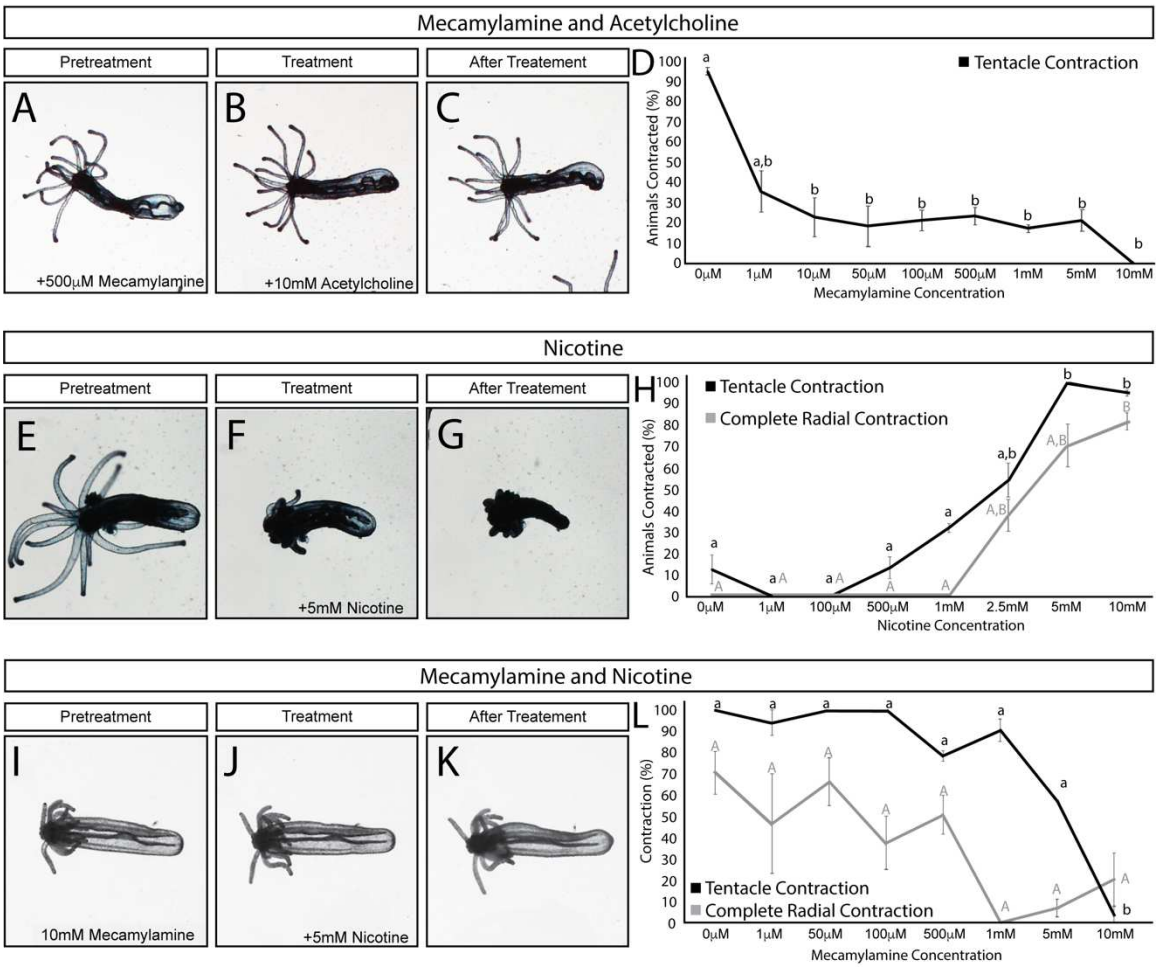

Figure 4.3:Pharmacological analysis of acetylcholine's role in tentacular contractions**.** (A-D) Acetylcholine-induced tentacle contractions in three-month old polyps pretreated with 0μM-10mM mecamylamine. At 0μM mecamylamine, 10mM acetylcholine induced tentacle contractions in 89 ± 2.32% of animals. This response dropped to 36 ±10.13% of animals at 1μM mecamylamine, though not significant ($p=0.095$). Acetylcholine-induced tentacle contractions occurred in 20% of animals when pretreated with 10μM-5mM mecamylamine and dropped to 0 ± 0% in animals treated with 10mM mecamylamine ($p\leq0.05$). (E-H) Nicotine-induced tentacle contractions occurred at 500μM with 13.33 ± 5.09% and increased to 54 ± 7.99% at 2.5mM, though these were not statistically different than the controls ($p>0.05$). At 5mM and 10mM, nicotine-induced tentacle contractions occurred in 100 ± 0% and 98 ± 1.36% of animals respectively, which was significantly different than the 0μM-2.5mM nicotine treatments ($p\leq0.05$). Nicotine-induced complete radial contractions were observed in 38 ± 7.43% of animals starting at 2.5mM nicotine. At 5mM and 10mM nicotine, 70 ± 10.0% and 82 ± 4.05% of animals respectively had complete radial contractions, these were significantly different than the controls ($p\leq0.05$). (I-L) Mecamylamine at lower concentrations (0μM-1mM) was not capable of blocking tentacular contractions. At 5mM, nicotine-induced tentacle contractions were reduced to 57.22 ± 16.4%, though not low enough to be significant ($p=0.433$). At 10mM mecamylamine, nicotine-induced tentacle contractions were significantly reduced to 3.7 ± 6.8% ($p\leq0.05$). Body contractions were not significantly reduced throughout the mecamylamine gradient, though at high levels (1mM-10mM mecamylamine) we did see a trend towards a reduction in the number of body contractions. These data were calculated using a one-way ANOVA (D) Acetylcholine-induced tentacle contractions in three-month old polyps pretreated with 0μM-10mM mecamylamine $F_{8,22}=14.03$, $p<0.001$; (H, black) Tentacle contraction in the response to nicotine at different time points $F_{7,17} = 43.15$, $p<0.001$. (H, gray) Body contraction in the response to nicotine at different time points

$F_{7,17} = 25.87$, $p<0.001$. (L, black) Tentacle contraction in three-month old polyps pretreated with 0μM-10mM mecamylamine $F_{7,16}=25.39$, $p<0.001$; (L, gray) Body contraction in three-month old polyps pretreated with 0μM-10mM mecamylamine $F_{6,14}=3.70$, $p<0.05$. Each experiment was performed N> 3 times with an $n \geq 7$/replicate. Points that do not share letters, either uppercase (in H and L) or lowercase (in D, H, L) are statistically different from each other.

To further confirm that acetylcholine and nicotine induced tentacle contractions occur due to binding to nicotinic acetylcholine receptors, and not due to off target effects, polyps were treated with a broad acetylcholine receptor antagonist, mecamylamine. Previous work has shown that mecamylamine functions to block acetylcholine within cnidarians, but has been used at varying concentrations (Mendes and De Freitas, 1984; Oliver et al., 2008) . Due to this we treated polyps with a dose response curve of mecamylamine (1μM to 10mM) to test the ability of mecamylamine to block tentacle contractions induced by 10mM acetylcholine (Figure 4.3A-D). Treatment with 1μM mecamylamine reduced acetylcholine induced tentacle contractions with a response in only 36.5% of animals tested (Figure 3D). At 10μM mecamylamine only ~20% of animals responded to 10mM acetylcholine (Figure 3D). Treatment with mecamylamine at 1mM and higher concentrations induced slight tentacle retractions, but no tentacle contractions (Figure 4.3A-D). None of the mecamylamine concentrations tested could significantly reduce the number of animals with nicotine induced radial muscle contractions, though from 1-10mM there was a trend towards no contractions (Figure 4.3I-L). ($p=0.400$). This ability for mecamylamine to block acetylcholine and nicotine induced tentacle contractions supports our hypothesis that acetylcholine is acting through acetylcholine receptors, within the tentacles. To further characterize the role of acetylcholine in regulating radial contractions, polyps were treated with mecamylamine and the number of peristaltic waves was quantified. Peristaltic waves are a continuous

wave of radial contractions which are initiated orally and then progress down towards the aboral end. Untreated polyps have one peristaltic wave/minute (Figure 4.2). Mecamylamine at concentrations of 500μM and higher significantly reduced peristaltic waves ($p \leq 0.05$) and the number of peristaltic waves initiated trended towards a reduction, though were not significantly reduced ($p \geq 0.05$) (Figure 4.2B). These data would suggest that acetylcholine plays a role in the regulation of both tentacle and radial contractions specifically through activation of nicotinic acetylcholine receptors.

Acetylcholine induced muscle contractions are due to neuronal activation

Acetylcholine within bilaterians is best known for its functions within neuronal and neuromuscular synapses. Despite data which supports a role in the regulation of muscle contraction it is unknown whether acetylcholine functions on neurons, muscle, or both (Ross, 1960; Kass-Simon and Passano, 1978; Mendes and De Freitas, 1984, 1984). To determine where acetylcholine functions in *Nematostella,* polyps were pretreated with lidocaine, a voltage-gated sodium channel blocker, which has been shown to function in *Nematostella* (Sheets and Hanck, 2003; Gur Barzilai et al., 2012) . If lidocaine is not capable of blocking acetylcholine induced tentacle contractions this would suggest that acetylcholine functions directly at the neuromuscular junctions. If lidocaine is capable of blocking tentacle contractions this would suggest that acetylcholine functions within a neuron upstream the neural circuitry that regulates tentacle contractions. Treatment with 5mM lidocaine, which has been previously shown to paralyze polyps, resulted in loss of acetylcholine induced tentacle contractions (Figure 4.4 D-I,P). Pretreatment with 5mM

lidocaine also blocked nicotine induced tentacle and radial contractions (Figure 4.4 M-O, Q). This loss of acetylcholine and nicotine induced contractions would suggest that acetylcholine functions within neurons and not at the neuromuscular junction. However, it is possible that off target effects from lidocaine could affect the musculature of *Nematostella*. These data, combined with previous publications, supports a conserved function of acetylcholine as a neurotransmitter within cnidarians, and likely functioned this way within the cnidarian ancestor. These conserved functions also supports the hypothesis that the cnidarian-bilaterian ancestor likely utilized acetylcholine as a neurotransmitter as well.

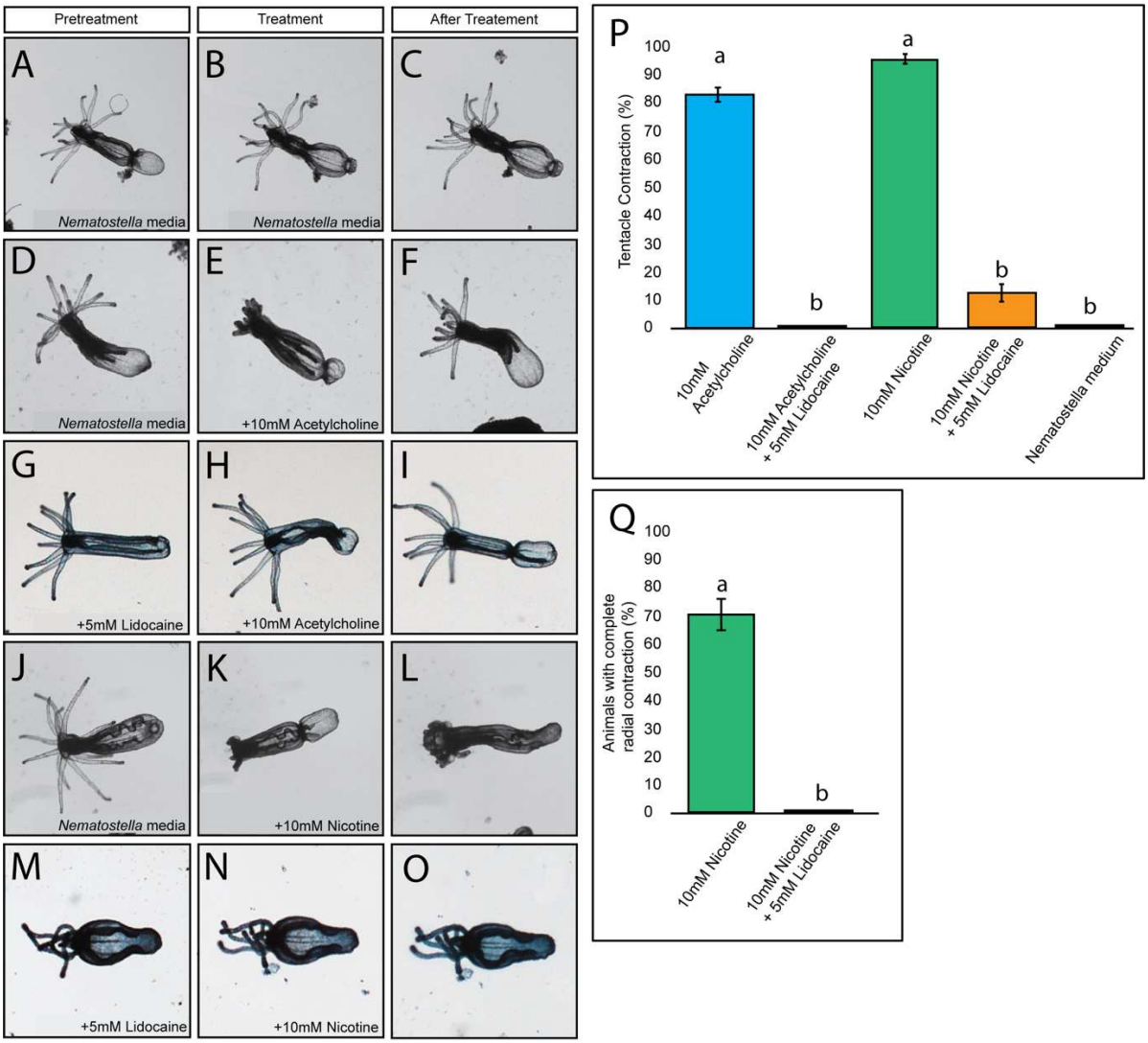

Figure 4.4: Lidocaine suppresses acetylcholine mediated tentacular contractions. Pretreatment with 10mM lidocaine resulted in loss of acetylcholine-induced tentacle contraction in all the juvenile polyps tested (A-C, G-I, P). This loss was statistically similar to controls (P) ($p \geq 0.05$). This was repeated in polyps pretreated with 10mM lidocaine and then 10mM nicotine (M-O, P). Samples pretreated with lidocaine had tentacular contractions that were significantly different from treatments with acetylcholine or nicotine alone ($p \leq 0.05\%$). Quantifications comparing the contraction of tentacles are summarized in P; bars that do not share letters indicate a significant difference between treatment groups. All images have the oral end directed to the left of the figure. P-values were calculated using a student t-test. Each experiment was performed N > 3 times with an n ≥ 7/replicate.

Nematostella possess 26 nicotinic acetylcholine receptors

The observed function of acetylcholine within neuronal chemical synapses suggested that it would be possible to identify a neuronal subtype involved in muscle contraction by

characterizing expression of nicotinic acetylcholine receptors. Previous work had identified 14 nAChRs but recent single cell sequencing analysis of polyps identified 8 additional receptors (Anctil, 2009; Sebé-Pedrós et al., 2018). This would suggest that the original identification these nAchRs was incomplete and should be reevaluated. BLAST, and updated RNAseq databases, were used to identify addition putative nAchRs within the published genome and nine additional AchRs were identified (Putnam et al., 2007). This brought the number of acetylcholine receptors up to 31 total. Five of these receptors lacked the cysteine loop necessary to form the acetylcholine binding pocket, and so were abandoned (Jones et al., 2005; Unwin, 2005). We then collected bilaterian mAchRs and nAchRs sequences, used GABAergic receptors on an outgroup, and performed a maximum likelihood phylogenetic analysis using RaxML and IQtree (Figure 4.5). Two previously published alignment methods were used for the phylogenetic analysis; an unedited alignment and an alignment consisting of the transmembrane domains and the double cysteines necessary for acetylcholine binding (Jones et al., 2005; Pedersen et al., 2019).

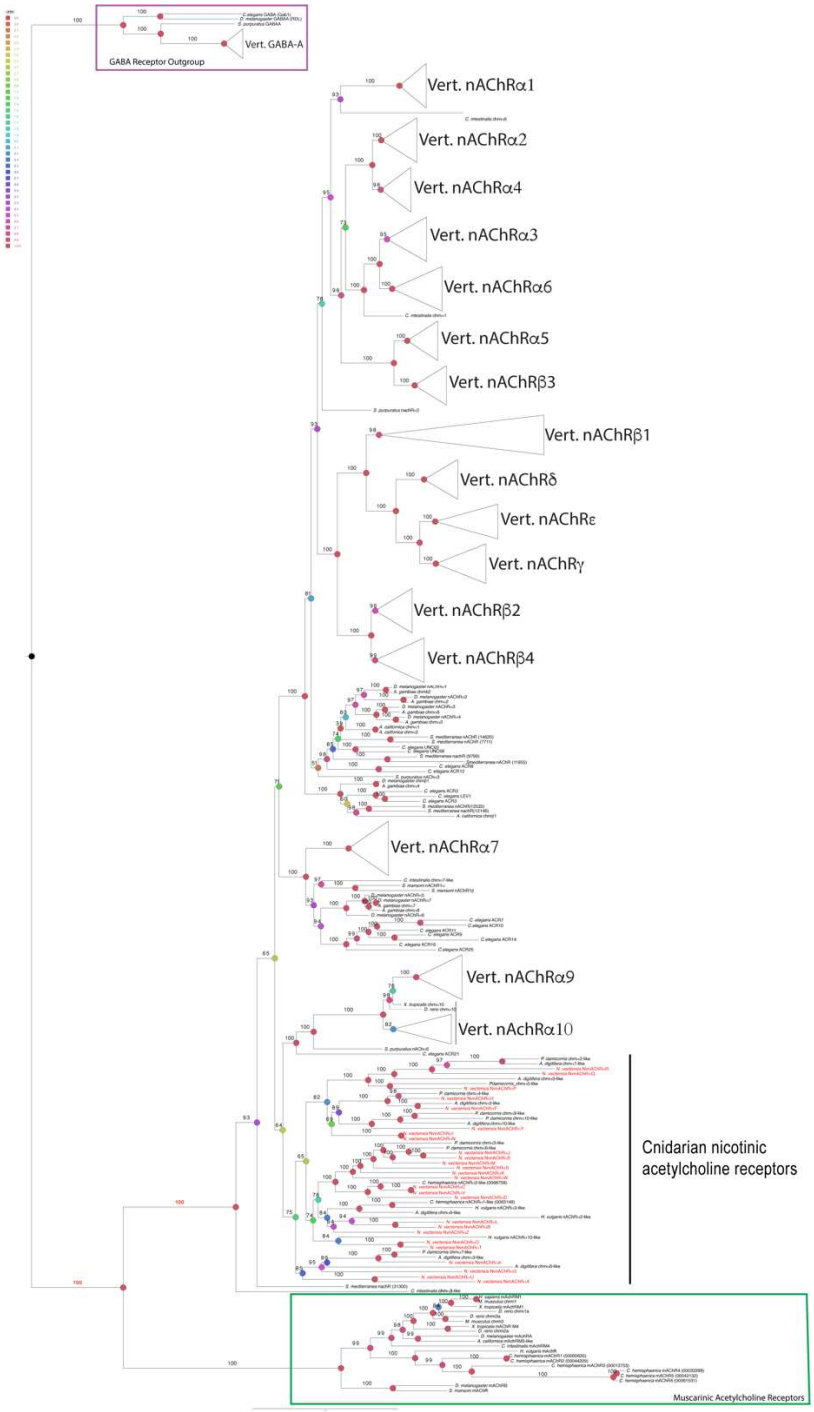

Figure 4.5: Phylogenetic analysis of unedited alignment of known and putative *AChR*s**.** Maximum likelihood tree, generated using IQ-tree, showing the relationship of potential cnidarian acetylcholine receptors to the known bilaterian nicotinic and muscarinic acetylcholine receptors. The GABA receptors, indicated by a purple box, served as the out-group for our analysis. Muscarinic receptors are indicated by a green box. The ultrafast bootstrap values for critical nodes of interest are written in red. Tree generated using alignment in Supplemental Table 2. Heat map also indicates ultrafast bootstrap values. *N. vectensis* sequences are in red text on tips of tree branches.

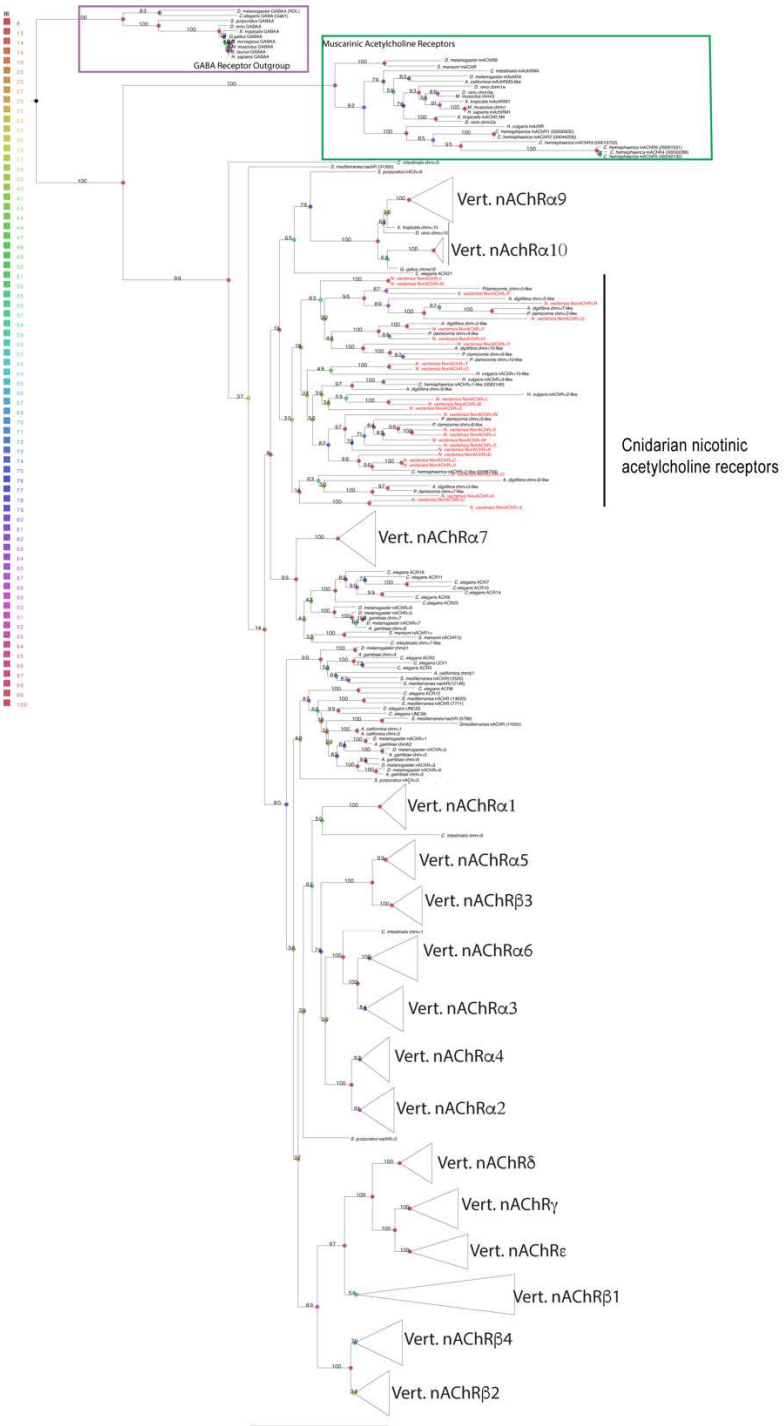

Figure 2.6: Unedited RaxML Phylogenetic tree. RaxML generated maximum likelihood tree determining the relationship of potential cnidarian acetylcholine receptors to the known bilaterian nicotinic and muscarinic acetylcholine receptors. The GABA receptors, indicated by a purple box, served as the outgroup for our analysis. Muscarinic receptors are indicated by a green box. The bootstrap values for critical nodes of interest are written in red.. Heat map also indicates bootstrap values. Nematostella sequences are in red text on tips of tree branches.

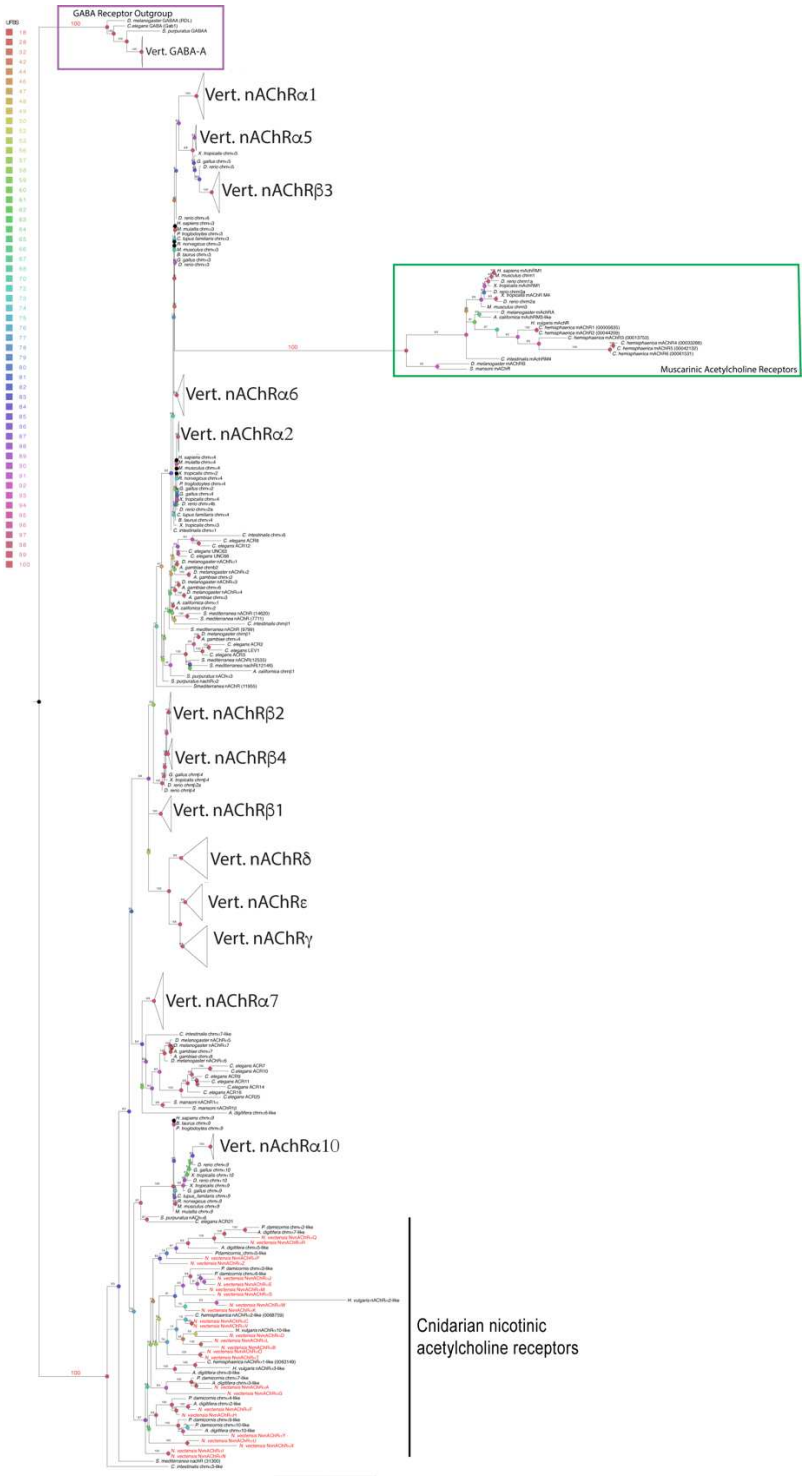

Figure 4.7: IQ-tree Phylogenetic tree using transmembrane domain and double cysteines**.** IQ-tree generated maximum likelihood tree determining the relationship of potential cnidarian acetylcholine receptors to the known bilaterian nicotinic and muscarinic acetylcholine receptors. The GABA receptors, indicated by a purple box, served as the outgroup for our analysis. Muscarinic receptors are indicated by a green box. ultrafast bootstrap values for critical nodes of interest are written in red. Tree generated Heat map also indicates ultrafast bootstrap values. *Nematostella* sequences are in red text on tips of tree branches.

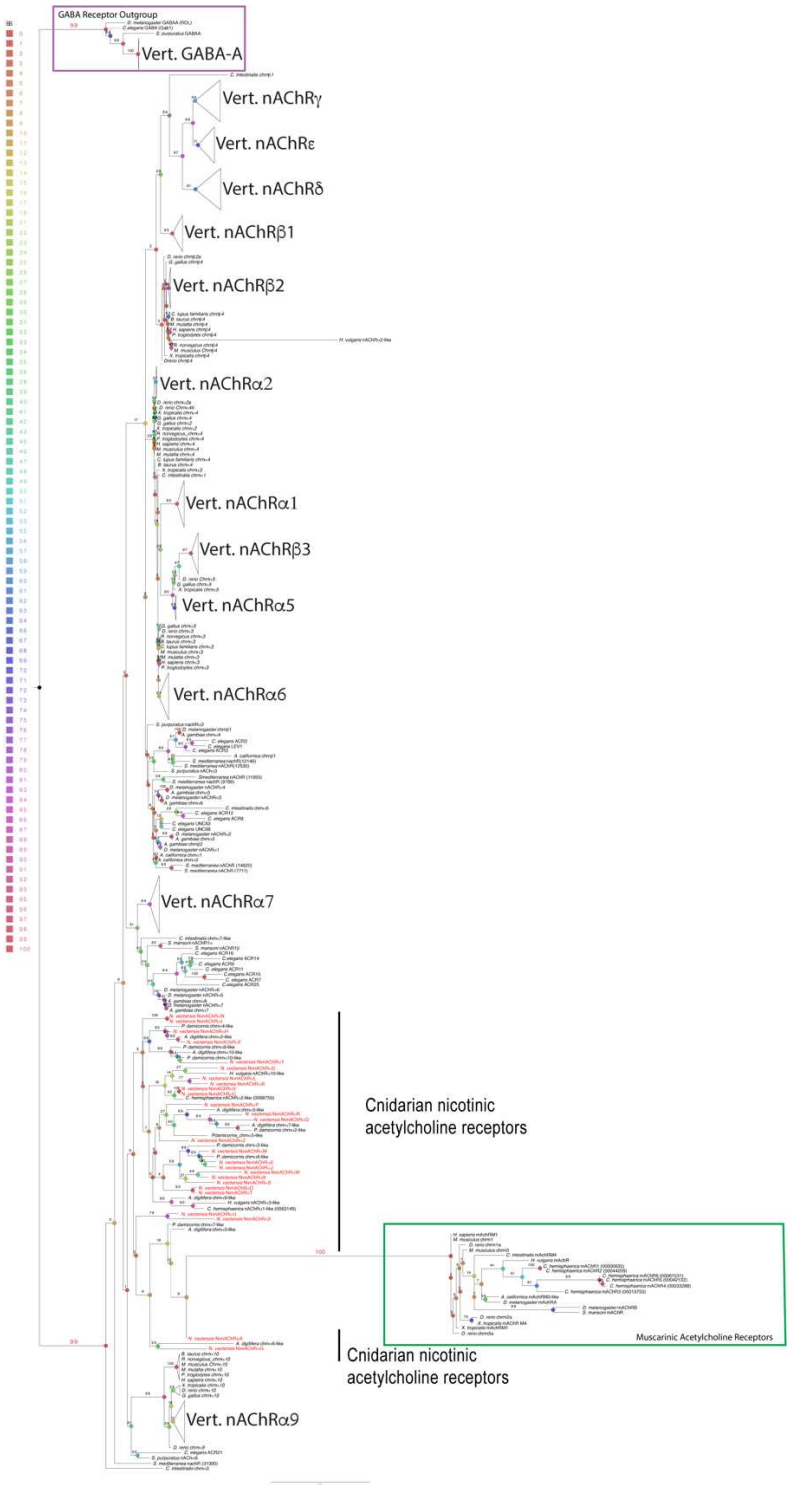

Figure 4.8: RaxML Phylogenetic tree using transmembrane domain and double cysteines**.** RaxML generated maximum likelihood tree determining the relationship of potential cnidarian acetylcholine receptors to the known bilaterian nicotinic and muscarinic acetylcholine receptors. The GABA receptors, indicated by a purple box, served as the outgroup for our analysis. Muscarinic receptors are indicated by a green box. The bootstrap values for critical nodes of interest are written in red.. Heat map also indicates bootstrap values. *Nematostella* sequences are in red text on tips of tree branches

All *Nematostella* AChRs clustered within known AChRs in trees generated using the unedited and TD alignments and clustered with other cnidarian acetylcholine receptors (UFBS = 100, 10 0) (BS = 100, 98) (Figure 4.5-4.8). All muscarinic receptors, including the single *Hydra* mAChR and the six *C. hemisphaerica* mAChRs, formed their own clade (UFBS = 100; BS = 100). None of the potential *Nematostella* sequences clustered with the muscarinic receptors and all sequences lacked the Q207(M3)/Q163(M2) and L204 motif necessary for G-coupled signaling in mAChrs, which supports previous reports suggesting that *Nematostella* do not possess mAChRs (Figure 4.5-4.8) (Anctil, 2009; Kruse et al., 2012). Phylogenetic placement of the muscarinic clade was dependent on the alignment edit and the phylogenetic analysis. IQtree and RaxML trees generated with the unedited alignment placed the muscarinic receptors as sister to the nicotinic receptors, but phylogenies generated using the edited alignments placed the muscarinic clade as sister to the bilaterian nAchα3 clade, or nested within the cnidarian receptors (Figure 4.5-4.7 UFBS = 100, BS = 100). These data here support that all acetylcholine receptors identified in *Nematostella* are nAChRs. As there is no consensus on the naming strategy for *Nematostella* acetylcholine receptors, the 26 genes identified here have been named NvnAChRαA–NvnAChRαZ (Table 4.1). This naming structure was used so as not to confuse receptors with established subunits which are classified using a number to define orthologous receptors.

All analyses performed support that all *Nematostella* genes, including the 14 previously undescribed acetylcholine receptors, presented here are AchRs and belong to the nAChR family. These phylogenetic data provided evidence to support previous reports suggesting

independent radiation of cnidarian and bilaterian nAChRs. We also observed evidence to support that gene duplication events occurred within the *Nematostella* nAChRs. Several receptors, NvnAChRαJ and NvnAChRαE, NvnAChRαC and NvnAChRαV, and NvnAChRαI and NvnAChRαN, are always sister with each other and could potentially be paralogs.

Our Name	JGI: Protein ID	NvERTx	Anctil et al. 2009 (Genome)	Sebes et al. 2018 (Single Cell RNA seq.)	Sinigaglia et al. 2015 (*in situ*)	JGI/Warner et al. 2018 (RNA-seq)
NvnAChRαA	31824	NvERTx.4.110720				31824/NvERTx.4.110720
NvnAChRαB	50745	NvERTx.4.143847				50745/NvERTx.4.143847
NvnAChRαC	11255	NvERTx.4.141630				11255/NvERTx.4.141630
NvnAChRαD	214990	NvERTx.4.137798	214990*	214990* (N/tlM)		
NvnAChRαE	91941	NvERTx.4.75581	91941*	91941* (N/tlM)		
NvnAChRαF	61041	NvERTx.4.55041				61041/NvERTx.4.55041*
NvnAChRαG	85724	NvERTx.4.110720		85724* (N/tlM)		
NvnAChRαH	85091	NvERTx.4.88235	85091*			
NvnAChRαI	205808	NvERTx.4.61521	205808*	205808* (N/tlM)		
NvnAChRαJ	199721	NvERTx.4.82387	199721*		ao145* (AO)	
NvnAChRαK	110265	NvERTx.4.147304	110265*		ao19* (AO)	
NvnAChRαL	205856	NvERTx.4.61144				205856/NvERTx.4.61144
NvnAChRαM	32916	NvERTx.4.161999				32916/NvERTx.4.161999
NvnAChRαN	205855	NvERTx.4.63946	205855			
NvnAChRαO	40806	NvERTx.4.31008				40806/NvERTx.4.31008
NvnAChRαP	87907	NvERTx.4.85000				87907/NvERTx.4.85000
NvnAChRαQ	198343	NvERTx.4.152487	198343*			
NvnAChRαR	198927	NvERTx.4.153628	198927*	198927* (N/tlM)		
NvnAChRαS	200917	NvERTx.4.111130	200917			
NvnAChRαT	40919	NvERTx.4.145232	40919			
NvnAChRαU	91696	NvERTx.4.52490	91696	91696* (N/M)		
NvnAChRαV	216224	NvERTx.4.141630		216224* (N/tlM/G)		
NvnAChRαW	57113	NvERTx.4.97064		57113 (N/G)		
NvnAChRαX	91371	NvERTx.4.56195		91371 (N/M)		
NvnAChRαY	79911	NvERTx.4.127752		79911 (N/M)		
NvnAChRαZ	97337	NvERTx.4.72427		97337* (N/M)		
Previously Identified Ach. Receptors that are removed in this study						
All missing Cysteine Loop	240779	NvERTx.4.60558	240779*	240779* (tlM)		
	247410	NvERTx.4.76805	247410			
	22673	NvERTx.4.133515		22673 (N/tlM)		
	2281	NvERTx.4.56575		2281 (N/M)		
	205764	NvERTx.4.109818				205764/NvERTx.4.109818*

Table 4.1: Naming mechanisms for Acetylcholine receptors in *Nematostella*. A collection of previously identified, named, and characterized acetylcholine receptors gathered from the literature, BLAST searches of the JGI Nematostella genome (https://genome.jgi.doe.gov/Nemve1/Nemve1.home.html), and identified from BLAST searches of the NvERTx database (https://genome.jgi.doe.gov/pages/search-for-genes.jsf?organism=Nemve1). Confirmed nicotinic acetylcholine receptors are listed in the top portion of the table and were renamed NvnAChRαA-Z. Previously identified receptors that lack necessary features of nAChRs were excluded from analysis and are listed in the bottom portion of the table. Previously published expression patterns for acetylcholine receptors, and the publication they were described in, are indicated for each gene. N= neurons, M= muscle, tlM= tentacular and/or longitudinal muscle, G=Gonad, AO=apical organ. Asterisk indicates genes we obtained mRNA in situ hybridization patterns for in Figure 4.

Spatiotemporal expression of acetylcholine receptors supports neuronal and non-neuronal roles of acetylcholine

With the identification of 26 different acetylcholine receptors we then attempted to characterize their spatial expression, with goal of identifying a nAChRs positive neurons.

Single-cell sequencing previously identified expression of nAChRs within neurons and tentacles or longitudinal muscles (Sebé-Pedrós et al., 2018). All nAChRs identified in the tentacular and longitudinal musculature were cloned (*NvnAChRαD, NvnAChRαE, NvnAChRαG, NvnAChRαI, NvnAChRαR,* and *NvnAChRαV*). *NvnAChRαD, E, and R* were confirmed to be expressed within the tentacles with *NvnAChRαD and NvnAChRαE* expressed in the ectoderm near the distal end of the tentacles (Figure 4.9D, H, T, Figure 4.10). At larval stages *NvnAChRαD and NvnAChRαE* were expressed in the developing endoderm with *NvnAChRαE* also expressed in the developing tentacle buds and enriched in the endoderm at the aboral pole(Figure 4.9B, C, F, and Figure 4.9G). *NvnAChRαR* appears to be ubiquitously expressed at low-levels during larval and tentacle bud stages (Figure 4.9R, S). At polyps stages *NvnAChRαR* is broadly expressed throughout the tentacle ectoderm which could suggest expression within tentacle muscles though would also suggest that it is not specific to muscle cells (Figure 4.9T). The broad expression patterns for *NvnAChRαD, E, and R* supports the possibility for both a cell signaling and neuronal roles for these receptors. During development and in juvenile polyps, *NvnAChRαI, NvnAChRαG,* and *NvnAChRαV* are expressed in cells around the pharynx (Figure 4.9L, P, X). The *in situ* expression pattern of *NvnAChRαV* is consistent with previous reports of expression in the developing gonad Figure 4.9). *NvnAChRαI* and *NvnAChRαG* were not reported to be expressed in gonads so it is unclear if are false negatives in the data or are expressed in a distinct population of cells (Sebé-Pedrós et al., 2018). Despite similarities in expression, the expression patterns of *NvnAChRαV, NvnAChRαI, and NvnAChRαG* are not identical. *NvnAChRαI* and *NvnAChRαG* are expressed in smaller domains than *NvnAChRαV* (Compare Figure 4.9L, P, X).

NvnAChRαU and *NvnAChRαZ* have been reported to be broadly expressed in muscle cells (Sebé-Pedrós et al., 2018). Yet *NvnAChRαU* expression within the developing and juvenile polyp pharynx is similar to *NvnAChRαG, NvnAChRαI*, and *NvnAChRαV* (Figure 4.9AA, AB). While, *NvnAChRαZ* seemed be ubiquitous expressed at low levels in planula stages and at later stages were undetectable, however it has been reported to be expressed at high levels after 114hpf (Figure 4.9AD, AF; Figure 4.11). The inability to detect expression of *NvnAChRαG, NvnAChRαI, NvnAChRαV,* and *NvnAChRαU* within muscle or neuronal cells was surprising. One possible explanation for this could be that these genes are expressed at low levels in neurons and/or muscle making detection by *in situ* hybridization difficult in those cell types. The *in situ* patterns obtained here suggests that, despite previously identified expression of *NvnAChRαD, NvnAChRαE, NvnAChRαR, and NvnAChRαZ* within musculature and neurons, these receptors are likely not exclusively to those cells types.

Within bilaterians acetylcholine has also been shown to play a role in cell to cell signaling, proliferation, and differentiation (Wessler and Kirkpatrick, 2008; Maouche et al., 2009). To identify whether these roles exist within *Nematostella* we also characterized the expression of receptors not known to be expressed in neurons or muscle (*NvnAChRαH, NvnAChRαJ, NvnAChRαK, NvnAChRαQ, NvnAChRαB, NvnAChRαC*. and *NvnAChRαF*). *NvnAChRαH* expressed started in the larval pharynx, then expressed broadly in the endoderm of forming tentacle buds, and as polyps expressed around the pharynx in a similar expression to *NvnAChRαG, NvnAChRαI, NvnAChRαU,* and *NvnAChRαV* (Figure 4.9AG–AJ). *NvnAChRαB* is expressed in a scattered salt and pepper

pattern in developing and formed tentacles (Figure 4.9AW– AZ). *NvnAChRαC* is first expressed in a scattered salt and pepper pattern within the planula endoderm (Figure 4.9BB). At the tentacle bud stage, expression became restricted to the endodermal tissue beneath the tentacle tips (Figure 4.9BD). *NvnAChRαF* expression started at the late planula/tentacle bud stage in the endodermal tissue, where the tentacles had begun to develop (Figure 4.9BG). At the juvenile polyp stage, *NvnAChRαF* expression became restricted to a few cells near the base of the tentacles (Figure 5BH). Previous work reported that *NvnAChRαB, C,* and *F* are not expressed in neurons but the scattered salt and pepper pattern of likely represents expression in differentiated cell types. We also found that *NvnAChRαQ*, which was not identified in previous single-cell RNA sequencing, was expressed in the tentacles and in the body column, sharing some overlap with the ectodermal expression of *NvnAChRαR, D, and E* (Figure 4.9A–H, AS–AV). *NvnAChRαJ* and *NvnAChRαK* (aka, 199721/ao145 and 110265/ao19, respectively) were expressed in the apical organ ectoderm of planula larvae, consistent with previously observed expression patterns, this apical expression was then lost in juvenile polyps (Figure 5AK–AR) (Sinigaglia et al., 2015). Within free-swimming bivalves larvae acetylcholine signaling has been linked to metamorphosis, and the apical organ is linked to settlement and metamorphosis in some corals(Strader et al., 2018). This aboral expression of could suggest that *NvnAChRαJ* and *NvnAChRαK* play a conserved role for acetylcholine in anthozoan cnidarian metamorphosis.

Seven of the 14 expression patterns recovered (*NvnAChRαD, E, R, H, J, K, Q, and V*) had expression patterns more consistent with cell signaling or developmental patterning than

restricted roles in neurons and/or muscle. Bilaterian AChRs function within multiple non-neuronal cell types, neuronal cells, and muscles cells. Although we were unable to generate probes for all of the predicted NvnAChRs, our expression data argue for both neuronal and non-neuronal functions for acetylcholine and these roles were likely present in the cnidarian–bilaterian ancestor nAChR.

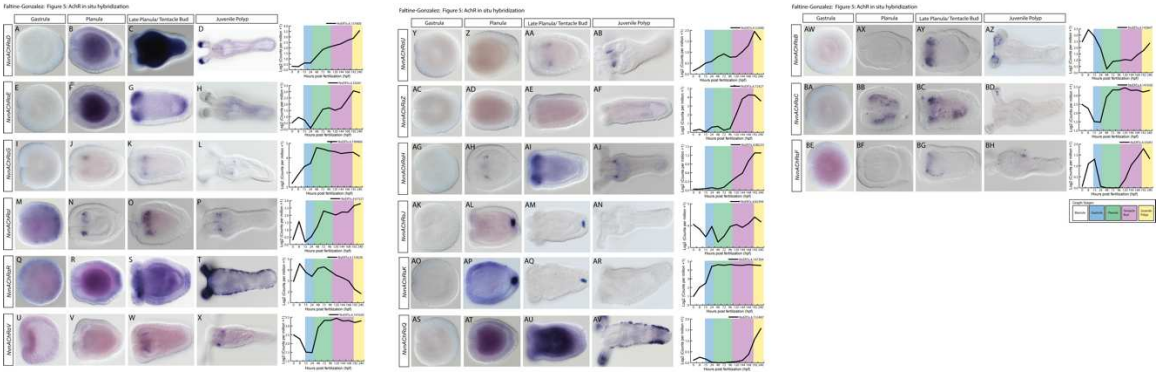

Figure 4.9: Expression patterns of *Nematostella* nicotinic acetylcholine receptor genes. *NvnAChRαD* was broadly expressed in the planula and tentacle bud stages but then became restricted to the endodermal tips of the tentacles (A-D). *NvnAChRαE* expression begun during the planula stages and then became restricted to the tentacle buds at the tentacle bud stage. By the polyp stage, expression was restricted to a band in the tentacles (E-H). *NvnAChRαG* expression begun in the planula within the developing pharynx, and this pharyngeal expression was maintained into the juvenile polyp stage (I-L). *NvnAChRαI* expression started in a scattered salt and pepper pattern at the aboral end, then restricted to the developing pharynx in the planula and was maintained here in the juvenile polyp (M-P). *NvnAChRαR* expression started broadly within the gastrula, planula, and tentacle bud stages, and this broad expression was maintained in the endoderm of the juvenile polyps (Q-T). *NvnAChRαV* expression started at the late planula stage within the pharynx, and expression was maintained there in the juvenile polyps (U-X). *NvnAChRαU* expression started at the late planula/early tentacle bud stage in the developing pharynx, and was maintained there in the juvenile polyps (Y-AB). We did not observe any expression of *NvnAChRαZ,* despite RNA sequencing data suggesting expression after 144hpf (AC-AF). Expression of *NvnAChRαH* started at the planula stage in the developing pharynx, and was maintained there in the juvenile polyps (AG-AJ). *NvnAChRαJ* and *NvnAChRαK* expression both started in the planula stages, continued being expressed into the tentacle bud stage at the apical tuft, and was lost by the juvenile polyp stage (AK-AR). *NvnAChRαQ* was first broadly expressed at the planula and tentacle bud stages, then became restricted to endodermal tentacle and aboral ectoderm (AS-AV). A scattered salt and pepper expression of *NvnAChRαB* was observed in the developing tentacles, and the tentacles of the juvenile polyps (AW-AZ). *NvnAChRαC* expression was observed at the planula stages as a scattered salt and pepper pattern in the endoderm until the juvenile polyp stage, when expression was restricted to the tentacle tips (BA- BD). *NvnAChRαF* was expressed at the late planula stages within a few cells of the developing tentacles; this expression became restricted to a cluster of cells at the basal end of the tentacles (BE-BH). Graphs at the end of each row consists of the temporal expression according to previously published RNA-seq. data (Warner et al., 2018). Within the graphs, white= blastula, blue=gastrula, green=planula, red=late planula/tentacle bud, and yellow= juvenile polyp stages. All images have the oral end directed to the left.

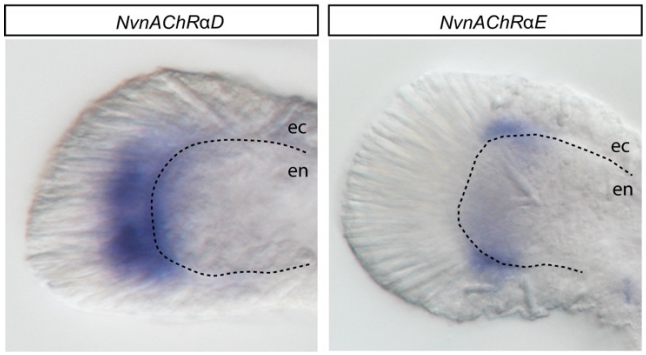

Figure 4.10: Expression of *NvnAChRαD* and *NvnAChRαE* in the tentacles**.** Expression of *NvnAChRαD* and *NvnAChRαE* are restricted to the tentacular ectoderm. Dotted line separates the ectoderm and endodermal tissue layers. ec = ectoderm, en =endoderm.

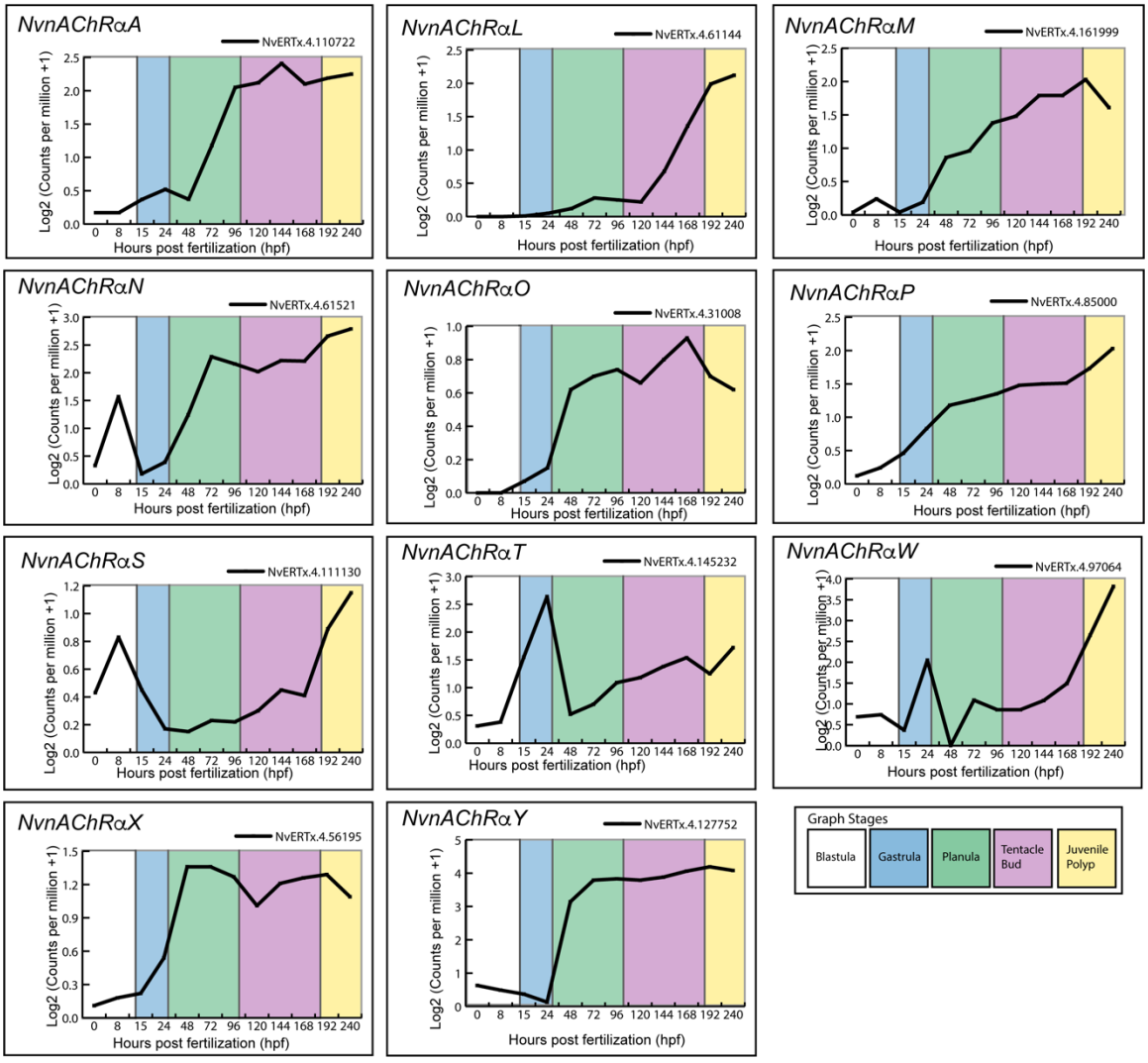

Figure 4.11: Expression profiles for NvnAChRs without in situ expression profiles. Expression profiles, in log2 (counts per million +1) were collected from the NvERTx database for those receptors that could not be cloned. White regions indicate the blastula stage, blue labels the gastrula stage, green labels the free-swimming planula stage, red labels the tentacle bud stage, and yellow labels the juvenile polyp stage.

Discussion

Acetylcholine modulates muscular contraction through upstream nicotinic acetylcholine receptor positive neurons

The original goal of this aim was to identify cholinergic neurons with the longterm goal of identifying their developmental trajectory. Before cholinergic neurons could be identified the role of acetylcholine needed to be confirmed within *Nematostella*. Here we

show that treatment with acetylcholine results in tentacle contractions (Figure 4.1). Nicotine induced tentacle contraction further supported this role for acetylcholine in mediating tentacle contractions. Interestingly, nicotine was capable of inducing whole body radial contractions, which was not observed which was not observed with the acetylcholine treatments. As nicotine is cell permeable, allowing access to endodermal tissue, while acetylcholine is not this could suggest that acetylcholine also modulates radial contractions. We showed that both these tentacle and radial contractions were blocked when polyps were pretreated with mecamylamine. Mecamylamine also reduced peristaltic wave contractions, these data further support a role of acetylcholine in modulating tentacle and radial contractions. Lastly pretreatment with the voltage-gated sodium channel blocker, lidocaine, was able to inhibit all acetylcholine or nicotine induced contractions. These pharmacological experiments support the hypothesis that acetylcholine functions as a neurotransmitter and likely through acetylcholine receptors expressed within neurons that modulate muscle contraction.

Within bilaterians lidocaine has been observed to inhibit smooth muscle contractions through muscarinic receptors within bilaterians (Kai et al., 1993). Lidocaine does not disrupt nAChRs, there are no muscarinic receptors in the *Nematostella* genome(Putnam et al., 2007). The two *Nematostella* genes that cluster most closely with muscarinic receptors in a subset of our phylogenies (NvnAChRαA and NvnAChRαG) are also not expressed in tentacles or radial muscle cells (Table 4.1; Figure 4.9I–L) (Sebé-Pedrós et al., 2018). Together, these observations allow us to argue that the inhibition of muscular contractions are not due to known off targets effects of lidocaine on the tentacle

musculature. However, it is possible that an unidentified protein expressed in muscles could be affected by an off-target of lidocaine, or that lidocaine could inhibit *Nematostella* NvnAChRs themselves. Currently there is no evidence supporting direct activation of muscle by acetylcholine, as such future experiments aimed at further characterization of nAChR function at the cellular level are necessary in *Nematostella*.

Expression of nicotinic acetylcholine receptors suggests neuronal and non-neuronal roles for acetylcholine in *Nematostella*.

Previous research found 14 nicotinic acetylcholine receptors within the genome of *Nematostella*, more recent single cell sequencing found 8 more nicotinic acetylcholine receptors, and our own BLAST analysis found 9 more (Putnam et al., 2007; Anctil, 2009; Sebé-Pedrós et al., 2018). The phylogenetic analysis performed here found that 26 of these 31 sequences were true nicotinic acetylcholine receptors and found no muscarinic acetylcholine receptors (Figure 4.5-4.8). Once these genes were identified developmental time series for performed for 16/26 with the goal to use *in situ* hybridization to identify these nAChR positive neurons. Instead, we observed expression of *NvnAChRαD, NvnAChRαE*, and *NvnAChRαR* within the tentacle ectoderm, where the tentacular contractile muscles reside (Figure 4.9 A–H, Q–T, Figure 4.10) [3,46]. *NvnAChRαD* and *NvnAChRαE* expression overlapped with the tentacular longitudinal muscles, and *NvnAChRαR* is expressed throughout the tentacles in a broad domain likely containing both neuron and muscle cells. None of the *NvnAChR* genes have expression patterns consistent with being expressed within radial muscle cells, though single-cell RNAseq data would suggest that *NvnAChRαX–Z* and *NvnAChRαU* are likely candidates to be

expressed in radial muscles (Sebé-Pedrós et al., 2018). *NvnAChRαC* expression which would suggest expression in endodermal neurons that could regulate radial muscles, but *NvnAChRαC* was not identified in neurons by single–cell RNAseq [3]. Its possible that *in situ* hybridization is not sensitive enough to detect low expression levels of these receptors within neurons. More detailed analysis of single-cell RNAseq data coupled with functional studies at single cell resolution are necessary to determine which cells require acetylcholine to induce contractions of *Nematostella* musculature. Despite this our data suggests a conserved role for nAChRs and acetylcholine as neurotransmitters.

This aim focused on the identification of a neuronal role for acetylcholine, but within multiple metazoans, it has been found to also function in non-neuronal roles (Anctil, 1985; Wessler and Kirkpatrick, 2008; Di Sansebastiano et al., 2014). We found that in *Nematostella* the receptors *NvnAChRαD, E, R, H, J, K, Q,* and *V* all had patterns that are consistent with non-neural functions (Figure 4.9). Many of these genes were expressed in dynamic developmental patterns and were broadly expressed in a tissue during larval stages (such as in the tentacle bud, the apical organ, or pan-endodermally), but then subsided. The broad non-cell-type-specific pattern that is dynamic during development is more consistent with a role in patterning than it is with a defined neuronal or muscle function. However, it does not eliminate the notion that those genes could be functioning at chemical synapses in the neurons and/or muscles in which they are expressed. *NvnAChRαB*, *NvnAChRαC*, and *NvnAChRαF*, all had a scattered salt and pepper expression in the juvenile polyp pharynx (Figure 4.9AW–BH). None of these genes were identified as neuronal, muscular, cnidocyte, or gland cells in the single-cell RNA-

sequencing data set. It is unclear if cells expressing *NvnAChRαB*, *NvnAChRαC*, and *NvnAChRαF* represent an unknown cell type or represent false negatives in the single-cell RNA-sequencing data (Sebé-Pedrós et al., 2018). Two receptors have expression consistent with a role for acetylcholine in metamorphosis. *NvnAChRαJ* and *NvnAChRαK* are expressed in the apical organ in late stage planula (Figure 4.9 O, S) (Sinigaglia et al., 2015). Acetylcholine has been found to be involved in the settlement and metamorphosis of free-swimming bivalve larvae including *Pinctada maxima, Crassostrea gigas, Mytilus edulis,* and *Mytilus galloprovincialis* as well as within coral planula larvae (Sánchez-Lazo et al., 2012; Strader et al., 2018) . The presence of broad expression patterns that are consistent with roles in development for 7 of the 15 genes tested here suggests that non-neuronal functions likely existed for the ancestral nAChRs that radiated in the cnidarian and bilaterian lineages.

The evolution of nicotinic acetylcholine receptors in *Nematostella* and its implications for the evolution of acetylcholine function in metazoans

The data presented here was not capable of identifying nAchR positive neuronal subtypes but does provide some insight on the evolution of acetylcholine function and receptors. We found that the 26 acetylcholine receptors identified in this study are more closely related to other cnidarian receptors than to any of the bilaterian acetylcholine receptors (Figure 4.5). This finding combined with the lack of nicotinic acetylcholine receptor sequences within the published genomes of ctenophores and poriferans would suggest that the nAChrs were present in the cnidarian-bilaterian ancestor (Srivastava et al., 2008, 2010; Ryan et al., 2013; Moroz et al., 2014; Moroz and Kohn, 2016). This would also

suggest that the cnidarian and bilaterian receptors then radiated within each lineage independently. This independent radiation is further supported by the way the protostome–deuterostome nAChRs largely form independent clades suggesting that small number of nicotinic acetylcholine receptors were found in protostome–deuterostome ancestor. A similar phenomenon has been suggested in muscarinic family evolution, which suggests independent expansion of muscarinic receptors in protostome and deuterostome lineages (Pedersen et al., 2018).

We found no support for a *Nematostella* muscarinic acetylcholine receptors but previous work identified one cnidarian muscarinic receptor in Hydra (Collin et al., 2013). BLAST search of the *Clytia hemisphaerica* genome performed in this study found six muscarinic acetylcholine receptors (Figure 4.5-4.8) (Leclère et al., 2019). Interestingly, no cnidarian muscarinic acetylcholine receptors have been identified outside of the hydrozoans. This could suggest that muscarinic receptors were present in the cnidarian–bilaterian ancestor, but were lost in anthozoans. However, an improved understanding of cnidarian muscarinic receptors is required to better determine the gain–loss patterns and evolution of mAChRs in animals. This would also explain the differing response to atropine seen within pharmacological studies between hydrozoans and anthozoans (Kass-Simon and Pierobon, 2007).

The widespread role for acetylcholine-mediated contractions in cnidarians (Figs. 4.1-4.4), its conserved expression in neurons and muscles (Figure 4.9), and the fact that 11 of the *Nematostella* receptors are expressed in neurons and/or muscle, make for a strong

argument that the neuronal role of nAChRs was present in stem cnidarians (Kass-Simon and Passano, 1978; Mendes and De Freitas, 1984; Scemes and Mendes, 1986; Oliver et al., 2008). The broadly identified neuronal function for nAChRs in cnidarians and bilaterians would suggests that the neuronal functions of nAChRs arose coincidentally at or near the base of nAChR evolution prior to the cnidarian–bilaterian divergence. Lastly, the identification of multiple nAChRs supports non-neuronal functions for acetylcholine in *Nematostella* and would suggest that these functions predate neuronal roles.

Responses to acetylcholine are best characterized within bilaterians but clear responses have been identified within basal metazoans, fungi, and plants lacking acetylcholine receptors (Dani and Bertrand, 2007; Wessler and Kirkpatrick, 2008; Di Sansebastiano et al., 2014; Bamel et al., 2016). The enzymes necessary for acetylcholine synthesis have been identified within metazoans, plants, and single-celled organisms, while acetylcholine has been isolated from bacteria, fungi, plant, and metazoan extracts (Horiuchi et al., 2003; Kawashima et al., 2007). In the fungi, *Candida albicans*, acetylcholine inhibits biofilm formation (Rajendran et al., 2015). Acetylcholine treatment within plants has shown effects on growth regulation, cellular differentiation, water homeostasis, and photosynthesis (Di Sansebastiano et al., 2014; Bamel et al., 2016). Treatment of acetylcholine in ctenophores and poriferans, have shown increased luminescence excitation and prolonged cycles of rhythmic contraction, respectively (Anctil, 1985, 1985; Ellwanger and Nickel, 2006). These observations make for a strong argument that the non-neuronal acetylcholine signaling predated the neuronal functions described for nAChRs and mAChRs. However, it is unclear if the non-neuronal functions

for bilaterian nAChRs and mAChRs arose within the bilaterians or nearer the base of nicotinic and muscarinic receptor evolution.

Material and Methods

Phylogenetic analysis

Bilaterian protein sequences were found using keyword searches (e.g., nicotinic acetylcholine receptor, muscarinic acetylcholine receptor, GABAergic receptor, and glycine receptor) to identify sequences within multiple genomic databases (mouse genome informatics, flybase, wormbase, zfin, and NCBI). Non-*Nematostella* cnidarian protein sequences were collected using bilaterian protein sequences blasted on NCBI or the *Clytia hemisphaerica* genome browser (Leclère et al., 2019). *Nematostella*-coding sequences were collected by blasting bilaterian and cnidarian nicotinic or muscarinic acetylcholine receptor sequences against the *Nematostella* genome (https ://genom e.jgi.doe.gov/pages /search-for-genes.jsf?organ ism=Nemve 1), and the NvERTx database (Warner et al., 2018). Putative AChRs identified by BLAST hits were then selected and uploaded to ApE v2.0.47, where they were translated. The largest open reading frames identified in the *Nematostella*-coding sequences were then used for protein alignment (Paradis et al., 2004). All protein sequences were uploaded into MEGA v7.0.25 software, exported, and then, an MAFFT alignment was performed using the CIPRES gateway (Miller et al., 2010; Kumar et al., 2016) . We excluded all *Nematostella* sequences missing characteristic residues required for acetylcholine binding. Phylogenetic analyses were performed using two previously published AChR alignments. The published alignments are unedited

protein sequences, and an edited alignment that included the double cysteines necessary for acetylcholine binding and the transmembrane domains (T1–T4) (Li et al., 2016; Pedersen et al., 2019) . Known bilaterian muscarinic acetylcholine receptors and the single published cnidarian muscarinic acetylcholine receptors were included to determine if any *Nematostella* sequences cluster within the muscarinic clade. To expand the number of cnidarian muscarinic acetylcholine receptors we also mined the *Clytia hemisphaerica* genome to identify any potential muscarinic acetylcholine receptors (Leclère et al., 2019). Phylogenies were generated using RaxML and IQ tree with GABA receptors serving as the out-group (Stamatakis, 2014; Nguyen et al., 2015)(Figure 4.5-4.8). We determined the LG phylogenetic evolution model using IQ-tree protein Model Finder (Nguyen et al., 2015). The phylogenetic trees were made utilizing IQ tree and RaxML with ultrafast bootstrapping or bootstrapping repeated 1000 times, respectively (Stamatakis, 2014; Nguyen et al., 2015).

Animal care

Adult *Nematostella* were maintained at Lehigh University in 17 °C incubators. Culture and spawning of animals were performed according to previously published protocols (Havrilak et al., 2017b). Embryos were raised at 22 °C until fixation at the required stage.

In situ hybridization

Each gene was sub-cloned into pGEM-T (Promega) from mixed stage cDNA using the primers listed in Additional file 4: Table S1. Embryo fixation, RNA probe synthesis, *in situ* hybridization, and immunohistochemistry protocols were performed as

previously described (Layden et al., 2016; Havrilak et al., 2017b). Juvenile polyps were fixed for 2h as previously described [31]. When *in situs* returned no pattern, we attempted to remake the probe and repeated the in situ. No expression represents at least two attempts to determine a spatio-temporal pattern.

Pharmaceutical treatments

All stock concentrations were generated by resuspending pharmaceutical reagents in Nematostella medium [1/3X artificial seawater (ASW)]. Reagents used were Acetylcholine hydrochloride (Sigma-Aldrich Cat#A6625), Nicotine hydrogen tartrate salt (Sigma-Aldrich Cat#SML1236), mecamylamine hydrochloride (Sigma-Aldrich Cat.#M9020), and lidocaine (Sigma-Aldrich Cat.#L7757). Concentrations for Acetylcholine, nicotine, and mecamylamine were experimentally determined (see "Results"). Lidocaine was used at a concentration of 5 mM, which was previously shown to be the effective for blocking *Nematostella* voltage-gated sodium channels (Gur Barzilai et al., 2012). To perform pharmacological treatments, polyps were moved into a concave depression slide for imaging and left to relax until the majority of polyps re-extended their tentacles. Animals that failed to relax after moving were excluded from further analysis. Once the majority of animals relaxed, animals were video recorded for 1 min to assess baseline activity. At the 1 min mark, acetylcholine–chloride or nicotine was added to the depression slide and all contractions were quantified. Because the previous experiments suggested that there is a delay in the effect of some compounds, we continued to monitor animals for an additional 5 min to ensure no additional contractions occurred. Lidocaine and mecamylamine inhibitors were added to animals in *Nematostella*

medium 20min prior to application of nicotine or acetylcholine. The 20 min pretreatment were chosen based on the previous observations in Nematostella (Gur Barzilai et al., 2012). Tentacle contractions were measured for each animal and given a score of either complete contraction of all tentacles (1), a complete contraction of ≥ half, but not all of the tentacles (0.5), or no tentacle contraction (0). The total contractions were summed for each treatment and the percentage of contractions per animal was then calculated. We then calculated the mean among the trials. Peristaltic initiation contractions were defined as any inward contraction perpendicular to the oral–aboral axis that occurred within the body column. Peristaltic wave contractions were defined as any propagation of radial contractions along the oral–aboral axis of the body column. Peristaltic initiation contractions and peristaltic wave contractions were then quantified as either being a contraction (1), or no contraction (0). We calculated the percent of animals that contracted per total number of animals tested for each trail. We then calculated the mean for the trials. Controls were performed by adding a volume of *Nematostella* medium equal to the volume of stock pharmaceutical reagent added to the concave imaging slide. Statistical significance was determined using a one-way ANOVA with the Games-Howell post hoc analysis, due to unequal variance, performed in SPSS or a student's t test using Microsoft Excel, when appropriate. Animals used for one experiment were not reused for any subsequent experiments.

Imaging

Images for *in situ* hybridization were acquired on a Nikon NTi with a Nikon DS-Ri2 color camera using the Nikon elements software. Time series were performed on a Nikon

Eclipse E1000 with a Nikon camera and analyzed on the Nikon elements software. Time series images were analyzed using the Fiji software v.2.0.0-rc-54/1.51 g(Schindelin et al., 2012). All images were edited using Adobe Illustrator and Photoshop and videos were edited using Adobe Premiere Pro (Adobe Inc.).

Chapter 5: Summary and Concluding Remarks

This dissertation focused on characterizing how individual neuronal cell types are patterned and then characterizing a functional role for these neurons within adult polyps. In chapter two I used shRNAs to functionally characterize individual downstream targets of *NvsoxB(2)* and *Nvath-like,* identified a *NvsoxB(2)* only progenitor population, and identified a role of *NvfoxD3-like* in cnidocyte patterning. I then characterized how axial markers and Wnt activity along the oral-aboral axis function to pattern individual neuronal subtypes. Finally, I characterized the role of acetylcholine in the neuronal circuitry which regulates tentacle and radial body column contractions. Each chapter established the foundational research from which multiple avenues of neuroscience can be explored within *Nematostella*.

In chapter two, I identified multiple transcription factors downstream either the progenitor marker *NvsoxB(2)* or the *NvsoxB(2)/Nvath-like* progenitor population. Previous research already established the expression patterns for all of these markers within gastrula and the adult cell types they are expressed within (Layden et al., 2016; Sebé-Pedrós et al., 2018). These data suggest that these downstream markers consist of broad regulators of cell type identity and individual cell types. Future work should focus on characterizing the function of these transcription factors. This could be done with shRNA mediated knockdown of each individual transcription factor, characterize how these genes interact with each other resulting in the establishment of a gene regulatory network. Recent single-cell sequencing technology has provided high resolution of the developmental trajectories necessary for the specification of multiple cell types (Farrell et al., 2018; Siebert et al., 2019; Lemaire et al., 2021). This method could be used from

early blastula to late gastrula stages to broadly characterize the developmental trajectory for multiple neurons, cnidocytes, and secretory cells early during development. The combination of single-cell sequencing data and the shRNA mediated functional assays would significantly improve our understanding of cell type differentiation in *Nematostella.*

In chapter 3, I identified how axial information along the oral-aboral axis is used to pattern individual neuronal subtypes restricted along this axis within *Nematostella*. We argued that the presence of *Nvsix3/6* binding domains within the upstream regulatory domains of *NvLWamide, Nvserum amyloidA-like,* and *Nvfoxq2d* supports direct regulation of these subtypes by *Nvsix3/6*. However, future work should characterize how removal of these binding domain effects expression of transgenic reporters. Additionally, we hypothesized that the endodermal marker *NvotxC* functions to pattern structures and endodermal neurons. Knockdown of *NvotxC* should be performed and the effects of this knockdown on endodermal patterning should be characterized. The role of *NvotxC* on neuronal patterning will be harder to perform since an endodermal neuronal marker has not been identified yet. However, using a broad neuronal marker, like *Nvelav1*, might provide some insight on how NvotxC patterns neurons. These experiments would provide a more detailed mechanism for how these spatial domain genes pattern both ectodermal and endodermal nervous systems.

In chapter 4, I characterized a role for acetylcholine in the regulation of tentacle and radial muscle contraction. However, the goal of this aim was to identify a potential motor

neuron and characterize its developmental trajectory. We found data which supports the hypothesis that acetylcholine functions upstream this muscular contraction pathway. One method to identify motor neurons is to observe whether any of our current neural transgenic markers innervate muscle tissue. Alternatively, if the goal is to identify a functional neuron then we could characterize the functions within published transgenic lines. Utilization of neuronal promoters driving expression of GCaMP, a calcium indicator, has been used to characterize the circuits necessary for multiple behaviors within hydra (Dupre and Yuste, 2017). A similar mechanism could be utilized here to determine the function of neuronal subtypes, like *NvLWamide*, whose developmental trajectory has already been partially characterized (Layden et al., 2012; Havrilak et al., 2017b).

In summary this dissertation examined different mechanisms to pattern and identifying functional neuronal subtypes. The performance of novel high resolution single cell sequencing early during development and synthesis of traditional neuroscience techniques within *Nematostella vectensis* could expand on the research identified here. The combination of these data sets could establish an extremely detailed understanding of cnidarian neuroscience for this first time within a cnidarian model. This level of detail would allow for more informed hypotheses about the evolution of nervous system and nervous system patterning across metazoans.

References

Amiel, A.R., Johnston, H., Chock, T., Dahlin, P., Iglesias, M., Layden, M., Röttinger, E., and Martindale, M.Q. 2017. A bipolar role of the transcription factor ERG for cnidarian germ layer formation and apical domain patterning. *Dev. Biol.* 430: 346–361.

Anctil, M. 1985. Cholinergic and monoaminergic mechanisms associated with control of bioluminescence in the ctenophore Mnemiopsis leidyi. *J. Exp. Biol.* 238: 225–238.

Anctil, M. 2009. Chemical transmission in the sea anemone Nematostella vectensis: A genomic perspective. *Comp. Biochem. Physiol. - Part Genomics Proteomics* 4: 268–289.

Babonis, L.S., and Martindale, M.Q. 2017. PaxA, but not PaxC, is required for cnidocyte development in the sea anemone Nematostella vectensis. *EvoDevo* 8: 1–20.

Bamel, K., Gupta, R., and Gupta, S.C. 2016. Acetylcholine suppresses shoot formation and callusing in leaf explants of \textlessi\textgreaterin vitro\textless/i\textgreater raised seedlings of tomato, \textlessi\textgreaterLycopersicon esculentum\textless/i\textgreater Miller var. Pusa Ruby. *Plant Signal. Behav.* 11: e1187355.

Berndt, A.J.E., Tang, J.C.Y., Ridyard, M.S., Lian, T., Keatings, K., and Allan, D.W. 2015. Gene Regulatory Mechanisms Underlying the Spatial and Temporal Regulation of Target-Dependent Gene Expression in Drosophila Neurons. *PLoS Genet.* 11: 1–27.

Busengdal, H., and Rentzsch, F. 2017. Unipotent progenitors contribute to the generation of sensory cell types in the nervous system of the cnidarian Nematostella vectensis. *Dev. Biol.* 1–10.

Bylund, M., Andersson, E., Novitch, B.G., and Muhr, J. 2003. Vertebrate neurogenesis is counteracted by Sox1–3 activity. *Nat. Neurosci.* 6: 1162–1168.

Cannon, J.T., Vellutini, B.C., Smith, J., Ronquist, F., Jondelius, U., and Hejnol, A. 2016. Xenacoelomorpha is the sister group to Nephrozoa. *Nature* 530: 89–93.

Cau, E., and Wilson, S.W. 2003. Ash1a and Neurogenin1 function downstream of Floating head to regulate epiphysial neurogenesis. *Development* 130: 2455–2466.

Chapman, J.A., Kirkness, E.F., Simakov, O., Hampson, S.E., Mitros, T., Weinmaier, T., Rattei, T., Balasubramanian, P.G., Borman, J., Busam, D., et al. 2010. The dynamic genome of Hydra. *Nature* 464: 592–596.

Cheatle Jarvela, A.M., Yankura, K.A., and Hinman, V.F. 2016. A gene regulatory network for apical organ neurogenesis and its spatial control in sea star embryos. *Development*.

Collin, C., Hauser, F., De Valdivia, E.G., Li, S., Reisenberger, J., Carlsen, E.M.M., Khan, Z., Hansen, N.O., Puhm, F., Søndergaard, L., et al. 2013. Two types of muscarinic acetylcholine receptors in Drosophila and other arthropods. *Cell. Mol. Life Sci.* 70: 3231–3242.

Dani, J.A., and Bertrand, D. 2007. Nicotinic Acetylcholine Receptors and Nicotinic Cholinergic Mechanisms of the Central Nervous System. *Annu. Rev. Pharmacol. Toxicol.* 47: 699–729.

Darras, S., Fritzenwanker, J.H., Uhlinger, K.R., Farrelly, E., Pani, A.M., Hurley, I.A., Norris, R.P., Osovitz, M., Terasaki, M., Wu, M., et al. 2018. Anteroposterior axis patterning by early canonical Wnt signaling during hemichordate development. *PLOS Biol.* 16: e2003698.

Di Sansebastiano, G.P., Fornaciari, S., Barozzi, F., Piro, G., and Arru, L. 2014. New insights on plant cell elongation: A role for acetylcholine. *Int. J. Mol. Sci.* 15: 4565–4582.

Dottori, M., Gross, M., Labosky, P., and Goulding, M. The winged-helix transcription factor Foxd3 suppresses interneuron differentiation and promotes neural crest cell fate. 12.

Dupre, C., and Yuste, R. 2017. Non-overlapping Neural Networks in Hydra vulgaris. *Curr. Biol.* 27: 1085–1097.

Ellwanger, K., and Nickel, M. 2006. Neuroactive substances specifically modulate rhythmic body contractions in the nerveless metazoon Tethya wilhelma (Demospongiae, Porifera). *Front. Zool.* 3: 1–14.

Farrell, J.A., Wang, Y., Riesenfeld, S.J., Shekhar, K., Regev, A., and Schier, A.F. 2018. Single-cell reconstruction of developmental trajectories during zebrafish embryogenesis. *Science* 360: eaar3131.

Gavilán, B., Perea-Atienza, E., and Martínez, P. 2016. Xenacoelomorpha: a case of independent nervous system centralization? *Philos. Trans. R. Soc. B Biol. Sci.* 371: 20150039.

Graham, V., Khudyakov, J., Ellis, P., and Pevny, L. 2003. SOX2 Functions to Maintain Neural Progenitor Identity. *Neuron* 39: 749–765.

Guillemot, F. 2007. Spatial and temporal specification of neural fates by transcription factor codes. *Development* 134: 3771–3780.

Gur Barzilai, M., Reitzel, A.M., Kraus, J.E.M., Gordon, D., Technau, U., Gurevitz, M., and Moran, Y. 2012. Convergent Evolution of Sodium Ion Selectivity in Metazoan Neuronal Signaling. *Cell Rep.* 2: 242–248.

Havrilak, J.A., Al-Shaer, L., Baban, N., Akinci, N., and Layden, M.J. 2021. Characterization of the dynamics and variability of neuronal subtype responses during growth, degrowth, and regeneration of Nematostella vectensis. *BMC Biol.* 19: 104.

Havrilak, J.A., Faltine-gonzalez, D., Fodera, D., Simpson, A.C., Magie, R., Layden, M.J., Havrilak, J.A., Faltine-gonzalez, D., Wen, Y., Fodera, D., et al. 2017a. Author ' s Accepted Manuscript development. *Dev. Biol.*

Havrilak, J.A., Faltine-Gonzalez, D., Wen, Y., Fodera, D., Simpson, A.C., Magie, C.R., and Layden, M.J. 2017b. Characterization of NvLWamide-like neurons reveals stereotypy in Nematostella nerve net development. *Dev. Biol.* 431: 336–346.

Havrilak, J.A., Faltine-Gonzalez, D., Wen, Y., Fodera, D., Simpson, A.C., Magie, C.R., and Layden, M.J. 2017c. Characterization Of NvLWamide-Like Neurons Reveals Stereotypy In Nematostella Nerve Net Development. *BioRxiv* 0–1.

He, S., Del Viso, F., Chen, C.Y., Ikmi, A., Kroesen, A.E., and Gibson, M.C. 2018. An axial Hox code controls tissue segmentation and body patterning in Nematostella vectensis. *Science* 361: 1377–1380.

Holland, L.Z., Carvalho, J.E., Escriva, H., Laudet, V., Schubert, M., Shimeld, S.M., and Yu, J.-K. 2013. Evolution of bilaterian central nervous systems: a single origin? *EvoDevo* 4: 27.

Horiuchi, Y., Kimura, R., Kato, N., Fujii, T., Seki, M., Endo, T., Kato, T., and Kawashima, K. 2003. Evolutional study on acetylcholine expression. *Life Sci.* 72: 1745–1756.

Ikmi, A., McKinney, S.A., Delventhal, K.M., and Gibson, M.C. 2014. TALEN and CRISPR/Cas9-mediated genome editing in the early-branching metazoan Nematostella vectensis. *Nat. Commun.* 5: 5486.

Jones, A.K., Grauso, M., and Sattelle, D.B. 2005. The nicotinic acetylcholine receptor gene family of the malaria mosquito, Anopheles gambiae. *Genomics* 85: 176–187.

Kai, T., Nishimura, J., Kobayashi, S., Takahashi, S., Yoshitake, J., and Kanaide, H. 1993. Effects of lidocaine on intracellular Ca2+ and tension in airway smooth muscle. *Anesthesiology*.

Kass-Simon, G., and Passano, L.M. 1978. A neuropharmacological analysis of the pacemakers and conducting tissues ofHydra attenuata. *J. Comp. Physiol.* 128: 71–79.

Kass-Simon, G., and Pierobon, P. 2007. Cnidarian chemical neurotransmission, an updated overview. *Comp. Biochem. Physiol. - Mol. Integr. Physiol.* 146: 9–25.

Kawashima, K., Misawa, H., Moriwaki, Y., Fujii, Y.X., Fujii, T., Horiuchi, Y., Yamada, T., Imanaka, T., and Kamekura, M. 2007. Ubiquitous expression of acetylcholine and its biological functions in life forms without nervous systems. *Life Sci.* 80: 2206–2209.

Kraus, Y., Aman, A., Technau, U., and Genikhovich, G. 2016. Pre-bilaterian origin of the blastoporal axial organizer. *Nat. Commun.* 7: 1–9.

Kruse, A.C., Hu, J., Pan, A.C., Arlow, D.H., Rosenbaum, D.M., Rosemond, E., Green, H.F., Liu, T., Chae, P.S., Dror, R.O., et al. 2012. Structure and dynamics of the M3 muscarinic acetylcholine receptor. *Nature* 482: 552–556.

Kumar, S., Stecher, G., and Tamura, K. 2016. MEGA7: Molecular Evolutionary Genetics Analysis Version 7.0 for Bigger Datasets. *Mol. Biol. Evol.* 33: 1870–1874.

Lagutin, O.V. 2003. Six3 repression of Wnt signaling in the anterior neuroectoderm is essential for vertebrate forebrain development. *Genes Dev.* 17: 368–379.

Layden, M.J., Boekhout, M., and Martindale, M.Q. 2012. Nematostella vectensis achaete-scute homolog NvashA regulates embryonic ectodermal neurogenesis and represents an ancient component of the metazoan neural specification pathway. *Development* 139: 1013–1022.

Layden, M.J., Johnston, H., Amiel, A.R., Havrilak, J., Steinworth, B., Chock, T., Röttinger, E., and Martindale, M.Q. 2016. MAPK signaling is necessary for neurogenesis in Nematostella vectensis. *BMC Biol.* 14: 61.

Layden, M.J., and Martindale, M.Q. 2014. Non-canonical Notch signaling represents an ancestral mechanism to regulate neural differentiation. *EvoDevo* 5: 30.

Layden, M.J., Röttinger, E., Wolenski, F.S., Gilmore, T.D., and Martindale, M.Q. 2013. Microinjection of mRNA or morpholinos for reverse genetic analysis in the starlet sea anemone, Nematostella vectensis. *Nat. Protoc.* 8: 924–934.

Lebedeva, T., Aman, A.J., Graf, T., Niedermoser, I., Zimmermann, B., Kraus, Y., Schatka, M., Demilly, A., Technau, U., and Genikhovich, G. 2021. Cnidarian-bilaterian comparison reveals the ancestral regulatory logic of the β-catenin dependent axial patterning. *Nat. Commun.* 12: 4032.

Leclère, L., Bause, M., Sinigaglia, C., Steger, J., and Rentzsch, F. 2016. Development of the aboral domain in *Nematostella* requires *β -catenin* and the opposing activities of *S ix3/6* and *F rizzled5/8*. *Development* 143: 1766–1777.

Leclère, L., Horin, C., Chevalier, S., Lapébie, P., Dru, P., Peron, S., Jager, M., Condamine, T., Pottin, K., Romano, S., et al. 2019. The genome of the jellyfish Clytia hemisphaerica and the evolution of the cnidarian life-cycle. *Nat. Ecol. Evol.* 3: 801–810.

Lemaire, L.A., Cao, C., Yoon, P.H., Long, J., and Levine, M. 2021. The hypothalamus predates the origin of vertebrates. *Sci. Adv.* 7: eabf7452.

Li, M.D., Yang, Z., Guo, H., and Dash, B. 2016. Evolutionary Relationship of Nicotinic Acetylcholine Receptor Subunits in Both Vertebrate and Invertebrate Species. In Nicotinic Acetylcholine Receptor Technologies, M.D. Li, ed. (New York, NY: Springer New York), pp. 227–254.

Lister, J.A., Cooper, C., Nguyen, K., Modrell, M., Grant, K., and Raible, D.W. 2006. Zebrafish Foxd3 is required for development of a subset of neural crest derivatives. *Dev. Biol.* 290: 92–104.

Lowe, C.J., Terasaki, M., Wu, M., Freeman, R.M., Runft, L., Kwan, K., Haigo, S., Aronowicz, J., Lander, E., Gruber, C., et al. 2006. Dorsoventral Patterning in Hemichordates: Insights into Early Chordate Evolution. *PLoS Biol.* 4: e291.

Madelaine, R., Garric, L., and Blader, P. 2011. Partially redundant proneural function reveals the importance of timing during zebrafish olfactory neurogenesis. *Development* 138: 4753–4762.

Maouche, K., Polette, M., Jolly, T., Medjber, K., Cloëz-Tayarani, I., Changeux, J.P., Burlet, H., Terryn, C., Coraux, C., Zahm, J.M., et al. 2009. A7 Nicotinic Acetylcholine Receptor Regulates Airway Epithelium Differentiation By Controlling Basal Cell Proliferation. *Am. J. Pathol.* 175: 1868–1882.

Marlow, H., Matus, D.Q., and Martindale, M.Q. 2013. Ectopic activation of the canonical wnt signaling pathway affects ectodermal patterning along the primary axis during larval development in the anthozoan Nematostella vectensis. *Dev. Biol.* 380: 324–334.

Marlow, H.Q., Srivastava, M., Matus, D.Q., Rokhsar, D., and Martindale, M.Q. 2009. Anatomy and development of the nervous system of Nematostella vectensis, an anthozoan cnidarian. *Dev. Neurobiol.* 69: 235–254.

Martín-Durán, J.M., and Hejnol, A. 2021. A developmental perspective on the evolution of the nervous system. *Dev. Biol.* 475: 181–192.

Martín-Durán, J.M., Pang, K., Børve, A., Lê, H.S., Furu, A., Cannon, J.T., Jondelius, U., and Hejnol, A. 2018. Convergent evolution of bilaterian nerve cords. *Nature* 553: 45–50.

Mazza, M.E., Pang, K., Martindale, M.Q., and Finnerty, J.R. 2007. Genomic organization, gene structure, and developmental expression of three Clusteredotx genes in the sea anemoneNematostella vectensis. *J. Exp. Zoolog. B Mol. Dev. Evol.* 308B: 494–506.

McClay, D.R., Miranda, E., and Feinberg, S.L. 2018. Neurogenesis in the sea urchin embryo is initiated uniquely in three domains. *Development* 145: dev167742.

Mendes, E.G., and De Freitas, J. 1984. The responses of isolated preparations of Bunodosoma Caissarum (Correa, 1964) (Cnidaria, Anthozoa) to drugs. *Comp. Biochem. Physiol. Part C Comp.* 79: 375–382.

Miller, M.A., Pfeiffer, W., and Schwartz, T. 2010. Creating the CIPRES Science Gateway for inference of large phylogenetic trees. *2010 Gatew. Comput. Environ. Workshop GCE 2010*.

Moroz, L.L., Kocot, K.M., Citarella, M.R., Dosung, S., Norekian, T.P., Povolotskaya, I.S., Grigorenko, A.P., Dailey, C., Berezikov, E., Buckley, K.M., et al. 2014. The ctenophore genome and the evolutionary origins of neural systems. *Nature* 510: 109–114.

Moroz, L.L., and Kohn, A.B. 2016. Independent origins of neurons and synapses: Insights from ctenophores. *Philos. Trans. R. Soc. B Biol. Sci.* 371:.

Nakanishi, N., and Martindale, M.Q. 2018. CRISPR knockouts reveal an endogenous role for ancient neuropeptides in regulating developmental timing in a sea anemone. *ELife* 7: e39742.

Nakanishi, N., Renfer, E., Technau, U., and Rentzsch, F. 2012. Nervous systems of the sea anemone Nematostella vectensis are generated by ectoderm and endoderm and shaped by distinct mechanisms. *Development* 139: 347–357.

Nguyen, L.-T., Schmidt, H.A., von Haeseler, A., and Minh, B.Q. 2015. IQ-TREE: A Fast and Effective Stochastic Algorithm for Estimating Maximum-Likelihood Phylogenies. *Mol. Biol. Evol.* 32: 268–274.

Oliver, D., Brinkmann, M., Sieger, T., and Thurm, U. 2008. Hydrozoan nematocytes send and receive synaptic signals induced by mechano-chemical stimuli. *J. Exp. Biol.* 211: 2876–2888.

Oliver, G., Mailhos, A., Wehr, R., Copeland, N.G., Jenkins, N.A., and Gruss, P. 1995. Six3, a murine homologue of the sine oculis gene, demarcates the most anterior border of the developing neural plate and is expressed during eye development. *Development* 121: 4045–4055.

Pani, A.M., Mullarkey, E.E., Aronowicz, J., Assimacopoulos, S., Grove, E.A., and Lowe, C.J. 2012. Ancient deuterostome origins of vertebrate brain signalling centres. *Nature* 483: 289–294.

Paradis, E., Claude, J., and Strimmer, K. 2004. APE: Analyses of phylogenetics and evolution in R language. *Bioinformatics* 20: 289–290.

Pedersen, J.E., Bergqvist, C.A., and Larhammar, D. 2018. Evolution of the Muscarinic Acetylcholine Receptors in Vertebrates. *Eneuro* 5: ENEURO.0340-18.2018.

Pedersen, J.E., Bergqvist, C.A., and Larhammar, D. 2019. Evolution of vertebrate nicotinic acetylcholine receptors. *BMC Evol. Biol.* 19: 1–21.

Putnam, N.H., Srivastava, M., Hellsten, U., Dirks, B., Chapman, J., Salamov, A., Terry, A., Shapiro, H., Lindquist, E., Kapitonov, V.V., et al. 2007. Sea anemone genome reveals ancestral eumetazoan gene repertoire and genomic organization. *Science* 317: 86–94.

Rajendran, R., Borghi, E., Falleni, M., Perdoni, F., Tosi, D., Lappin, D.F., O'Donnell, L., Greetham, D., Ramage, G., and Nile, C. 2015. Acetylcholine Protects against Candida albicans Infection by Inhibiting Biofilm Formation and Promoting Hemocyte Function in a Galleria mellonella Infection Model. *Eukaryot. Cell* 14: 834–844.

Range, R.C., and Wei, Z. 2017. Correction: An anterior signaling center patterns and sizes the anterior neuroectoderm of the sea urchin embryo. *Development* 144: 1579–1579.

Renfer, E., Amon-Hassenzahl, A., Steinmetz, P.R.H., and Technau, U. 2010. A muscle-specific transgenic reporter line of the sea anemone, Nematostella vectensis. *Proc. Natl. Acad. Sci.* 107: 104–108.

Richards, G.S., and Rentzsch, F. 2014. Transgenic analysis of a SoxB gene reveals neural progenitor cells in the cnidarian Nematostella vectensis. *Development* 141: 4681–4689.

Richards, G.S., and Rentzsch, F. 2015. Regulation of Nematostella neural progenitors by SoxB, Notch and bHLH genes. *Development* 142: 3332–3342.

Ross, D.M. 1960. THE EFFECTS OF IONS AND DRUGS ON NEURO- MUSCULAR PREPARATIONS OF SEA ANEMONES. *J Exp Biol* 37: 732–752.

Ryan, J.F., Pang, K., Schnitzler, C.E., Nguyen, A.-D.A.D., Moreland, R.T., Simmons, D.K., Koch, B.J., Francis, W.R., Havlak, P., Smith, S.A., et al. 2013. The genome of the ctenophore Mnemiopsis leidyi and its implications for cell type evolution. *Science* 342: 1242592–1242592.

Sánchez-Lazo, C., Martínez-Pita, I., Young, T., and Alfaro, A.C. 2012. Induction of settlement in larvae of the mussel Mytilus galloprovincialis using neuroactive compounds. *Aquaculture* 344–349: 210–215.

Scemes, E., and De-Freitas, J.C. 1989. Electrophysiology of the swimming system of hydromedusae and the effects of atropine-induced crumpling. *Braz. J. Med. Biol. Res. Rev. Bras. Pesqui. Medicas E Biol.* 22: 189–198.

Scemes, E., and Mendes, E.G. 1986. Cholinergic mechanism in Liriope tetraphylla (Cnidaria, Hydrozoa). *Comp. Biochem. Physiol. Part C Comp.* 83: 171–178.

Schindelin, J., Arganda-Carreras, I., Frise, E., Kaynig, V., Longair, M., Pietzsch, T., Preibisch, S., Rueden, C., Saalfeld, S., Schmid, B., et al. 2012. Fiji: An open-source platform for biological-image analysis.

Sebé-Pedrós, A., Saudemont, B., Chomsky, E., Plessier, F., Mailhé, M.P., Renno, J., Loe-Mie, Y., Lifshitz, A., Mukamel, Z., Schmutz, S., et al. 2018. Cnidarian Cell Type Diversity and Regulation Revealed by Whole-Organism Single-Cell RNA-Seq. *Cell* 173: 1520-1534.e20.

Sheets, M.F., and Hanck, D.A. 2003. Molecular Action of Lidocaine on the Voltage Sensors of Sodium Channels. *J. Gen. Physiol.* 121: 163–175.

Shinzato, C., Shoguchi, E., Kawashima, T., Hamada, M., Hisata, K., Tanaka, M., Fujie, M., Fujiwara, M., Koyanagi, R., Ikuta, T., et al. 2011. Using the Acropora digitifera genome to understand coral responses to environmental change. *Nature* 476: 320–323.

Siebert, S., Farrell, J.A., Cazet, J.F., Abeykoon, Y., Primack, A.S., Schnitzler, C.E., and Juliano, C.E. 2019. Stem cell differentiation trajectories in *Hydra* resolved at single-cell resolution. *Science* 365: eaav9314.

Simpson, P. Notchand the choice of cell fate in Drosophila neuroepithelium. 3.

Singer, R.H. 1964. EFFECT OF NEUROPHARMACOLOGICAL DRUGS ON LIGHT RESPONSE OF HYDRA PIRADI. In ANATOMICAL RECORD, (WILEY-LISS DIV JOHN WILEY & SONS INC, 605 THIRD AVE, NEW YORK, NY 10158-0012), p. 402.

Sinigaglia, C., Busengdal, H., Leclère, L., Technau, U., and Rentzsch, F. 2013. The Bilaterian Head Patterning Gene six3/6 Controls Aboral Domain Development in a Cnidarian. *PLoS Biol.* 11:.

Sinigaglia, C., Busengdal, H., Lerner, A., Oliveri, P., and Rentzsch, F. 2015. Molecular characterization of the apical organ of the anthozoan Nematostella vectensis. *Dev. Biol.* 398: 120–133.

Srivastava, M., Begovic, E., Chapman, J., Putnam, N.H., Hellsten, U., Kawashima, T., Kuo, A., Mitros, T., Salamov, A., Carpenter, M.L., et al. 2008. The Trichoplax genome and the nature of placozoans. *Nature* 454: 955–960.

Srivastava, M., Simakov, O., Chapman, J., Fahey, B., Gauthier, M.E.A., Mitros, T., Richards, G.S., Conaco, C., Dacre, M., Hellsten, U., et al. 2010. The Amphimedon queenslandica genome and the evolution of animal complexity. *Nature* 466: 720–726.

Stamatakis, A. 2014. RAxML version 8: a tool for phylogenetic analysis and post-analysis of large phylogenies. *Bioinformatics* 30: 1312–1313.

Steinmetz, P.R., Urbach, R., Posnien, N., Eriksson, J., Kostyuchenko, R.P., Brena, C., Guy, K., Akam, M., Bucher, G., and Arendt, D. 2010. Six3 demarcates the anterior-most developing brain region in bilaterian animals. *EvoDevo* 1: 14.

Steinmetz, P.R.H., Aman, A., Kraus, J.E.M., and Technau, U. 2017. Gut-like ectodermal tissue in a sea anemone challenges germ layer homology. *Nat. Ecol. Evol.* 1: 1535–1542.

Strader, M.E., Aglyamova, G.V., and Matz, M.V. 2018. Molecular characterization of larval development from fertilization to metamorphosis in a reef-building coral. *BMC Genomics* 19: 1–17.

Sunagar, K., Columbus-Shenkar, Y.Y., Fridrich, A., Gutkovich, N., Aharoni, R., and Moran, Y. 2018. Cell type-specific expression profiling unravels the development and evolution of stinging cells in sea anemone. *BMC Biol.* 16: 1–16.

Tournière, O., Busengdal, H., Gahan, J.M., and Rentzsch, F. 2021. *Insm1* -expressing neurons and secretory cells develop from a common pool of progenitors in the sea anemone *Nematostella vectensis* (Developmental Biology).

Tournière, O., Dolan, D., Richards, G.S., Sunagar, K., Columbus-Shenkar, Y.Y., Moran, Y., and Rentzsch, F. 2020. NvPOU4/Brain3 Functions as a Terminal Selector Gene in the Nervous System of the Cnidarian Nematostella vectensis. *Cell Rep.* 30: 4473-4489.e5.

Unwin, N. 2005. Refined structure of the nicotinic acetylcholine receptor at 4 \AA resolution. *J. Mol. Biol.* 346: 967–989.

Vallstedt, A., Muhr, J., Pattyn, A., Pierani, A., Mendelsohn, M., Sander, M., Jessell, T.M., and Ericson, J. 2001. Different Levels of Repressor Activity Assign Redundant and Specific Roles to Nkx6 Genes in Motor Neuron and Interneuron Specification. *Neuron* 31: 743–755.

Warner, J.F., Guerlais, V., Amiel, A.R., Johnston, H., Nedoncelle, K., and Röttinger, E. 2018. NvERTx: A gene expression database to compare embryogenesis and regeneration in the sea anemone *Nematostella vectensis*. *Development* dev.162867.

Webster, N.B., Corbet, M., Sur, A., and Meyer, N.P. 2021. Role of BMP signaling during early development of the annelid Capitella teleta. *Dev. Biol.* S0012160621001536.

Wessler, I., and Kirkpatrick, C.J. 2008. Acetylcholine beyond neurons: The non-neuronal cholinergic system in humans. *Br. J. Pharmacol.* 154: 1558–1571.

Zimmermann, B., Robb, S.M.C., Genikhovich, G., Fropf, W.J., Weilguny, L., He, S., Chen, S., Lovegrove-Walsh, J., Hill, E.M., Ragkousi, K., et al. 2020. Sea anemone genomes reveal ancestral metazoan chromosomal macrosynteny (Genomics).

Dylan Z. Faltine-Gonzalez

111 Research Drive Iacocca Hall B217, Bethlehem, PA 18018

Education

PhD Integrative Biology — Lehigh University, Bethlehem, PA 2015-2021

B.S. Marine Biology — University of Hawaii at Manoa, Honolulu, HI 2010-2014

Research Experience

Doctoral Student Lehigh University 2015-2021
Advisor: Dr. Michael J. Layden

Undergraduate Researcher Békesy Laboratory for Neurobiology, University of Hawaii at Manoa 2013-2014
Advisor: Dr. Daniel K. Hartline

Undergraduate Summer Researcher Gerstner Sloan Kettering/CHOOSE Development 2013-2014
Advisor: Dr. Alexandra Joyner

Undergraduate Researcher Kewalo Marine Lab, University of Hawaii at Manoa 2012-2013
Advisor: Dr. Mark Q. Martindale

Publications

3. Faltine-Gonzalez, D.Z., Layden, M.J. Oral-aboral patterning regulates neural subtype specification in *Nematostella vectensis. In prep.*

2. Faltine-Gonzalez, D.Z., Layden, M.J. Characterization of nAChRs in *Nematostella vectensi*s supports neuronal and non-neuronal role in the cnidarian-bilaterian common ancestor. *EvoDevo*. 2019;10:27

1. Havrilak, J.A., **Faltine-Gonzalez, D.Z.,**Wen, Y., Fodera, D., Simpson, A.C., Magie, C.R., Layden, M.J.. Characterization of *NvLWamide-like*+ neurons reveals stereotypy in *Nematostella* nerve net. *Developmental Biology*. 2017 Sep 6.

Presentations

15. *Neural patterning in the cnidarian Nematostella vectensis* 2021
Oral presentation at Cnidofest

14. *Characterizing neuronal subtype specification in Nematostella vectensis* 2020
Invited speaker at Desales University

13. *Characterizing neuronal subtype specification in Nematostella vectensis* 2020
Oral presentation at Society for Integrative and Comparative Biology

12. *Determining the role of oral-aboral patterning on neurogenesis in the sea anemone, Nematostella vectensis* 2019
Oral presentation at Mid-Atlantic Regional Society for Developmental Biology 2019

11. *Identification of neural subtype patterning in the anthozoan Nematostella vectensis* 2018
Oral presentation at Cnidofest 2018

10. *Determining the regulation of myoepithelial contraction within the anthozoan Nematostella vecentsis* 2017
Poster presentation at The Diversification of Early Emerging Metazoans: A window into Animal Evolution?

9*. Characterization of the Nematostella vectensis NvLwamide transgenic line reveals stereotypy in the cnidarian nerve net* 2016
Poster presentation at the Society for Developmental Biology 2016 international meeting

8. *Determining the role of NvashA in endodermal neurogenesis* 2016
Oral presentation at the Lehigh valley Ecology and Evolution meeting

7. *Adrenergic signaling modulates long bone growth and chondrocyte functions in vivo* 2015
Poster presentation at the Society for Developmental Biology International meeting

6. *Adrenergic signaling regulates long bone growth and chondrocyte function in vivo* 2014
Poster presented at the Society for Developmental Biology International meeting

5. *Changes in phototaxis of Bestiolina similis during naupliar development* 2014
Poster presented at the Ocean Science Meeting (OSM)

4. *The nervous system's role in symmetrical development of limb bones* 2013
Poster presented at Gerstner Sloan-Kettering undergraduate research program symposium

3. *The development of visual systems in marine zooplankton* 2013
Oral presentation at the University of Hawaii spring honors symposium

2. *Do Opsins regulate cnidocyte firing in Nematostella vectensis* 2013
Poster presented at the Society of Integrative and Comparative Biology

1. *Do Opsins regulate cnidocyte firing in Nematostella vectensis* 2012
Poster presented at Annual Biomedical Conference for Minority Students Meeting

Awards

Lehigh University College of Arts and Sciences Dean's Research Award Fellowship	Spring 2021
Lehigh University Nemes Fellowship	Spring 2019, Fall 2020
Cnidofest 2018 Travel Award	2018
Graduate Assistance in Areas of National Needs (GAANN) Fellowship , Lehigh University	2015-2016
CHOOSE Development Fellowship	2013-2015
Society of Developmental Biology undergraduate poster competition runner up	2014
Minorities Access to Research Careers Fellowship , University of Hawaii at Manoa	2012-2014
Society of Integrative and Comparative Biology Broadening Participation Travel Grant , University of Hawaii at Manoa	2012

Teaching Experiences

Teaching Assistant — Lehigh University

Bios325: Microbiology Lab	Spring 2020
BioS375: Methods in Developmental Biology Lab	Fall 2018, Fall 2019

BioS376: Developmental Biology	Spring 2018
BioS275: Experimental Neuroscience Lab	Spring 2018
BioS279: Experimental Molecular Neuroscience Laboratory	Fall 2017
BioS043/BioS118: SEA-phage program	Fall 2016-Sping 2017

Mentor Experiences

Krishna Patel- Lehigh University Undergraduate	Fall 2019- Spring 2020
Brooke Shaefer- Lehigh University Undergraduate	Fall 2019- Spring 2020
Eric Mintz – Lehigh University Undergraduate	Spring 2019
Rachel Swope – Lehigh University Undergraduate	Spring 2019
Caroline Jennings – Lehigh University Undergraduate	Fall 2018-Spring 2019
Alexandra Mease — BDSI Summer Undergraduate, Lehigh University	Summer 2016-Spring 2018
Jessie Brill — BDSI Summer Undergraduate, Lehigh University	Summer 2016
Paul Bang — BDSI Summer Undergraduate, Lehigh University	Summer 2016
Sydney Yang — RARE Summer Undergraduate, Lehigh University	Summer 2016
Anuroop Alberts — RARE Summer Undergraduate, Lehigh University	Summer 2016-Spring 2018